Dissertation

Submitted to the
Combined Faculty of Natural Sciences and Mathematics
of the
Ruperto-Carola University Heidelberg

For the degree:

Doctor of Natural Sciences

Presented by
Pharmacist Ali Ghanem

Born in Reading, Great Britain

Oral Examination: 25/September/2018

On the Regulation and Multiple Functions of the Key Gluconeogenic Enzyme Fbp1 in Rapidly Proliferating Cells: Insights from Yeast and Breast Cancer Cells

1st Referee: Prof. Dr. Stefan Wölfl

2nd Referee: PD Dr. Tobias Dick

Acknowledgements:

While I am solely responsible for this thesis, my overall achievements during the last five years are the product of fruitful interaction with diverse and very special people, who helped me realise my potential in reaching this milestone. It is therefore my delight to express my warmest gratitude to those people, whom I have been very fortunate to know and work with.

First and foremost I would like to show my utmost appreciation for my supervisor Prof. Dr. Stefan Wölfl for his unlimited and continued support on various fronts throughout my PhD. Many thanks for your immense guidance, supervision and patience. Above all, thank you for being a true mentor and sharing a uniquely exciting academic and life experience. Thanks to your continuous encouragement and help, the last five years have granted me an invaluable chance for learning and growing, so I may now hope that the once dreamy inexperienced fresh graduate from faraway could now dare look forward to a promising scientific future. To me you will always be a role model to look up to both as a meritorious scientist and a superb human being.

I am also indebted to my second supervisor Dr. Tobias Dick for his constructive and enriching feedback and valuable suggestions in my TAC meetings and the time invested attending those meetings, reading reports and eventually reading my thesis. Also thank you for inspiring my interest in Redox Biology that I hope will reflect on my future career.

I am as well very thankful to Prof. Dr. Gert Fricker for the very motivating and encouraging feedback in my TAC meetings, and for the valuable time taken to attend the meetings, read the annual reports and read and evaluate my thesis.

Gratitude is also due to Prof. Dr. Markus Hecker for kindly agreeing to join the examiners' panel of my thesis defence.

I am also deeply grateful to the German Academic Exchange Service (DAAD) for enabling me to pursue my PhD by providing a doctoral scholarship. I am particularly thankful to the Section Scholarship Programs for the Middle East and North Africa (ST33) and especially Ms. Birgit Klaes, my contact person in the DAAD, for her patience and immense support in handling all the inquiries and communications.

Through my PhD I also enjoyed being a member of the HBIGS international graduate school. This came with many privileges ranging from receiving a travel grant and attending diverse core and career courses to the participation in diverse social activities. I also enjoyed being one of the student speakers for HBIGS for one year and attending two inspiring HBIGS retreats. This was all made possible by the efforts of Dr. Rolf Lutz, Ms. Sandra Martini and Ms. Martina Galvan, to whom I am also truly grateful.

It is no secret that preparing a PhD is a huge endeavour to undertake with difficulties and setbacks lurking at every corner. In face of all this I was absolutely privileged to be surrounded with splendid lab mates, whose friendship and support guarded me from frustration and helped me keep on through the most challenging of times.

Dr. Julia Lochead, you have been and will always be a marvellous friend. I couldn't possibly imagine my first three years in Heidelberg without your splendid positivity and our evening office conversations. You took good care of the Padawan until he became a Jedi (yup I quoted Star Wars, and it's damn time I watched it) and thus have become the elder sister I never had.

Dr. Mohamed Abu el Maaty (still getting used to the Dr. part), a great fella and the coolest bro of them all. I am totally grateful for all the exciting conversations; on science, career prospects, world politics, Syrian-Egyptian (comparative studies) and also for refreshing my interest in the very motivating and energetic rap music! Always remain an overachiever, and never give up your dreams!

Dr. Suzan Can, it has been an absolute delight getting to know you and a privilege to share the experience of restructuring and supervising the biochemistry practical course. Thank you

for your patience in helping me to improve my German and for the many classical concerts we attended. Always keep your elegance and your classy taste in everything!
Dr. Hamed Alburzinia for your immense support during my initial months in Heidelberg, for introducing me to cell culture basics, and showing the whereabouts of the lab in addition to corresponding with me before I had moved to Heidelberg. I totally enjoyed and appreciated our conversations, which improved my understanding of how research and academia work.
Dr. Pavlo Holenya, one of my oldest friends in Heidelberg and a great neighbour. Thank you for your support in the early days and for the lengthy interesting conversations on the way back and from work. Also thanks for patiently introducing me to the ins and outs of the biochemistry course we supervised in my first two years.
Dr. Xinlai Cheng, sharing an office with you and getting inspired by your successful career progress has been a privilege. Still remember your help with my enormous luggage on my first day in Heidelberg! I wish you all the best and soon the professorship you deserve.
Dr. Shahrouz Ghafoory, it has been great getting to know you, and very inspiring to witness your courage in starting a late but impressive scientific career. Always keep your inner youth!
Dr. Mariela Huichalaf, a totally cheerful colleague and friend. It was delightful to know you, and very impressing to see your persistence and capability to self-educate.
Dr. Mircea Tric, I am very grateful to your supportive attitude and motivating words. I immensely enjoyed our continuous space exploration discussions and our visit to the Königstuhl Sternwarte! Always keep up being the jolly and multi-talented person you are.
Jannick Theobald, (soon-to-be Dr. too!), a splendid friend, jolly fella and the best “equal lead-author” of them all! It has been my absolute delight to get to know you and contribute to your cutting-edge project. Also thank you for pushing me to improve my knowledge of very local and distinct German expressions (even if done forcibly!). Always keep your creative and entrepreneurial spirit, and always be a citizen of the world! (Even if you wouldn’t admit it!)
Fadi Almouhanna, a splendid friend, compatriot and an undergrad study colleague. It has been a delight seeing you embark on a promising track towards a hopefully brilliant PhD. Our lengthy conversations, spanning from science and economics to everyday gossip, were always enjoyable and very often helped me cope with the daily stress of PhD life. Thank you for being a great friend, and looking forward to celebrating your PhD soon.
Yasamin Dabiri, a truly brilliant scholar with an impressively sharp memory, ambitious scientist and a lovely friend and office neighbour. I am truly thankful for our enjoyable and useful scientific discussions, especially on probing the apoptotic markers! I am also truly impressed by your insights into the human nature, behaviour and psychology. Always be the pure, honest and energetically ambitious individual you are!
Rodrigo Gama-Brambilla, a remarkably polite person, and a truly open-minded citizen of the world. Thanks for being a great friend and a positively spirited person. I wish you all the best with your PhD and many exciting world-journeys.
Biljana Blagojevic, a lovely smart and ambitious friend. It has been delightful getting to know you and seeing you paving your way towards a successful PhD. keep up maximizing both the hard work and fun in your life.
I was also absolutely delighted to get to know other current and former lab mates and visiting postdocs: Lisa Neuner, Anastasia Zuieva, Mario Lederle, Dr. Jee Young Kim, Dr. Christian Guijarro, Dr. Uttam Budhathoki, Dr. Ncog van Bui, Dr. Jing-Jing Zhang, and Dr. Catharina Scholl and wish them all the best with their current and future endeavours.
I am truly thankful to both Dr Ana Kitanovic and Ms. Jinda Holzwarth for their previous work on Fbp1 regulation and mutational screening in yeast, which set foundation to the yeast part of my thesis project. I mostly know both through their writings, and I am very grateful to their well-performed and documented research that enabled me to explore the multiple function of Fbp1 in *S cerevisiae*.
It was also my privilege to supervise a handful of brilliant students through their internships in the Wölfl lab. Anna-Maria Melzer, an exceptionally smart and truly enthusiastic and dedicated student. Thank you for your contribution, your great working ethics and the many mutually

inspiring discussions. Also thank you for all the super delicious cakes you baked, which only left us looking forward for more!
Linh Trong, Hannah Glennemeier-Marke, Danny Baltissen and Laura Neises, you are all truly outstanding and I am very thankful for the good fortunes allowing us to work together.
I was also privileged to have a handful of good friends among other students in the lab; Jameson Poon, Julia Schessner and Julia Braun have all been great friends with whom I enjoyed very rewarding communication and great memories. I am also very grateful to Julia Schüler for thoroughly reading and improving the German summary (Zusammenfassung) of this thesis.
I have also been absolutely fortunate to work with uniquely talented technicians. Specifically, I would like to thank Anna Dreger for her vital support, impressive positivity, delightful attitude and great working ethic. It has been a privilege to participate in your teaching and supervision and see you progress towards a successful career. I was also privileged to work with Saskia Schmitteckert, Viola Mayer, Thomas Kolenda, Alina Sperl, Ann-Cathrin Gregotsch, Nicole Klotz and Marleen Heiß. I wish you all the best with your current and future endeavours.
I am also massively grateful to my collaborators, who allowed me to broaden the spectrum of this work.
I am very thankful to Dr. Esther Zaal at Utrecht University, for her help in metabolite quantification both for my thesis project and mostly for a major side project. Gratitude is also due to Prof. Dr. Celia Berkers, the PhD supervisor Of Esther Zaal and head of the Metabolomics Group in the Biomolecular Mass-Spec Division at Utrecht University.
I am also very grateful to our collaborators at the Division of Functional Genome Analysis, lab of Prof. Dr Jörg Hocheisel in the DKFZ. Special thanks are due to Andrea Bauer for performing the wide-scale transcriptional profiling on MDA-MB231 cells allowing us to draw very promising conclusions regarding Fbp1 anti-proliferative functions.
I am also thankful to Laura-Ines Böhler, from the lab of Prof. Dr. Hugo Marti for giving me access to their hypoxic bench, which contributed to the findings reported in this thesis.
During my PhD years in Heidelberg I was also very fortunate to make some very unique friends that significantly impacted the quality of my life and broadened my horizons in ways reflecting directly and indirectly on my merit as a scientist.
Of these I would like to specify Dr. Felix Weyer, a fellow scientist, an amazing friend and an inspiringly pure and brave person. I am sincerely grateful for your very welcoming, helpful and motivating attitude.
I am also very thankful to the following friends with a true impact on my life and thoughts during my PhD: Dr. Alistair Middleton, Dr. Michael Lang, Dr. Florian Huber, Philip Kemp, Dr. Markus Bartles, Dr. Julian Kellner and Dr. Lorenz Thomas.
I am truly grateful to Dr. Edmond Homsy for his warmly welcoming and inclusive attitude. I am truly inspired by your success story as one of the first pioneering Syrians in Germany, and your sincere efforts to establish a sense of dialogue and community among our compatriots in Heidelberg.
I am really grateful to Dr. Jan Brodsky, thank you for warmly welcoming me in Germany, during my first two visits, and after moving to Heidelberg. I immensely enjoy our outings and conversations, and your very authentic experience in life and science and your wittily expressed opinions.
Much gratitude is also due towards the place and people who provided me with the basic foundation to embark on a scientific career. I am immensely grateful to all my professors and educators in the Faculty of Pharmacy at Damascus University and to my study friends and colleagues there. Thank you for challenging all the difficulties to provide your deserving students with good knowledge and education and for always aspiring to the best despite every hardship.
I am also truly thankful to the Goethe Institute in Damascus, and all my teachers there, for teaching me very proper German, and granting me the first opportunity to visit Germany. I

hope that one day Goethe Institute will be re-opened in Damascus, regaining its vast positive educational and culture influence.
I am also immensely grateful to my splendid friend Dr. Nawar Dalila, thank you for your substantial support and very useful and experienced counselling, which were vital to my decision to study pharmacy and later to survive and excel at my studies back in Damascus. I am also very grateful for vital help during my early days in Germany, and the enjoyable stays in Göttingen, your lovely doctoral hometown.
Big milestones often make me reflect on my upbringing and early years. When I do, I am always deeply grateful to an amazing person who saw a flare of intelligence and curiosity in me very early on, and boundlessly encouraged me to think logically, and critically and most importantly to always have fun doing so. My uncle and splendid friend Dr. Munzer Ghanem, thank you for being an inspiration and a source of joy and positivity.
I am also immensely grateful, and could never show enough gratitude to Mrs. Julia Cotton and Dr. Greg cotton. I have been massively privileged to have you as non-biological family from the first day of my life. I am deeply thankful for the priceless support you have given me on every front throughout my PhD years, and my whole life. Also many thanks for the life mentoring, the endless exciting discussions that have substantially influenced and often even shaped my thought, world-views and life goals. I am also deeply grateful for the amazing time I spent visiting you this year, for your infinitely welcoming attitude, that made me feel truly at home. I loved being back in my birth home, and being on so many journeys with you. It all has been a very inspiring, perspective-changing and heart-touching experience. I wish you both everything amazing in life and look forward to our future adventures!
My brilliant little sister, Leen Ghanem, and the one and only original “Loulou”. We have been there for each other through everything, and I would never wish it to be otherwise. I might have inspired you (a cliché thing with elder siblings) but more often than you think, your courage, honesty, sensitivity, hard work and patience have been an endless source of motivation and inspiration to me! Always keep your glamour, and never underestimate you talents and potential!
I physically wouldn’t be here if not for my parents. Similarly this work wouldn’t exist if it weren’t for their exceptional nature as parents and as splendid individuals too.
My mother Nawal Laika, and my father Dr. Iyad Ghanem, I can never be thankful enough for all what you have done for me. You have given so much to ensure that we get the best of everything, and always made the right choice of investing in our education, refinement and quality of life, despite all the challenges. Even more impressive is your persistence on the right values of honesty, straightforwardness freedom of thought and expression, openness and creativity. You have struggled so hard to ensure that we grow with these values, despite the often-adverse conditions and surroundings that mostly rewarded quite different, and less constructive values. Thanks to this struggle I could grow to be a true “global citizen” who can freely travel, learn and appreciate this world. You also always kept your faith in me, and made sure my self-confidence never eroded, even in the toughest times. If not for all this, I am certain I would not be here right now, finalising this thesis, and looking forward to a potentially exciting scientific career. I hope I would one day eventually amount to the son you deserve, and that I would be successful enough to reflect the magnitude of your investment in me.

Table of Contents:

Name: Ali Ghanem
Title: On the Regulation and Multiple Functions of the Key Gluconeogenic Enzyme Fbp1 in Rapidly Proliferating Cells: Insights from Yeast and Breast Cancer Cells
Supervisor: Prof. Dr. Stefan Wölfl

Summary

Rewired cancer metabolism sprang into the spotlight this century as a crucial aspect of the malignant transformation. Being the century of the DNA, most 20th century cancer research focused on approaching cancer as a direct result of accumulated mutations while overlooking the metabolic aspects. Albeit very insightful on the origin of the disease, this approach has fallen short of eradicating cancer. Hence efforts in oncology research embarked on exploring other aspects in a bid for a whole-rounded anti-cancer approach. Consequently, last decade has seen accelerating breakthroughs in elucidating the metabolic adaptation of cancer cells to provide the requirements of rapid proliferation and the implication thereof as potential drug targets.

Basic metabolic networks and enzymes show large degree of evolutionary conservation between eukaryotes. Moreover, yeast and cancer share the major metabolic hallmark of aerobic glycolysis, demonstrate comparable proliferative tendencies, comparable cell cycle regulation and also undergo apoptosis akin to higher eukaryotes. This multiple overlap makes yeast an attractive model for addressing glucose metabolism as a driver for rapid proliferation.

This thesis features the results of my investigation into the regulation and effects of the key gluconeogenic enzyme fructose 1,6 bis-phosphatase Fbp1 in two distinct eukaryotic systems: the budding yeast *Saccharomyces cerevisiae* and human breast cancer cell lines. Based on previous research pointing out links between Fbp1 and the particular type of DNA damage elicited by methyl methanesulfonate. When exposed to MMS, Fbp1 is transcriptionally upregulated as a part of the response to DNA methylation. Fbp1, on the other hand, bestows an increased MMS-sensitisation upon yeast. I devised a mutational analysis of evolutionary conserved residues to address the mechanism of this additional phenotype, the results of which demonstrated that the enzymatic activity could also be decoupled from further MMS sensitisation, hence suggesting a non-catalytic origin of the additional effect.

I then embarked on investigating the effects of Fbp1 in breast cancer cell lines of both luminal and basal-like lineages. The findings I present make the case for an anti proliferative role of Fbp1 as an outcome of diminished glucose sensitivity, uptake and a shift from glycolysis to higher mitochondrial activity. Moreover, Fbp1 exhibited a pro oxidative role in cell lines manifested in increased ROS accumulation and sensitivity to oxidative agents. My findings also provide transcriptional evidence of a Wide - scale cell-cycle inhibitory outcome of Fbp1 ectopic expression in Fbp1-deficient MDA-MB231. Intriguingly, I observed that Fbp1-deficient basal like breast cancer cells acquired the capability to post-transcriptionally breakdown ectopic Fbp1 upon long-term stable over-expression. I also demonstrated that this degradation occurs through the proteasome and exclusively upon the long-term selection of cells with ectopic Fbp1.

An overview indicates multiple similarities of Fbp1 effects in yeast and cancer cell systems. In general, Fbp1 has comparable effects on proliferation, glycolysis, and Redox balance in both systems. The proteasomal degradation of Fbp1 in cells draws another parallel to the regulation of this enzyme in yeast since the so called “catabolite degradation” of Fbp1 had been long described and well-studied in yeast.

Nevertheless, when compared, the two corresponding mutations in yeast and human Fbp1 had distinct consequences for catalytic activity and enzyme stability in each system., therefore hinting at structural differences in the activation mechanisms and at different interaction partners in the two systems.

Altogether, the results presented in this thesis endorse Fbp1 as a quasi tumour suppressor and emphasise the potential therapeutic significance of approaches that can de-repress Fbp1 in cancers lacking it and prevent its ablation in cancers that express it.

Zusammenfassung

Im letzten Jahrhundert gehörte Stoffwechselwandel in Tumoren zu den wichtigsten erforschten Aspekten der malignen Transformation. Im letzten Jahrhundert wurde Krebs hauptsächlich als direktes Ergebnis der Akkumulation bestimmter Mutationen betrachtet, während die Regulation des Metabolismus der Krebszellen zum größten Teil übersehen wurde. Obwohl die Mutationstheorie essentiell für das Verständnis der Tumorentstehung ist, reicht sie nicht aus, um den Krebs vollständig zu vermeiden oder auszulöschen, aus diesem Grund hat sich Krebsforschung auf andere Aspekte fokussiert, um ein ganzheitliches Vorgehen gegen Krebs zu ermöglichen. Aufgrund der schnellen Profliferation benötigen Tumore einen reprogrammierten Stoffwechsel, um die essenziellen Bausteine und die Energie für das schnelle Wachstum zu besorgen.

Die zentralen metabolischen Wege sind in allen Eukaryoten evolutionär konserviert Ferner haben sowohl Tumore als auch eukaryote Mikroorganismen, wie z.B. Saccharomyces die Tendenz zur aeroben Glykolyse und schnelleren Proliferation. Zudem zeigen beide eine vergleichbare Regulierung des Zellzyklus und Apoptose. Aus den oben genannten Gründen bietet *Saccharomyces cerevisiae* ein einfaches zelluläres Model für die Untersuchung von schnellen Proliferation in Beziehung zur aeroben Glycolyse (Warburg Effekt).

In dieser Doktorarbeit stelle ich die Ergebnisse meiner Forschung dar, über die Regulation und Wirkungen des Enzyms Fruktose-1,6-bisphosphatase in zwei unterschiedlichen eukaryotischen Systemen; i) die Bierhefe *Saccharomyces cerevisiae* und ii) humane Brustkrebszelllinien.

Ergebnisse bisheriger Forschung an *S. cerevisiae* haben Zusammenhänge zwischen Fbp1 und den von MMS verursachten DNA-Schäden gezeigt. Eine MMS-Behandlung induziert die Transkription von Fbp1. Die verstärkte Expression von FBP1 wiederum steigert die Empfindlichkeit gegenüber der MMS-Behandlung. Um den Mechanismus dieser neuen Funktion des Fbp1-Enzyms zu erforschen, habe ich ein Mutagenese-

Screening von evolutionär konservierten Aminosäuren mit struktureller und funktioneller Relevanz entworfen. Durch die Mutagenese habe ich die Möglichkeit nachgewiesen, die FBPase- Katalyse von der MMS- Sensitivierung zu entkoppeln.

Weiterhin habe ich die Funktionen von Fbp1 in Brustkrebs-Zelllinien mit einem basalen oder ductalen Ursprung untersucht. Allgemein zeigen meine Ergebnisse eine antiproliverative Wirkung von Fbp1 als Folge von abnehmender Glukoseempfindlichkeit und -aufnahme sowie inhibierter Glykolyse

Ferner wirkt Fbp1 pro-oxidativ in den untersuchten Zellen, da vermehrt ROS und eine erhöhte Empfindlichkeit gegenüber oxidierenden Einflüssen beobachtet werden. Dazu weisen meine Ergebnisse auf eine FBP1-verursachte Zellzyklus Inhibierung hin, wie eine weitreichende Herabregulierung der Transkription mehrerer Zellzyklusfaktoren nach Fbp1-Überexpression in MDA-MB231 Zellen.

Interessanterweise habe ich einen bisher unbekannten proteasomalen Abbau der Fbp1 in MDA-MB231 Zellen bewiesen. Ein ähnlicher Mechanismus ist für *S cerevisiae* bereits gut beschrieben.

Trotz unterschiedlicher Effekte zweier überlappender Mutationen in Human und Hefe-Fbp1-Orthologen, die zu signifikanten strukturellen Unterschieden führen, beweist diese Arbeit mehrfachlich die Ähnlichkeit in der Regulierung und metabolische Wirkung von Fbp1.

Allgemein unterstützen meine Ergebnisse eine vermutete Tumoursupressor-Wirkung für Fbp1 und zeigen somit eine mögliche therapeutische und präventive Relevanz für die De-repression und Aktivierung dieses Enzyms im Kontext mit Krebs.

List of abbreviations:

2-DG: 2-deoxy-glucose2-NBDG:

2-(*N*-(7-Nitrobenz-2-oxa-1,3-diazol-4-yl)Amino)-2-Deoxyglucose

Abs: Absorbance

Ac-CoA: Acetyl-Coenzyme-A

ACC: Acetyl-Coenzyme-A carboxylase

pACC: Phospho Acetyl-Coenzyme-A carboxylase l

AKT (PKB): protein kinase B

AMP: Adenosine Mono-Phosphate

AMPK: AMP-activated protein kinase

pAMPK: phospho AMP-activated Protein Kinase

ATP: Adenosine Tri-Phosphate

AURKA: Aurora kinase K

BLBC: Basal like breast cancer

Cenp-E: Centromere-Associated Protein E

CFU: Colony-Forming Unit

CMV: Cytomegalovirus

CRISPR: Clustard Regularly INterspaced Short Palindromic Repeats

DMEM: Dulbecco's Modified Eagle's Medium

DMSO: Dimethyl Sulfoxide

DNA: Deoxyribunucleic Acid

E. coli: *Escherichia coli*

ER: Estrogen Receptor

EGF: Epidermal Growth Factor

EMT: Epithelial-Mesenchymal Transition

F6P: Fructose 6 Phopshate

F1,6bP: Fructose 1,6 bis-Phosphate

F2,6bP: Fructose 2,6 bis-Phosphate

FACS: Fluorescence-Assisted Cell Sorting

FADH2: Flavin adenine dinucleotide (Reduced)

FBP1: Fructose 1,6 bisphosphatase (pertaining strictly to the protein)

Fbp1: Fructose 1,6 bisphosphatase (general term for the mRNA, protein or function/s)

fbp1: Fructose 1,6 bisphosphatase (pertaining strictly to the gene)

FBPase: Fructose 1,6 bisphosphatase (ning strictly to the catalytic activity)

G6P: Glucose-6-Phosphate

G6PDH: Glucose-6-Phosphate Dehydrogenase

HCC: hepatocellular carcinoma

HDR: Homology-Directed-Repair

Her2: Human epidermal growth factor receptor 2

Hif1α: Hypoxia-Inducible Factor alpha

JC-1: 5,5,6,6-Tetrachloro-1,1,3,3-tetraethylbenzimidazolylcarbocyanine iodide

kRas: Kirsten Rat sarcoma viral oncogene

LDH2: Lactate Dehydrogenase 2

MMS: methyl methanesulfonate

mTOR: mammalian Target of Rapamycin

NaCl: natrium chloride

NADH: Nicotinamide adenine dinucleotide (Reduced)

NAD^+: Nicotinamide adenine dinucleotide (Oxidised)

NADPH: Nicotinamide adenine dinucleotide phosphate (Reduced)

$NADP^+$: Nicotinamide adenine dinucleotide phosphate (Oxidised)

OD: optical density

OE: over-expression

OXPHOS: oxidative phosphorylation

PBS: Phosphate-Buffered Saline

PDK: Pyruvate Dehydrogenase Kinase

PEG: polyethyline glycole

PFK1: Phosphofructokinase1

PFK2: Phosphofructokinase2

PGI: Phosphu-gluco isomerase

PPP: Pentose Phosphate Pathway

RedOx: Reduction/Oxidation

RNA: Ribonucleic acid

mRNA: Messenger Ribonucleic acid

ROS: Reactive Oxygen Species

S.cerevisiae: *Saccharomyces cerevisiae*

SDEG: Synthetic Dropout Ethanol Glycerol (yeast culture medium)

SD-Ura: Synthetic Dropout medium without uracil

SDS: Sodium Dodecyl Sulfate

SDS-PAGE: SDS-Polyacrylamide Gel Electrophoresis

SNF: Sucrose Non-Fermineting

SRB: Sulforhodamine B

TCA: Tricarboxylic acid cycle

TCA: Trichloroacetic Acid

TGF-α: Transforming Growth Factor-alpha

TXNIP: Theoredoxic Interacting Protein

YNB: Yeast Nitrogen Base.

YPD: Yeast Peptone Dextrose (Culture medium)

I- Introduction

"Biologists must constantly keep in mind that what they see was not designed but rather evolved". Francis Crick

I-I Glucose as the main hub of cellular carbon metabolism

Simplistically speaking, accessible energy and building blocks of macromolecules are the two very essential prerequisites of survival and expansion of living cells. Metabolism provides the interactive and readily responsive network that connects and diverts the flow of energy and matter within the cell according to its needs and priorities. Hence, a fully differentiated non-dividing cell e.g. a neuron or a muscle cell, has its metabolism wired for optimised respiration, and ATP production to maintain its continued integrity and energy-demanding specific function. Whereas rapidly proliferating cells e.g. a developing embryo [1], a tumour or a unicellular organism exhibit completely different metabolic priorities [2], which reflect in their metabolism tilting towards anabolism to create the necessary macromolecules for the daughter cells [3]. However, a secure energy flux is still needed for maintaining glycolysis, anabolic processes and intracellular homeostasis [4, 5].

Carbon is the building block of life as we know it [6], it is also the main floating source of energy and biomaterial in the ecosystem [7], and in the extracellular compartments of multicultural organisms [8]. Extracellular energy floats in form of covalent carbon bonds, and is then converted by the cells into more readily accessible phosphate-bond energy. The larger the carbon-based molecule is, the more steps it needs to be broken down to readily catabolisable blocks, hence larger carbon molecules including fat play the role of energy storage. Glucose, however, is in the central intersection of carbon based anabolism and catabolism, initial intracellular phosphorylation by hexokinases at C6 traps glucose within the cell [9], and renders it available for a plethora of different pathways depending on the momentary requirements of the cell [10]. Glycolysis is the main initial catabolic pathway of glucose, providing pyruvate for the TCA, nevertheless it is also the stem, from which the synthetic pathways of several amino acids branch, making it a necessary entry step for protein anabolism

[11, 12]. The output of full glycolysis is 2 molecules of pyruvate and 4 molecules of ATP, pyruvate is either fermented into lactate, converted into aliphatic amino acids or further decarboxylated to form Ac-CoA the entry molecule of the TCA, which allows the complete decomposition of the remaining carbon bonds and the conversion of their energy into ATP and reductive equivalents; NADH and FADH2 [13]. The TCA is also the source of the precursors for denovo fatty acid synthesis and the synthesis of various amino acids.

In the aforementioned regard, glycolysis is seen as a central rate determinant for cellular energy production, anabolism and consequently proliferation. Besides glycolysis, G6P can undergo an alternative catabolic fate through the pentose phosphate shunt. The latter is a more specifically anabolic pathway fuelling growing and dividing cells with much needed ribose for de-novo nucleotide synthesis, and NADPH the main anabolic source of reductive equivalents needed for the synthesis of lipids required for all cellular membranes[14]. The pentose phosphate shunt is also an essential anti-oxidant pathway, which allows the cells to maintain their reducing equivalents to counter redox imbalance and maintain a strongly reductive cytosole [14, 15]. Consistently, the pentose phosphate pathway is induced in proliferative and anabolic programs, including by aberrantly over activated oncogenes in tumours (e.g. mTOR, kRas) [16, 17], whereas tumour suppressors (e.g. p53, AMPK) inhibit this pathway [18, 19]. While cells can break down glucose via glycolysis, gluconeogenesis enables the intracellular synthesis of glucose starting from TCA-derived precursors [20]. Since Glucose-6-phosphate is the entry molecule to the essential pentose phosphate shunt, it follows that even in energy abundant situations minimal levels of glucose-6-phosphate remain indispensable to secure enough PPP flux to maintain RedOx homeostasis and fuel de-novo nucleotide synthesis. This makes gluconeogenesis absolutely important for cell survival in absence of extracellular glucose sources. Despite its importance in glucose absence, when glucose is abundant, gluconeogenesis can be very disruptive to cellular metabolism due to energy consuming futile cycles. Therefore, the flux through both glycolysis, and gluconeogenesis are tightly regulated. In higher organisms including humans this regulation is achieved via pancreatic and hepatic hormones that reflect the glucose availability in the circulation.

I-II PFK1 and Fbp1; the evolutionary conserved gauges of glucose consumption and production

1. Regulation in mammals:

Glycolysis and gluconeogenesis share most of their enzymes, these catalyze reversible reactions according to substrates availability. The two pathways diverge in 4 steps that are catalyzed by enzymes unique for each pathway [21]. This allows the separate regulation of each pathway to avoid futile cycling[22-24].

Since most intracellular glucose is kept in a phosphorylated state followed by reversible isomerisation to fructose 6 phosphate, the following step in glycolysis is decisive to the flux through glycolysis as a whole. The second phosphorylation of glucose is catalyzed by phosphofructokinase (PFK1), this enzyme is specific for glycolysis, and it sets the rate of the pathway as a whole [25, 26]. PFK1 is allosterically regulated by a multitude of factors guaranteeing that glycolysis rate is adjusted according to cells' requirements [25, 27, 28]. The reverse step of the second phosphorylation of glucose is the dephosphorylation of fructose-1,6-bisphosphatase regenerating fructose-6-phosphate and inorganic phosphate. This step constitutes the main bottleneck in the gluconeogenesis pathway, and is catalyzed by the rate limiting enzyme fructose 1,6 bisphosphatase FBP1 [29]. A kin to PFK1, FBP1 is subject to complex allosteric regulation in mammals. The plethora of allosteric regulators work on PFK1 and FBP1 in an opposite manner, the abundance of glycolytic products citrate and ATP convey a signal of saturation onto the glycolytic pathway by inhibiting PFK1 in a classic negative feedback mechanism in which final products of pathways inhibit key enzymes of these pathways [30, 31]. Meanwhile the abundance of energy (low AMP concentrations) [32], and TCA intermediates (citrate) has an indirect permissive effect of gluconeogenesis to allow cells to make use of the high energy in anabolism and energy storage in more stable forms including glycogen [33]. In addition to direct intracellular factors PFK1 and FBP1 are also under the control of the glucose homeostasis hormones, insulin and glucagon. The former is an anabolic hormone secreted upon feeding and increasing blood glucose levels, and the latter is a catabolic hormone secreted in fasting periods. This hormonal duet maintains blood glucose levels within a physiologically tolerable range, and it does so

in part via regulating glycolysis and gluconeogenesis [34]. The effects of insulin and glucacon oppositely diverge on PFK1 and FBP1 via regulating an intracellular switch consisting of a dual-function enzyme phosphofruktokinase2/ fructose-2,6-bis-phosphatase PFK2/F2,6BPase [34, 35]. During fasting glucagon favours gluconeogenesis by indirectly deactivating the PFK2 function and maintaining the F2,6BPase function, which in turn depletes F2,6bP leading to increased gluconeogenesis flux via lifting the allosteric inhibition of F2,6bp and down regulated glycolysis via the lack of allosteric activation of F2,6bP on this enzyme[27, 36].

In summary, FBP1 and PFK1 constitute the two most important major switches of gluconeogenesis and glycolysis respectively and they integrate regulatory signals that inversely affect these two pathways to meet both the specific demands of the cell and those of the whole organism. It is also worth mentioning that while glycolysis is a ubiquitous pathway in all cells, albeit at markedly different rates, gluconeogenesis is restricted to certain specialised organs and tissues including the liver, where gluconeogenesis is instrumentalised to meet the glucose demands of the whole organism and maintain homeostasis.

2. Regulation in unicellular organisms:

Unicellular organisms, on the other hand, are hard wired to use any environmental abundance to achieve faster proliferation and therefore dominate their environment. Hence unicellular metabolism is wired to support rapid proliferation, in the case of *S. cerevisiae* and many other eukaryotes and prokaryotes. This means maximizing the glycolytic flux with most of the resulting pyruvate being fermented to ethanol or lactate. Through largely avoiding respiration, cells can secure maximized glycolysis without reaching energy saturation. This allows maximal glucose uptake and incorporation of glycolytic intermediates as building blocks to support anabolism resulting in fast production of macromolecules important for fast respiration. To achieve this, yeast among many other organisms uses glucose itself as the main signal steering their metabolism. Glucose repression transcriptionally prevents the expression of respiration and gluconeogenesis genes, including fructose 1,6 bisphosphatase. As mentioned earlier, it is pivotal to down regulate gluconeogenesis while glycolysis is active in order to avoid futile cycling. While higher organisms

achieve this via posttranslational allosteric regulations, unicellular organisms respond directly and readily to glucose queues on a transcriptional level. Besides transcriptional control, glucose replenishment also mediates the immediate degradation of FBP. Altogether, FBP1 is expressed and degraded on demand in unicellular organisms, whereas mammalian cells required to perform gluconeonenesis maintain constant levels of the alosterically-regulated protein.

I-III Contrasts between unicellular and multicellular metabolism control

The fundamental differences in metabolism between unicellular organisms and differentiated cells in higher organisms are attributed to having different objectives to be met for securing selective evolutionary advantage for the organism [37, 38]. The survival of a unicellular organism is majorly dependent on its fitness and superiority in direct competition against other organisms (members of the same species or other species) for the nutrients in the environment. Whilst the survival of a multi-cellular organism is rather dependent upon the successful cooperation of differentiated cells to maintain the organism's homeostasis and sustain efficiency on the systemic level of the organism as a whole [39]. Therefore, the regulation of metabolic pathways including glucose and general carbon metabolism is determined by the requirements of the organism and differs between tissues and organs depending on their role and specific metabolic requirements. Similar considerations underpin the regulation of cell proliferation and differentiation in a multi-cellular organism.

The interplay of intracellular cell cycle regulation and extracellular biochemical queues (hormones, growth factors) keeps cellular proliferation under control so that the growth and regenerative requirements are met while excessive aberrant proliferation is avoided, the immune system also functions as a second line of defence by obliterating any cells that seem to defy this control.

I-IV Metabolic reprogramming in cancer: parallels to unicellular metabolism. (A regressive fall back onto an ancient and selfish metabolic programme)

Cancer is in part the result of a failing multicellular homeostatic control and defence [40]. In the course of their malignant transformation, cancer cells escape all intracellular checkpoints (e.g cell cycle, DNA integrity checkpoints) [41] and

extracellular gauges [42] (e.g. reliance on growth signals and hormones, vigilance of the immune system) and limitations (e.g. energy supply and molecular substrate) on their proliferation, and proceed to acquiring traits that favour their own proliferation on the expense of the organism as a whole [43, 44]. The more the deviation from the natural differentiation line the worse the prognosis [45]. In this light, cancer can be described as a rebellion of a single cell and its transformed lineage against the multicellular harmony that reigns over differentiated tissues and organs [46-48]. Intriguingly, cancer cells also seem to revert to a metabolic program similar to that of unicellular organisms. It is well established that cancer cells undergo metabolic reprogramming shifting their reliance from TCA and OXPHOS towards glycolysis as a primary pathway for ATP production under aerobic conditions [49-51]. Hypoxia inducible factor Hif1a is one major player fostering this metabolic shift [50]. Several upstream regulators involved in the abnormal stabilization of Hif1α subunit in normoxic conditions are evolutionary conserved between yeast and mammals, these include mTOR/TOR1, AMPK/SNF and the oncogene AKT/Scf9 [50-52]. In addition to the generally up-regulated glycolysis, tumors have different predominant isozymes catalyzing some of the glycolytic reactions, including Glut1, HK2, and PKM2. These enzymes show similarities in their regulation specifications and overexpression levels to those of the yeast glycolytic pathway [51]. This also holds true for the TCA, which gets repressed through inhibition of its entry enzyme PDH, whose activity is quenched due to HIF1a-mediated over- expression of PDK [50]. HIF1 also induces the overexpression of LDH2, a highly active isoform of lactate dehydrogenase rendering cancerous cells into aerobic fermenters akin to unicellular organisms[53]. All these similarities point to a “devolution” undergone by malignantly transformed cells, in which a single-cell fixated evolutionary-rooted metabolic program overwrites the metabolic preferences defined by the multicellular context of differentiated cells [46, 47]. Indeed, there are evolutionary views that suggest an independent phylogeny of cancers placing them in a separate place of the evolutionary tree from the organisms, in which they arise [40, 54].

I-V Cancers down regulate gluconeogenesis: metabolic and proliferative advantages

Aerobic glycolysis might seem less energetically efficient, but it is only so when considering a scarce amount of glucose is available, this limitation is overcome by the multicellular physiological condition that provides a continuous supply of glucose[55]. Cancer cells rewire their metabolism to give optimal support for their accelerated proliferation, this also includes discarding any inefficient pathways whose energetic cost can burden the cell and hold back its growth and proliferation [2, 56]. Gluconeogenesis is one example of the aforementioned costly pathways; it exists to ensure that the organism as a whole averts deleterious hypoglycemia during fasting and intense activity[57]. However, for individual cells, gluconeogenesis is less efficient compared to taking up glucose and funnelling it through glycolysis. Cancer cells particularly enhance their glucose uptake capacity by upregulating the expression and membrane localization of glucose transporters[58]. Considered with the fact that circulation offers a constant supply of glucose, high capacity of glucose uptake enables cancer cells to have a constant abundance of glucose, which would render gluconeogenesis obsolete as long as cells receive enough blood supply.

Indeed, evidence from various tumour types indicates that cancerous cells abandon gluconeogenesis mostly by epigenetically silencing fructose 1,6 bis-phosphatase [59-64]. FBP1 is a rate limiting and key enzyme for this pathway, and silencing amounts to a complete shutdown of gluconeogenesis. Liver tumours exhibit drastic epigenetic silencing of FBP1. Very recently, the derepression of FBP1 in hepatocellular carcinoma HCC cell lines successfully suppressed glycolysis and reversed the tumour metabolic reprogramming. In renal clear cell carcinoma, FBP1 repression is indispensable for the initial tumorigenesis and malignant transformation. Breast tumours vary in regard to FBP1 expression. FBP1 is highly expressed in primary luminal breast cancers with relatively good prognosis. While it is absent in basal-like breast cancers, including the triple negative breast cancers, all usually exhibit dire prognoses. Metastases from FBP1-positive breast tumours also lack FBP1, consistent epigenetic repression of FBP1 was observed as part of the EMT-program conferring further aggressiveness, invasive and metastatic traits to breast cancerous cells. Intriguingly, the ectopic introduction of FBP1 was enough to prevent Snail-induced EMT; this suggests that FBP1 loss is an essential step for EMT to occur. The knockdown of FBP1 in originally FBP1-positive ductal breast cancer cells

correlated to increased glycolytic flux, more colonies in culture and larger xenograft tumours. Consistently, the ectopic expression in FBP1 in basal like “triple negative” cell lines partially reversed the glycolytic phenotype and halted back growth, colony and tumour formation. Taken together the aforementioned results suggest a decisive role for FBP1 in determining the prognosis and outcome of breast cancers. Unlike in other types of cancer where FBP1-loss occurs early during tumour initiation, in breast cancer FBP1-repression commences in later stages of tumour development, acquisition of invasiveness and metastasis. This makes breast cancers a good model for understanding the roles of FBP1 in the context of cancer, in part because a better understanding could hopefully reveal novel ways of targeting the more aggressive FBP1-negative tumours, or even more ambitiously prevention of reverse the steps that lead to FBP1-repression in the first place.

I-VII DNA damage in cancer initiation, treatment and relapse

The discovery of the DNA as the genomic material and the elucidation of the genetic code[65, 66] heralded an understanding of cancer as an outcome of accumulated mutations that result from genomic instability[67, 68]. According to the somatic mutation theory, cancer initiation and progression occurs by evading various constraints of uncontrolled proliferation. To achieve this, cancerous cells and tumours as a whole need to acquire 6 malignant hallmarks, this happens as outcome labile genome and accumulated mutations[44, 69]. This model of cancer origin and progression provided an ample framework for understanding the mechanism of anti-cancer cytotoxicity of early discovered chemotherapies. The genomic instability of cancers, in addition to the continuous rapid proliferation renders cancer cells more sensitive to chemicals directly damaging the DNA or inhibiting nucleotide synthesis essential for DNA repair and replication[70, 71]. In spite of its decisive effect upon cancer treatment for decades to come, chemotherapy confronted the big challenge of relapse and resistance emerging in a vast majority of cases. Soon it became clear the heterogeneity of cancers meant that treatment resulted in a positive selection of more resisting cells. Moreover, the degree of DNA damage nec resulted in a selection of DNA damage necessary for killing the majority of tumour cells leaves an

amount of surviving cells with increased mutation rate enough for new resistant phenotypes to arise[72]. This paradox of DNA damage being both at the root of cancer and its basic treatment necessitates wider approaches targeting cancer cells beyond the genome. In addition to a plethora of upstream resistance mechanisms that depend on limiting the bioavailability of the drug within tumour cells[73], new molecular mechanisms have been discovered that rely on modulating the reaction of cancer cells to the treatment and hence evade cell death. These include the induction of DNA repair pathway, which requires active metabolism generating the necessary nucleotides and ATP molecules for DNA repair[74]. Other downstream resistance manoeuvres, to which metabolism also contributes, include changed cell cycle regulation, apoptosis inhibition, induction of morphological alteration and autophagy [72, 75, 76]. Therefore targeting cancer metabolism has emerged as a promising anti-cancer approach to target metabolic weaknesses in order to improve response and prevent relapse[3]. Therefore, understanding the interaction between different metabolic pathways and the responsiveness to various anticancer treatments is essential for development of treatment regimens combining both conventional and metabolism-targeting agents. In my thesis I further explore the relation between the regulation of gluconeogenesis as a result of various Fbp1 contexts and the sensitivity of rapidly proliferating cells to DNA damaging agents and other oxidative and metabolic cytotoxic treatments.

I-VII-I Premise, rationale and envisaged objectives

This thesis features my PhD research focusing on Fructose1,6 bis phosphatase and its effects in two distinct contexts; the dual role of FBP1 in the budding yeast *S.cerevisiae* on the one hand, and the metabolic, proliferative and phenotypic impact of FBP1 in breast cancer cell lines, on the other. The seemingly unconventional approach aims at drawing conclusions from the investigation of FBP1 in yeast that can be put into use to improve our understanding of the multiplex effect of this enzyme in cancerous cells. As mentioned above, there are several stark similarities in metabolic phenotypes and preferences between unicellular organisms and cancers. These make it plausible to harness the simplicity of unicellular organisms to model and probe certain aspects of tumour metabolism. Various considerations make yeast attractive to probe FBP1 in yeast; some are general advantages connected to

yeast as a model including its very well defined and easy to manipulate genome, yeast have a very fast growth and proliferation compared to mammalian cells and wide range evolutionary conservation compared to mammals. This last trait is of an advantage in our particular case; previous work from our lab identified Fbp1 as a response element of the DNA and protein damaging treatment of methyl methane-sulfonate MMS. A wide screen of transcriptional shifts following MMS treatment identified Fbp1 as one of the genes whose expression is induced within an hour of exposure to low doses of MMS.

Originally Fbp1 is subject to glucose repression in yeast, hence it is completely repressed in glucose replenished conditions. Nevertheless, MMS induces the expression of Fbp1 in glucose rich media. The deletion of Fbp1 uncovered functional/phenotypic relevance for post-MMS Fbp1 induction. Fbp1-deficient (*fbp1Δ*) cells exhibit less sensitivity to low doses of MMS. FBP1-deletion also abolished MMS-induced ROS accumulation. Similarly, FBP1-deficient cells exhibited less ROS induction upon chronological aging compared to wild-type cells of the same strains. This additional phenotype points out to a potential role of FBP1 in mediating genotoxicity. The aforementioned additional role can either stem from the enzymatic activity itself (e.g.: a result of changed glucose metabolism in absence of FBP1, or other metabolic products) or it can be due to an additional non-catalytic interaction of the protein. To address the origin of this functional and phenotypic duality of FBP1, a separation of the catalytic function from any other potential independent functions of the protein is necessary. This can be achieved by substituting functionally and structurally relevant residues, hence giving rise to analogues with reduced or completely annulled catalytic activity. Other aspects that can be altered via mutagenizing FBP1 are its subcellular localisation and its susceptibility to ubiquitination and subsequent degradation. The nuclear sub localization of the enzyme is of great interest due to reports on its non-catalytic function in the nuclei of human cancerous cells. In the nucleus, FBP1 interacts with Hif1a and prevents it from excreting its oncogenic transcriptional program. Manipulating the nuclear sub-localization of the enzyme in yeast can uncover any possible specific nuclear functions in yeast, especially in the context of the dual phenotype discussed above.

The work on yeast is aimed at understanding the roles of FBP1 in yeast as a system per se, as well as enriching our perspective for exploring the regulation and effects of the enzyme in cancerous cells.

To approach the issue in cancerous cells, I took on establishing and characterising models of FBP1 over-expressions and deletions in two breast cancer cell lines. My choice fell on breast cancer due to the heterogeneity of these tumours regarding FBP1 expression. Mainly, breast cancers fall into two broad categories; ductal and basal-like breast cancers. Tumours of the former type are primary tumours, epithelial in their morphology, hormone-dependent in their growth and are predominantly curable with high 5-year survival rates and generally good prognoses. In contrast, BLBCs are highly aggressive, metastatic tumours with mesenchymal morphology, hormone-independent, and have much worse prognosis. Among these tumours are the so-called triple negative breast cancers that lack the expression of Her2 receptors, the epithelial marker E-cadherin, and the estrogen receptor. These are clinically designated as particularly critical, and they always lack FBP1 expression. Primary ductal breast tumours, including treated and regressed ones, are prone to relapse and further gain of aggressiveness that results from an epithelial-to-mesenchymal transition EMT program, which confers further aggressiveness and the capability of metastasising. As already mentioned, FBP1 has a critical implication in this dynamic process. This makes breast cancer cells an ideal model to understand the impact of FBP1 on cancers in general, since they offer both contexts of FBP1 absence or presence.

II-Material and Methods

"What I cannot create, I do not understand". Richard Feynman

II-I Instruments and equipment

Yeast Culture:	
Shaking incubator: GFL3031	GFL, Burgwedel
Agar plates incubator: Unitherm150	Uniequip, Martinsried
CyBi® Well 96-channel simultaneous pipettor.	
Software: Opal Control	CyBi –Well, Jena
Cell Culture:	
CO_2 incubator: NuAire Autoflow NU5510E	NuAire, Minnesota
Centrifuge: Eppendorf 5702	Eppendorf AG, Hamburg
Water bath: GFL 1083	GFL, Burgwedel
Microscope: Nikon Eclipse	Nikon, Düsseldorf
Gel electrophoresis and immunoblotting:	
Gel electrophoresis set: Hoefer™ SE 260	Amersham, Little Chalfont
Power supply for gel electrophoresis: Enduro™	Labnet Int, Edison
Transfer device: BlueFlash-L	SERVA Electrophoresis, Heidelberg
Power supply for transfer: PowerStation 200	Labnet Int, Edison NJ
Analogue tube roller: Stuart SRT6	Stuart equipment
Stone, Staffordshire	
Western Blot camera:	
LAS3000 imager: CCD camera and intelligent dark box. Software: LAS300 Image Reader	FujiFilm, Minato (Tokio)
Bellydancer Mixer/Shaker Stovall Life Sciences	
Greensboro, NC	
Native protein extraction: Bead mill MM300	Retsch®, Haan
Cloning PCR and nucleic acid gel electrophoresis:	
RT-qPCR: qTower	Analytik Jena, Jena
Thermocycler: Eppendorf	Eppendorf, Hamburg
DNA/RNA Electrophoresis chamber: SubCell® GT	Bio-Rad, Hercules CA
Analysis instruments and devices:	
Plate reader: Tecan Infinite F200 pro	Tecan, Männedorf
Flow cytometer: FACS Guava easyCyte HT	Merck Millipore, Darmstadt
Bionas® 2500 analysing system	Bionas, Rostock

Lab essentials:	
Eppendorf Research® Pipettes: 10, 20, 200, 1000 µl	Eppendorf, Hamburg
Vortex Genie2®	Scientific Industries Inc ™, Bohemia NY
Thermomixer Comfort	Eppendorf, Hamburg
Pipette controller: PIPETBOYacu2	Integra Biosciences, Zizers
Mini centrifuge (Spin down device)	Labnet Int, Edison NJ
Automated dispensing systems:	
Multidrop™ Combi	Thermo Fisher Scientific Weltham, MA
VIAFLO® II Electronic pipettes VIAFLO Assist pipetting platform	Thermo Fisher Scientific Thermo Fisher Scientific

II-II Material

Yeast Culture

Utilized yeast strains

All yeast strains were used in their haploidic form. The BY4741 strain is derived from S288-C with a quadruple deletion of popular selectable markers. The wild-type WT and Fbp1-deletion *Δfbp1* of this strain were harnessed for the mutational analysis of FBP1 described in this thesis.

Table 1: Parental and transformed yeast strains with a BY4741 background.

	Genotype	**Plasmid**	**Source**
Parental Strains			
BY4741 wt	*MATa his3Δ1; leu2Δ0; met15Δ0; ura3Δ0*	-	EUROSCARF yeast collection
BY4741 *Δfbp1*	*MATa his3Δ1, leu2Δ0, met15Δ0, ura3Δ0; fbp1::KanMX4*	-	EUROSCARF yeast collection
Transformed strains			
BY4741 wt + vector	*MATa his3Δ1; leu2Δ0; met15Δ0; ura3Δ0*	pRS426 (empty)	This work
BY4741 wt + *Fbp1*	*MATa his3Δ1; leu2Δ0; met15Δ0; ura3Δ0*	pRS426 *Fbp1*	This work
BY4741 wt + *Fbp1* P1A	*MATa his3Δ1; leu2Δ0; met15Δ0; ura3Δ0*	pRS426 *Fbp1* P1A	This work
BY4741 wt + *Fbp1* N75A	*MATa his3Δ1; leu2Δ0; met15Δ0; ura3Δ0*	pRS426 *Fbp1* N75A	This work
BY4741 wt + *Fbp1* D79A	*MATa his3Δ1; leu2Δ0; met15Δ0; ura3Δ0*	pRS426 *Fbp1* D79A	This work
BY4741 wt +*Fbp1* E109A	*MATa his3Δ1; leu2Δ0; met15Δ0; ura3Δ0*	pRS426 *Fbp1* E109A	This work
BY4741 wt +*Fbp1* D131A	*MATa his3Δ1; leu2Δ0; met15Δ0; ura3Δ0*	pRS426 *Fbp1* D131A	This work
BY4741 wt +*Fbp1* S133A	*MATa his3Δ1; leu2Δ0; met15Δ0; ura3Δ0*	pRS426 *Fbp1* S133A	This work
BY4741 wt	*MATa his3Δ1; leu2Δ0; met15Δ0;*	pRS426 *Fbp1*	This work

+*Fbp1* F194A	*ura3Δ0*	F194A	
BY4741 wt +*Fbp1*H265A	*MATa his3Δ1; leu2Δ0; met15Δ0; ura3Δ0*	pRS426 *Fbp1*	This work
BY4741 wt +*Fbp1*H324A	*MATa his3Δ1; leu2Δ0; met15Δ0; ura3Δ0*	pRS426 *Fbp1*	This work
BY4741 *Δfbp1* + vector	*MATa his3Δ1; leu2Δ0; met15Δ0; ura3Δ0; fbp1::KanMX4*	pRS426 (empty)	This work
BY4741 *Δfbp1* + *Fbp1*	*MATa his3Δ1; leu2Δ0; met15Δ0; ura3Δ0; fbp1::KanMX4*	pRS426 *Fbp1*	This work
BY4741 *Δfbp1* + *Fbp1* P1A	*MATa his3Δ1; leu2Δ0; met15Δ0; ura3Δ0; fbp1::KanMX4*	pRS426 *Fbp1* P1A	This work
BY4741 *Δfbp1* + *Fbp1* N75A	*MATa his3Δ1; leu2Δ0; met15Δ0; ura3Δ0; fbp1::KanMX4*	pRS426 *Fbp1* N75A	This work
BY4741 *Δfbp1* + *Fbp1* D79A	*MATa his3Δ1; leu2Δ0; met15Δ0; ura3Δ0; fbp1::KanMX4*	pRS426 *Fbp1* D79A	This work
BY4741 *Δfbp1* +*Fbp1* E109A	*MATa his3Δ1; leu2Δ0; met15Δ0; ura3Δ0; fbp1::KanMX4*	pRS426 *Fbp1* E109A	This work
BY4741 *Δfbp1* +*Fbp1* D131A	*MATa his3Δ1; leu2Δ0; met15Δ0; ura3Δ0; fbp1::KanMX4*	pRS426 *Fbp1* D131A	This work
BY4741 *Δfbp1* +*Fbp1* S133A	*MATa his3Δ1; leu2Δ0; met15Δ0; ura3Δ0; fbp1::KanMX4*	pRS426 *Fbp1* S133A	This work
BY4741 *Δfbp1* +*Fbp1* F194A	*MATa his3Δ1; leu2Δ0; met15Δ0; ura3Δ0; fbp1::KanMX4*	pRS426 *Fbp1* F194A	This work
BY4741 *Δfbp1* +*Fbp1* D131A	*MATa his3Δ1; leu2Δ0; met15Δ0; ura3Δ0; fbp1::KanMX4*	pRS426 *Fbp1*	This work
BY4741 *Δfbp1* +*Fbp1*H265A	*MATa his3Δ1; leu2Δ0; met15Δ0; ura3Δ0; fbp1::KanMX4*	pRS426 *Fbp1*	This work
BY4741 *Δfbp1* +*Fbp1*H324A	*MATa his3Δ1; leu2Δ0; met15Δ0; ura3Δ0; fbp1::KanMX4*	pRS426 *Fbp1*	This work

The FF18984 strain is highly resistant to DNA damage and genotoxic treatment, it contains deactivating knock-ins of 4 selectable markers. It was used in this work to assess long-term oxidative stress upon MMS exposure.

Table 2: Parental and transformed yeast strains with FF18984 background.

	Genotype	**Plasmid**	**Source**
Parental Strains			
FF18984 wt	*MATa his7-1; leu2-3,112; lys2-1; ura3-52*	-	Provided by Prof. Dr. R. Walmsley Manchester, UK
FF18984 *Δfbp1*	*MATa his7-1; leu2-3,112; lys2-1; ura3-52; fbp1::KanMX4*	-	Dissertation Dr. A. Kitanovic
Transformed strains			
FF18984 wt + GFP	*MATa his7-1; leu2-3,112; lys2-1; ura3-52*	pGenActGFP	This work
FF18984 wt + *Fbp1*	*MATa his7-1; leu2-3,112; lys2-1; ura3-52*	pGenAct *Fbp1*	This work
FF18984 wt+ Grx1-roGFP2	*MATa his7-1; leu2-3,112; lys2-1; ura3-52*	p415TEF cyto Grx1-roGFP2	This work
FF18984*Δfbp1*+	*MATa his7-1; leu2-3,112; lys2-1;*	pGenActGFP	This work

GFP	*ura3-52; fbp1::KanMX4*		
FF18984*Δfbp1+* *Fbp1*	*MATa his7-1; leu2-3,112; lys2-1; ura3-52; fbp1::KanMX4*	pGenAct *Fbp1*	This work
FF18984*Δfbp1+* *Fbp1-GFP*	*MATa his7-1; leu2-3,112; lys2-1; ura3-52; fbp1::KanMX4*	pGenAct *Fbp1-GFP*	This work
FF18984*Δfbp1+* Grx1-roGFP2	*MATa his7-1; leu2-3,112; lys2-1; ura3-52; fbp1::KanMX4*	p415TEF cyto Grx1-roGFP2	This work

Yeast Plasmids

The over-expression vector of wild-type Fbp1 was established using the commercially available pRS426 plasmid with *ura3* selection marker and constitutive GPD promoter. Wild type yeast Fbp1 was cloned into this over-expression vector by Dr. Ana Kitanovic as part of her PhD work.

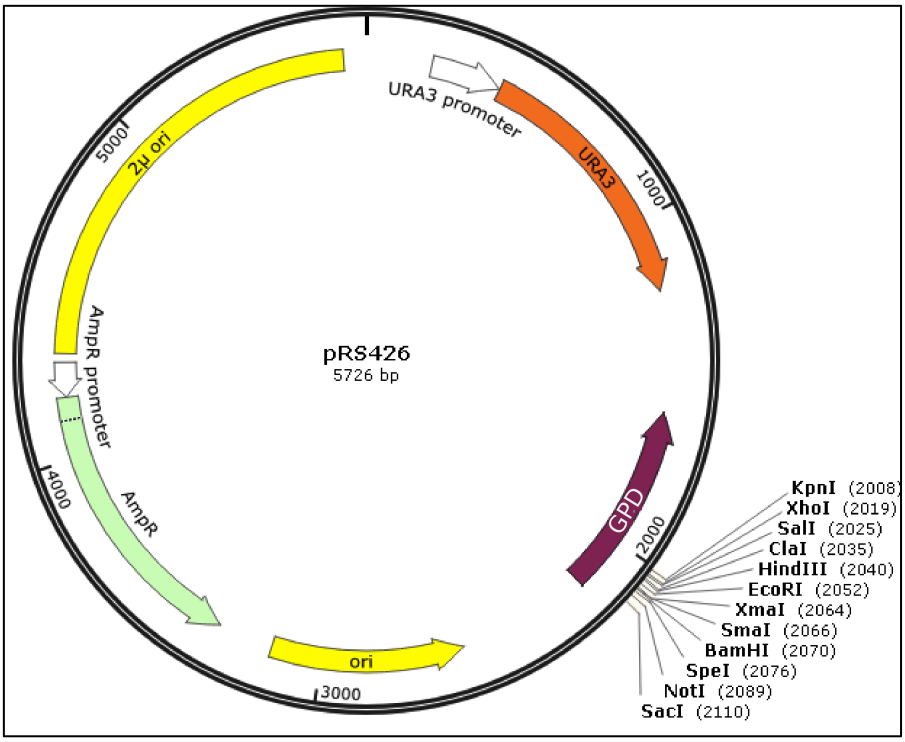

pRS426-GPD empty vector.

The plasmids containing mutated cassettes of Fbp1 were established using PCR site-directed mutagenesis. The following table includes all the yeast plasmids used in this work.

Table 3: yeast ectopic expression plasmids

Plasmid	Cloned Gene	Promoter	Selection	Source
pRS426-GPD (empty)	-	GPD	*Ura3*	Dr. T.Munder, Jena,Germany

pRS426-GPD *Fbp1* (wt)	*Fbp1*	GPD	*Ura3*	Dissertation Dr. A.Kitanovic
pRS426-GPD *Fbp1* P1A	*Fbp1* P1A	GPD	*Ura3*	Diploma thesis J. Holzwarth
pRS426-GPD *Fbp1* N75A	*Fbp1* N75A	GPD	*Ura3*	Diploma thesis J. Holzwarth
pRS426-GPD *Fbp1* D79A	*Fbp1* D79A	GPD	*Ura3*	Diploma thesis J. Holzwarth
pRS426-GPD *Fbp1* E109A	*Fbp1* E109A	GPD	*Ura3*	Diploma thesis J. Holzwarth
pRS426-GPD *Fbp1* D131A	*Fbp1* D131A	GPD	*Ura3*	Diploma thesis J. Holzwarth
pRS426-GPD *Fbp1* S133A	*Fbp1* S133A	GPD	*Ura3*	Diploma thesis J. Holzwarth
pRS426-GPD *Fbp1* F194A	*Fbp1* F194A	GPD	*Ura3*	Diploma thesis J. Holzwarth
pRS426-GPD *Fbp1*H265A	*Fbp1*H265A	GPD	*Ura3*	Diploma thesis J. Holzwarth
pRS426-GPD *Fbp1*H324A	*Fbp1*H324A	GPD	*Ura3*	Diploma thesis J. Holzwarth
pGenAct-*GFP*	*GFP*	Actin	*Ura3*	Prof. R.Walmsley, Manchester, UK
pGenAct-*Fbp1*	*Fbp1*	Actin	*Ura3*	Dissertation Dr. A. Kitanovic
pGenAct-*Fbp1-GFP*	*Fbp1-GFP*	Actin	*Ura3*	Dissertation Dr. A. Kitanovic
p415TEF cyto Grx1-roGFP2	*Grx1-roGFP2*	TEF1	*Leu2*	Dr. T. Dick DKFZ, Heidelberg

LB bacteria culture medium

Yeast extract 5g/l

NaCl 10g/l

Tryptone/peptone 10g/l

For plates: Agar 10g/l

Yeast culture media

General YPD medium

Ready YPD broth (Sigma-aldrich)

50 g for 1L.

For plates: 20 g/l agar.

Synthetic drop-out (SD) media

Yeast nitrogen base YNB without amino acids (Sigma-Aldrich®) 6.7 g/l

D-Glucose (CarlRoth®) 20 g/l

L-Lysine 100 mg/l

L-Leucin 100 mg/l

L-Histidine 100 mg/l

Uracil 20 mg/l

For plates: 20 g/l agar

Uracil or Leucin are eliminated from this formulation to yield SD-Ura or SD-Leu respectively.

Synthetic drop-out ethanol glycerol SDEG (non-fermentable) medium

Yeast nitrogen base YNB without amino acids (Sigma-Aldrich®) 6.7 g/l

Ethanol 20% *(v/v)*

Glycerol 20% *(v/v)*

L-Lysine 100 mg/l

L-Leucin 100 mg/l

L-Histidine 100 mg/l

Uracil 20 mg/l

For plates: 20 g/l agar

Uracil is eliminated from this formulation to yield SDEG-Ura.

Cell culture

Cell lines

Breast cancer cell lines representing luminal MCF-7 and basal-like MDA-MB-231 breast cancers were used.

Table 4: parental cell lines

	MCF-7 ATCC®	MDA-MB-231 ATCC®
Tissue of origin	Mammary gland	Mammary gland
Disease	adenocarcinoma	adenocarcinoma
Receptor expression/ Genotype	Estrogen receptor, E-Cadherin, Her-2	Triple-negative, EGF and TGF-α Receptors
FBP1 expression	+	-

Table 5: Full list of genetically altered cell-lines with different Fbp1 expression used in this work

	Plasmid(s)	Fbp1 Expression	Selection	Source
Parental cell lines:				
MCF-7	-	Endogenous	-	ATCC®
MDA-MB231	-	None	-	ATCC®
Stable Knock-out cell line				
MCF7-Fbp1$^{\Delta/\Delta}$	-Fbp1 double nickase -Fbp1 HDR	Silenced (Gene disruption)	Puromycin	This work
Stable Over-expressions				
MCF-7 Vector (empty)	pcDNA3.1(-)(empty)	Only endogenous	G418	This work
MCF-7 oeFBP1	pcDNA3.1(-)*Fbp1*	Endogenous& Over-expression	G418	This work
MCF-7 oeFBP1 N65A	pcDNA3.1(-)*Fbp1* N65A	Endogenous& oeFBP1 N65A	G418	This work
MCF-7 oeFBP1 P6A	pcDNA3.1(-)*Fbp1* P6A	Endogenous& FBP1 P6A	G418	This work
MCF7 Fbp1$^{\Delta/\Delta}$ oe yeastFBP1	pcDNA3.1(-)*Fbp1* yeastFBP1	Endogenous& yeastFBP1	G418	This work
MCF7-Fbp1$^{\Delta/\Delta}$ Vector (empty)	pcDNA3.1(-)(empty)	none		
MCF7-Fbp1$^{\Delta/\Delta}$ oeFBP1	pcDNA3.1(-)*Fbp1*	Over-expression	G418	This work
MCF7-Fbp1$^{\Delta/\Delta}$ oeFBP1 N65A	pcDNA3.1(-)*Fbp1* N65A	FBP1 N65A	G418	This work
MCF-7 Fbp1$^{\Delta/\Delta}$ oeFBP1 P6A	pcDNA3.1(-)*Fbp1* P6A	FBP1 P6A	G418	This work
MCF7 Fbp1$^{\Delta/\Delta}$ oe yeastFBP1	pcDNA3.1(-)*Fbp1* yeastFBP1	yeastFBP1	G418	This work
MDA-MB231 Vector (empty)	pcDNA3.1(-)(empty)	none	G418	This work
MDA-MB231 oeFbp1	pcDNA3.1(-)*Fbp1*	Over-expression	G418	This work
MDA-MB231 oeFbp1N65A	pcDNA3.1(-)*Fbp1* N65A	FBP1 N65A	G418	This work
MDA-MB231 oeFBP1 P6A	pcDNA3.1(-)*Fbp1* P6A	FBP1 P6A	G418	This work
MDA-MB231 oe yeastFBP1	pcDNA3.1(-)*Fbp1* yeastFBP1	yeastFBP1	G418	This work
MDA-MB231 oe yeastFBP1	pcDNA3.1(-)*Fbp1* yeastFBP1 P1A	yeastFBP1 P1A	G418	This work

To establish the over-expression of human and yeast Fbp1 in cancer cell lines, new vectors had to be constructed, desired mutations were then introduced into the vectors containing human or yeast Fbp1 using PCR site-directed mutagenesis. The

commercially available pcDNA3.1(-) vector with the mammalian-constitutive CMV promoter and Geneticin (G418) selectable marker was used to construct the required plasmids for Fbp1 expression in human cancer cells.

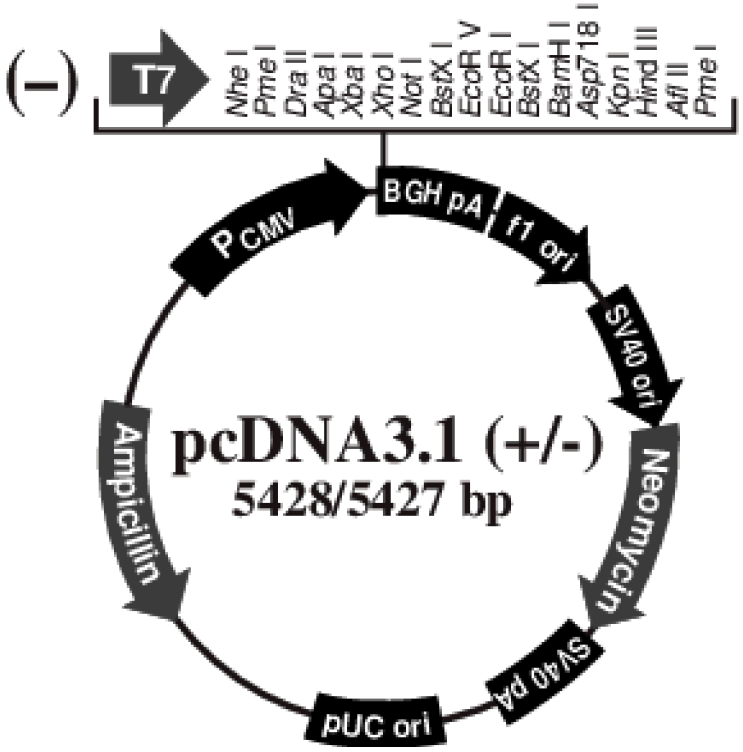

Table 6: List of the mammalian plasmids used in this work to ectopically express different forms of Fbp1 into cancer cell lines:

Plasmid	Cloned Gene	Promoter	Selection	Source
pcDNA3.1(-)	-	CMV	G418	This work
pcDNA3.1(-) *Fbp1*	*Fbp1*	CMV	G418	This work
pcDNA3.1(-) *Fbp1* P6A	*Fbp1* P6A	CMV	G418	This work
pcDNA3.1(-) *Fbp1* N65A	*Fbp1* N65A	CMV	G418	This work
pcDNA3.1(-) yeast *Fbp1*	yeast *Fbp1*	CMV	G418	This work
pcDNA3.1(-) yeast*Fbp1* P1A	Yeast *Fbp1* P1A	CMV	G418	This work

The stable knock-out of *fbp1* in MCF-7 was established using a combination of fbp1-specific CRISPR Cas-9 double-nickase and homology directed repair HDR plasmids. The plasmid pair was purchased from SantaCruz Biotechnology® catalog number: sc420299-NIC

Table 7: Human CRISPR-Cas9 deletion constructs:

Plasmid	Expressed Gene	Promoter	Selection	Source
FBPase double-nickase	Cas-9 (D10A) GFP	U6	-	SCBT®
FBPase HDR	Puromycin RFP	EF-1a	Puromycin	SCBT®

The pairs of cloning primers used for cloning Fbp1 into pcDNA3.1(-):

Human *Fbp1*:

Forward: `tttttgaattcATGGCTGACCAGGCGCC`

Reverse: `tttttaagctttcactgggcagagtgcttctc`

Yeast *Fbp1*:

Forward: tttttctcgagatgccaactctagtaaatg

Reverse: tttttaagcttctactgtgacttgccaat

Yeast *Fbp1 P1A:*

Forward: `tttttctcgagATGGCAACTCTAGTAAATGGACC`

Reverse: `TTTTTAAGCTTctactgtgacttgccaatatgg`

The expression plasmids of the mutated forms of human Fbp1 were constructed by mutagenizing the pre-cloned pcDNA3.1(-)*Fbp1* using the following site-directed mutagenesis primer pairs:

Fbp1 P6A:

Forward: `gctgaccaggcggccttcgacacggac`

Reverse: `gtccgtgtcgaaggccgcctggtcagc`

Fbp1 N65A:

Forward: `cattgctggttctaccgccgtgacaggtgatcaag`

Reverse: `cttgatcacctgtcacggcggtagaaccagcaatg`

Table 8: Real-time quantitative PCR primers

Gene	Primers
Human *fbp1*	**For:** GCCCCAATGGAAAGCTGAGA **Rev:** GTCTAACACGGCCTCCTTCC GAGCCCCAATGGAAAGCTGA **Rev:** ATGACGTCTAACACGGCCTC
Yeast *fbp1*	**For:** CAAGCCTTTCTCGGCTAGGT **Rev:** AGTTTTCCGTTGGGGCTCTT

CENPE	**For:** AAATTTAAAGGCGGGGCGG **Rev:** TGGGCAGTTTCTCCAAGTGA
UCH-L1	**For:** GGAAGGCCAATGTCGGGTAG **Rev:** GCAGGGTGTCCTCTGAACTG
TGFβ-R3	**For:** GTCGGCCTGATGGGGGTA **Rev:** GAATCGCGCAGGGAAAGTG
e-cadherin	**For:** CAGTTCAGACTCCAGCCCG **Rev**: CTGGCAGAGCCAAGAGGAG
TRIM-28	**For:** GGATGTACCAGGGGAGGAGT **Rev:** TACACGCTCACATTTCCGCT
MAGE-A3/6	**For:** TCGGTGAGGAGGCAAGGTTC **Rev:** CAGTGCTGACTCCTCTGCTC
MAGE-C2	**For:** ACGGCCATCTTGGGAATCTG **Rev:** TATGGTGGGAGGTCCCTCAG
Glutaminase	**For:** CTTTCCCCAAGGACAGGTGG **Rev:** CGGTTTGATTTTCCTTCCCGT
HIST2H2AC	**For:** GGCTCGGGACAACAAGAAGA **Rev:** AGAACGGCCTGGATGTTAGG
FAM38	**For:** TTCCAGACCGTCAAGCACAA **Rev:** GAGCACACAAACGAACACCC
AURKA	**For:** GGAAGACTTGGGTCCTTGGG **Rev:** GAACCGACAGGGGACTTGAC
β-Actin	**For:**CATTCCAAATATGAGATGCGTTCG **Rev**: GCTATCACCTCCCCTGTGTG
Vinculin	**For:** CAGTCAGACCCTTACTCAGTG **Rev:** CAGCCTCATCGAAGGTAAGGA
RPL-30	**For:** GGTGTCCATCACTACAGTGG **Rev:** GTCAGAGTCACCTGGATCAATG

Cell culture consumables

- **Cell culture media:**

  As a standard medium, **full Dulbecco modified Eagle medium DMEM** (Gibco®, Thermo Fisher Scientific) was used with **10% *(v/v)* FCS** (Gibco®, Thermo Fisher Scientific) in addition to penicillin streptomycin (final concentration= 50U/ml) (Gibco®, ThermoFischer Scientific).

- **Cell culture well plates:**

  CELLSTAR® 6 well cell culture plate (Greiner Bio-one, Kremsmünster)
  CELLSTAR® 12 well cell culture plate (Greiner Bio-one, Kremsmünster)
  CELLSTAR® 96 well cell culture plate (Greiner Bio-one, Kremsmünster)

- **Cell culture flasks:**

  Cellstar® T25 and T75 cell culture flasks with filter caps. (Greiner Bio-one, Kremsmünster)

Reagents and buffers:

- DNA gel electrophoresis:

- **Agarose gel:**

  1% *(w/v)* agarose, 1:10000 ethidium bromide (Stock solution: 1mg/ml), complete volume to 100 ml TAE or TBE buffer.

- **TAE Buffer (1X):**

  40 mM Tris (pH 7.6) 20 mM acetic acid 1 mM EDTA
- **TBE Buffer:**

  89 mM Tris (pH 7.6) 89 mM boric acid, 2 mM EDTA
- **DNA loading dye:**

  6X Loading Dye Solution (Fermentas® LifeSciences, Thermo Fisher Scientific) (10 mM Tris-HCl (pH 7.6), 0.03% bromophenol blue, 0.03 % xylene cyanol FF, 60 % glycerol and 60 mM EDTA.)
- **Protein marker:**

  Lambda DNA/PstI Marker, 24 (Fermentas® LifeSciences, Thermo Fisher Scientific)

- Western-blot

- **Polyacrylamide gels for SDS-PAGE:**

	15mL of 12% resolving gel	**5mL of 5% stacking gel**
H_2O	5.9	3.4
30 % acrylamide mix	5	0.83
1.5 M Tris-HCl pH8.8	3.8	-
1.0 M Tris-HCl pH6.8	-	0.63
10 % ammonium persulfate	0.15	0.05
TEMED	0.006	0.005

- **Anode buffer:**
- 25 mMTris;40 mM6-amino-n-capronic acid;10 % methanol; pH 9.4
- **Cathode Buffer:**
- 25 mMTris; 40 mM6--amino-capronic acid; 10% methanol; pH 9.4
- **TBS-Tween:**

  8.0 g/L NaCl; 0.2 g/L KCl; 3.0 g/L Tris;pH 7.4; 0.1% Tween.
- **Protein Loading dye:**

  PLB-10 mM Tris-HCl; 20% glycerol; 200 mM β-mercaptoethanol and 0.2%(v/v) Bromphenol-blue
- **SDS-PAGE running buffer:**

  250 mM glycin and 25 mM Tris -HCl.

II-III Methods

Molecular cloning and construction of plasmids

To ectopically express Fbp1 (with its different homologues and mutations) in cell lines, new plasmids had to be constructed with Fbp1 variants expressed under a mammalian promoter. For this purpose I started with the commercially available pcDNA3.1(-) vector (see material section).

A restriction cloning strategy was followed with restriction sites introduced on 5`end of each primer so that to flank the resulting Fbp1 PCR product. The restriction sites were chosen as to avoid cutting the insert and to have matching sites in the multiple cloning region of the pcDNA3.1 vector.

The following steps were implemented to construct the plasmids:

- PCR amplification of the product human or yeast Fbp1 (Using Phusion polymerase, NEB®).
- Column purification of the PCR product (
- Overnight restriction digest of the purified PCR product and the plasmid using matching restriction enzymes at 37° followed by a 20 min inactivation step at 80°.
- Gel purification of the digested vector and PCR product (insert) ().
- Overnight ligation of the vector and insert at molar ration of 1:3 (vector::insert) (T4 DNA ligase, NEB®).
- Transformation of the resulting ligation product into *E.coli*.
- Following transformation and selection, Mini-preps were made of picked colonies and these were sent for sequencing (Eurofins Genomics, Ebersberg).

PCR site-directed mutagenesis

To prepare the expression vectors of mutated human Fbp1 a site-directed PCR mutagenesis approach was harnessed using the Q5® Site-directed mutagenesis kit from NEB. The method depends upon the amplification of the entire plasmid using primers harbouring the desired single or double mismatch mutation, once amplified the mutation becomes integral to the Fbp1 cassette in the resulting amplified vector. The template is then degraded based on its unique DNA methylation pattern (the template is a plasmid prepared in bacteria, and therefore has a unique *E.coli*-associated methylation pattern compared to the unmodified PCR product) using the methylate-DNA specific DNPI restriction enzyme. Simultaneously, the yielded PCR

product is phosphorylated and ligated by enzymes that exist in the same mixture as DnpI.

A following over-view of the site-directed mutagenesis protocol provided with the utilized Q5® Site-Directed Mutagenesis NEB® kit:

- Mutagenesis Primers with the desired point mutations were designed using the NEBase Changer online tool from NEB®.
- PCR Amplification of the plasmid using Q5 polymerase (following the protocol provided with the kit).
- Digestion of the template plasmid, phosphorylation and ligation of the mutated product DNA using the KLD (kinase, ligase and DpnI treatment (5 minute incubation at room temperature) enzyme mix and buffer.
- Transformation of *E.coli* with the resulting mutated plasmid.

Preparation of chemically competent DH5α™ *E.coli* cells (Thermo Fischer Scientific)

- Bacteria were cultured in 2 ml LB over-night at 37°c.
- 1 ml of the over-night culture were then diluted up to 150 ml of LB medium, the culture was subsequently grown up to an $O.D_{600}$=0.6 (about 2.5-3 horus).
- Subsequently the cultured bacteria were pelleted and re-suspended in 15 ml TSB buffer (1*LB, 5% DMSO, 10 mM $MgCl_2$, $MgSO_4$, 10 mM PEG 4000).
- The TBS bacterial suspension was kept on ice for 10 minutes.
- The suspension was divided into individual 100 µl aliquots that were kept on dry ice and subsequently preserved at -80°c.

Transformation of chemically competent *E.coli*

- The following transformation mixture is prepared in an Eppendorf tube for each transformation in addition to one mock reaction (treated exactly similarly to the transformation, but excluding the plasmid DNA):
    - 20 µl KCM buffer (0.5 M KCl, 0.15 M $CaCl_2$ and 0.25 M $MgCl_2$).
    - 1 ng of a previously prepared plasmid DNA, or 10 µl (25 ng) of a ligation mixture for newly constructed plasmids.
    - Fill up to 100 µl with sterile water.
- An aliquot of chemically competent *E.Coli* was thawed on ice, and added onto the above mentioned transformation mixture.

- The resulting suspension of bacteria in the transformation mixture was incubated for 40 minutes on ice.
- Competent cells were then heat-shocked for precisely 45°at 42°c in a preheated water bath.
- The heat-shock was terminated by promptly placing the cells on ice.
- Subsequently cells were pelleted and plated on LB-agar containing 100 μg/ml Ampicillin.
- After over-night incubation, growing colonies were inoculated in 3 ml liquid LB with Ampicillin.
- On the following day, the resulting liquid colonies were harnessed to make mini plasmid preparations.
- In the case of newly cloned plasmids, samples were sent for sequencing to confirm that the correct construct had been obtained.

Transformation of *S.cerevisiae* using the lithium acetate method

Chemical genetic transformation of yeast was used to introduce expression vectors containing the wild-type and various mutated forms of Fbp1 and thus have them ectopically expressed under constitutive GPD or Actin promoter. For this I used the following modified protocol from the lithium acetate methods first introduced by Gietz and Woods (1995)[77].

I) Preparation of chemically competent yeast

- A single colony is inoculated in 3 ml general YPD medium and incubated for 24 h at 30°.
- 4 μl of the above mentioned pre-culture were inoculated in 50 ml YPD and incubated for 16 h (≈10 generations).
- Over-night culture was pelleted at 1000 xg for 5 minutes in 50 ml falcon tube.
- Cells were washed in 20 ml sterile water, pelleted and re-suspended in 1 ml sterile water, transferred into an Eppendorf tube and pelleted again.
- The cell pellet was re-suspended in a 0.1 M lithium acetate solution (500 μl for each 100 μl pellet).
- To reach chemical competency, cells were incubated in the lithium acetate suspension for 20 minutes at 30°c.

II) Transformation

- For each transformation and one additional mock (treated precisely like the transformations, but lacking plasmid DNA): denature 5 µl of the carrier DNA (Herring sperm DNA, Sigma-Aldrich®) by boiling for 10 minutes in a heating block and then moving the tubes promptly onto ice.
- For each transformation: 0.5 to 1 µg of plasmid DNA were taken and mixed with the carrier DNA.
- 100 µl of competent cells (prepared in one liter) were added to the carrier & plasmid DNA mixture followed by 20 min incubation at 30°c.
- 600 µl of LiAc (0.1 M) and PEG4000 (40 %) mixture were added to the cells. After mixing very well the suspension was incubated for 20 minutes at 30°c.
- 71 µl of sterile DMSO were added to each transformation (final concentration 10 %).
- Cell suspensions were heat-shocked for 15 minutes at 42°c (in an accurately preheated water bath).
- Following 15 minutes the heat-shock was terminated by promptly placing the cell suspensions on ice.
- After aspirating the supernatant, cells were resuspended in 800 µl YPD medium and moved into culture tubes containing 800 µl of YPD (final culture volume 1.6 ml).
- Cells were shaken for 3 h at 30°c.
- After being pelleted and washed once in sterile PBS, cells were pelleted again, re-suspended in 50 µl SD-Ura and plated on SD-Ura agar plates.
- Following 2 to 3 days of incubation, transformation plates were inspected for emerging colonies. Colonies were then picked and spread on new agar plates and successful transformation was phenotypically confirmed.

Transfection of cell lines and establishing stable over-expressions and deletions

I resorted to lipid-based transfection using Lipofectamin™3000 (Thermo Fisher®, Waltham MA) for introducing the desired expression vectors into cancer cell lines. The transfections were performed using the protocols provided with the transfection reagents. The following steps were adhered to:

- After trypsinisation cells were counted and seeded in a 6 well-plate at a density of 300.000-500.000 cells per well.
- Following 24 to 48 hours incubation and after reaching a confluency of 70% to 90%, cells were transfected.
- The transfection mixture was prepared by adding pre-mixed 2.5 μg plasmid DNA with 5 μl p3000 reagent in 125 μl Opti-MEM to pre-mixed 7.5 μl in 125 μl Opti-MEM, for each transformation
- The trnasfection mixtures were mixed by inverting the containing tubes and then incubated for 15 minutes at room temperature.
- 250 μl transfection mixture were pipetted onto each well, slowly and drop-wise.
- The 6 well-plates containing the newly transfected cells were subsequently shaken gently.
- Following 24 hours of incubation, medium was replaced and cells were further incubated for 24 more hours.

I) Establishing cell lineages with stable over-expression

- After giving cells 24 hours of recovery from the transfection, cells were treated with medium containing G418 sulphate (900 μg/ml for MCF-7, 1200 μg/ml for MDA-MB231).
- Medium with antibiotic was replaced once every 3 to 4 days.
- Following 3 to 4 weeks of selection in 6 well plate format (control non-transfected cells completely wiped out), transfected cells were trypsinised and transferred into a T25 cell culture flask.
- The G418 selection pressure was maintained as part of the cell culture medium in which the transfected cells were cultivated.
- Over-expression of Fbp1 was then verified on the mRNA and protein levels, using qPCR and immunoblotting, respectively.
-

II) Establishing the stable CRISPR-Cas9 deletion of Fbp1 in MCF-7

- To achieve the knock-out of fbp1 in MCF-7, cells were double transfected with a CRISPR-Cas9 Double Nickase (Cas9 D10A mutant) plasmid containing two gRNAs directed to the opposite strands of the fbp1 gene and a homology-

directed repair plasmid containing the selectable Puromycin resistance marker flanked with sequences matching the disruption site indicated by the gRNAs.

- 24 hours post-transfection, medium was replaced and cells were given 48 hours for recovery and developing Puromycin resistance.
- Subsequently cells were selected using 200 ng/ml Puromycin with medium containing the same concentration of Puromycin changed every 3 to 4 days.
- 6 weeks following transfection, cells were trypsinised and transferred into a T25 cell culture flask, and Puromycin was withdrawn from the culture medium.
- The successful deletion was verified on mRNA and Protein levels, and the resulting deletion cell lineage was continuously monitored to ensure the stability and irreversibility of the Fbp1 deletion.

Yeast spot assays (drop-tests)

i) Growth on non-fermentable carbon sources, drop test on SDEG medium

Starting from Mid-Log phase cultures, cell suspensions with the following dilution factors were prepared via serial dilution (1:10).

1:1; 1:10; 1:100; 1:1000; 1:10000; 1:100000.

Subsequently, 4 µl of each cell suspension of the examined yeast strains were adjacently dropped onto SDEG-agar. Agar plates were incubated for 48 h at 30 °C and then imaged to assess the growth of the strains over-expressing either wild type or mutant versions of Fbp1p.

ii) Sensitivity to MMS treatment

Starting from over-night cultures, cell-suspensions OD was adjusted to 10, and these suspensions were serially diluted (1:5) to yield suspensions with the following OD_{600} (10; 2; 0.4; 0.08; 0.0016; 0.00032). 4 µl of each suspension was then spotted onto freshly prepared SD-Ura plates containing varying concentrations of MMS (0.01% to 0.0175%).

The plates with 0.01% MMS, and those with 0.015% or 0.0175% MMS were incubated at 30 °C for 48 h and 72 h, respectively.

iii) Drop-test Image-Quantification

Spot-intensities from drop-tests were quantified using ImageJ, spot intensities from MMS plates were then normalized to those of the non-treated control, and values from mutants were normalized against the strain with wt Fbp1.

Continuous measurement of yeast growth in liquid medium

Over-night cultures were first diluted to an OD_{600} of 0.2, and shaken for 3 hours. Subsequently cultures were transferred into 96 round-bottom well-plates, 200 µl per well. Of each used cell type, three wells were treated with 0.02% MMS, and three wells with 0.01% MMS while four wells were kept untreated.

The 96 well plates were then incubated at 30°c inside the microplate reader (Tecan-Ultra). OD_{600} of each well was measured every hour for 32 h, 15 min of shaking within the plate reader preceded each measurement.

Protein extraction

Depending on the application, protein extracts were either prepared in native or denaturing conditions. Enzymatic activity measurements require intact protein folding, and thus necessitate protein extraction in non-denaturing conditions. While SDS-Page and immunoblotting are performed on denatured protein extracts.

Denaturing protein extraction

To extract total proteins from cells, $3*10^5$ to $5*10^5$ cells were seeded, following 24 to 48 hours of incubation cells were subjected to the desired treatment or medium conditions and then lysed in 6 M urea buffer containing the following protease inhibitors: (NaF, PMSF, Pepstatin, Aprotenine and $NaVO_4$). To lyse the cells, medium was aspirated, and 120 to 180 μl ice-cold 6 M Urea buffer were pipetted directly onto the cells. Subsequently, the cell culture plates were promptly placed on ice and then vortexed to ensure full homogenization in the Urea buffer. Afterwards, lysates were collected in Eppendorf tubes and then spun down at 13000 g for 15 minutes to get rid of the DNA. Lysates were subsequently stored at -20°C.

Native (non-denaturing) protein extraction

To preserve proteins folding and function, cells were mechanically lysed in mild non-denaturing conditions. Since the mechanical disruption of cells in a bead-mill set remains less efficient in completely breaking down cells and extracting their individual proteins, higher cell numbers were used to harness sufficient non-denatured protein for the enzymatic activity assays.

For this a one to 1.one and a half million cells were cultivated in cell-culture standard size Petri dishes and incubated with full DMEM (with G418 for cells harbouring plasmids) for 24 to 48 hours. Subsequently, cells were trypsinised, pelleted and lysed using the bead-mill according to the following protocol:

- Pellets were resuspended in 1ml ice-cold PBS and transferred into Eppendorf tubes, centrifuged again and resuspended in 1 ml fresh ice-cold PBS.
- 1 g of acid-washed glass-beads (Sigma-Aldrich) was added to the cell suspension.
- Cells were then homogenised by shaking at a frequency of 30 Hertz using the bead-mill.
- To avoid over-heating of the suspension due to rapid mixing and the resulting protein denaturation, homogenisation was performed in shaking/cooling rounds as follows:
- 5 minutes shaking followed by 5 minutes on ice, repeated 3 times and followed by a last homogenisation round of continuous 10 minutes.
- Finally the suspensions of beads and lysed cells were spun down at 16000*g for 15 minutes at 4°c and clear lysates were aspirated, moved into fresh Eppendorf tubes and stored at -20°c or immediately used for the enzymatic activity measurements.
-

Yeast nuclear/cytoplasmic protein extraction

Cells from over-night culture in SD-Ura medium were pelleted at 1000x *g*. Afterwards pellets were re-suspended in 1 ml 0,8 M NaCl containing 0,2 mg Zymolase and incubated for 30 min at room temperature. The resulting spheroplasts were then spun down and re-suspended in 1 ml 10 mM Tris containing protease inhibitors. Subsequently ca. 100 µl glass beads were added and spheroplasted cells were crushed using the bead mill homogeniser MM300 (Retsch) at full speed for 10 min followed by 10 min on ice. This homogenization/cooling cycle was repeated three times and lysates were obtained. Nuclei were isolated from the rest of the lysates using differential centrifugation at 1000 x *g* for 5 min. The supernatant containing the cytosolic fraction of the lysate was isolated and stored at -20°C, and the yielded pellet with the nuclear fraction was resuspended in 0.5 ml 10 mM Tris then centrifuged at 300 x g to remove the cell debris. The remaining supernatant after this step contains

the floating nuclei and was isolated and stored at -20°C. Both nuclear and cytosolic fractions were analyzed using SDS-Page followed by western blotting to investigate the presence of the various mutated forms of Fbp1p in transformed strains containing their respective overexpression vectors.

Determining total protein concentrations

Total protein concentrations in the lysates were determined using Bradford reaction. 10 µl of each lysates were mixed with 990 µl of Bradford reagent (Sigma-Aldrich) in Eppendorf tubes. Samples were then mixed and incubated for 5 minutes in the dark. Subsequently 3x300 µl of each sample were transferred into 96 well-plates and measured using the Tecan Ultra (Tecan, Germany) reader at 595 nm.

SDS-PAGE and immunoblotting

Proteins in denatured lysates were resolved on 10% polyacrylamide gel (SDS-PAGE) as described in (Laemmli, 1970)[78]. Afterwards, resolved proteins were blotted (transferred) from the resolving SDS-PAGE gel onto a PVDF membrane. Semi-dry protein transfer was used with anode and cathode buffer prepared as detailed in the above material section.

Subsequently, membranes were stained with ponceau S (5% ponceau S) and then washed in TBS-tween 1% *(v/v)* buffer and blocked in a 5% BSA solution in TBS-tween buffer for 1 hour, and then incubated with 1:1000 solution of one of the used primary antibodies. After the primary anti-body incubation, membranes were washed 3 times for 5 minutes each in TBS-tween 1 buffer and subsequently incubated in 1:5000 HRP-fused anti rabbit or anti mouse secondary (IgG) anti-body solutions for 1 hour. Finally, membranes were washed 3 x 5 minutes and developed in Western Lightning Plus-ECL (Perkin-Elmer, Germany). Signals were detected using the Fujifilm LAS-3000 imaging system and the AIDA software for image acquisition.

Quantification of western-blot signals

the intensities of the western-blot bands of target proteins were quantified using the Image-J histogram quantification tool. The intensity of the target protein signals was adjusted relative to the corresponding loading-control (beta-actin) bands.

Assessment of enzymatic activity in crude native protein extracts

i) FBPase activity

Total fructose 1,6 bis-phosphatase activity was measured using cytosolic protein extracts of over-night cultures of yeast cells as described by Skalecki et al. [79] The general principle of the assay depends on coupling FBPase catalysis to the formation of NADPH through the phospho-glucose isomerase PGI and glucose-6-phosphate dehydrogenase G6PD present in the reaction mix. Dephosphorylation of fructose 1,6 bis-phosphate by Fbp1 yields Fructose 6 phosphate, which is then converted to glucose 6 phsophate by PGI. G6P is then oxidized by G6PDH with $NADP^+$ getting reduced to NADPH.

Thus the ratio of the yielded F6P molecules and the NADPH is 1:1.

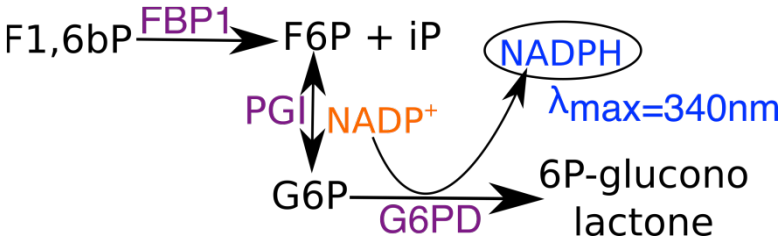

In practice, this measurement was performed in a 96 well plate format as follows:

3 x 10 µl of each native lysate to be tested were pipetted into 3 separate wells. Subsequently, the following components were mixed to constitute the full reaction mix:

Reaction buffer: 75 µl

PGI (5 U/µl): 0.15 µl (0.75U/reaction).

G6PD: (0.7 U/µl): 1 µl (0.70U/reaction).

$NADP^+$ (5 mM): 15 µl (final conc.= 0.5 mM)

Fructose1,6 bis-phosphasate (17mM): 1.5 mM (final conc.= 0.17 mM)

After thoroughly mixing the abovementioned components for the required number of reactions, 140 µl of the resulting reaction mixture were pipetted on each well containing the pre-pipetted protein lysates. Plates were then shaken for 2 minutes and then the kinetic measurement of absorption of the yielded NADPH (λ_{max}=340nm) was started. The FBPase activity was derived from the slope of the linear part of the increase in NADPH absorption over time, which reflected the reaction rates. The enzymatic activity was then calculated in mU/mg (total protein) using the following equation:

$$FBPase(mU/mg) = \frac{\left(OD_{340}^{t2}[mU] - OD_{340}^{t1}[mU]\right) * 161}{(t2 - t1) * \mathrm{Pr}otein(mg)}$$

ii) G6PD activity

The assessment of G6PD activity in crude native lysates depended on measuring the UV-absorption of the NADPH directly yielded by the reaction. The activity was measured in the presence of an excess amount of the substrate glucose-6-phosphate, hence rendering the reaction rate a function of the availability of the enzyme only. G6PD oxidizes glucose-6phosphate with $NADP^+$ as a cofactor yielding 6-phospho-glucono-lactone and reduced NADPH with a maximal absorption at λ_{max}=340nm.

This measurement was performed in a 96 well plate format as follows:

3x10 μl of each non-denatured lysated proteins to be tested were pipetted in 3 separate wells.

Subsequently, the following components were mixed to constitute the full reaction mix:

Reaction buffer: 50 mM Tris-HCl buffer (pH=8.2), 100 mM KCl, 5 mM $MgSO_4$.

Glucose-6-phosphate G6P: working concentration 50 μM

$NADP^+$: working concentration: 0.8 mM

After thoroughly mixing the abovementioned components for the required number of reactions, 140 μl of the resulting reaction mixture were pipetted on each well containing the pre-pipetted protein lysates. Plates were then shaken for 2 minutes and then the kinetic measurement of absorption of the yielded NADPH (λ_{max}=340nm) was started. The relative G6PD activity was derived from the slope of the linear part of the increase in NADPH absorption over time, which reflected the reaction rates.

FACS analysis

i) Yeast

Overnight liquid cultures were diluted to an OD_{600} of 0.1-0.2, and then grown into the log-phase (OD_{600} ≈0.4-0.6). Afterwards, cell suspensions were transferred into 96 round-bottom well plates. Cells were treated in the well plates in triplets and by following the intended duration of the treatment.

To quantify dead-cell fractions, propedium iodide was added to the medium (final

concentration 3 μg/ml). Following 5 minutes incubation in the dark, plates were shaken for 2 minutes and then acquired using the FACS Guava with an auto-sampler. The percentage of dead cells was then determined by quantifying the PI-positive cells.

ii) Cell culture

Fluorescence activated cell sorting FACS analysis was used to measure a variety of metabolic and viability markers in the cells. Cells were seeded in 12 well plates at a density of 50,000 cells/well in 1 ml full DMEM/well and incubated over-night. On the following day medium was aspirated, and cells were treated as indicated for each experiment). Following treatment, cells were incubated with the fluorescent probes (details and conditions for each fluorescent probe are listed below) then analysed using FACS Guava (Merck-Millipore, UK). All FACS acquisitions were automated and performed in a 96 well-plate setting.

Measuring glucose uptake using fluorescently labelled 2-Deoxy-Glucose 2-NBDG

Akin to 2-deoxyglucose, 2-NBDG is taken up by cells and phosphorylated. The resulting 6-Phopsho-2-NBDG is sequestered in the cytosole and cannot undergo further glycolytic steps. Therefore, it accumulates in the cells and is used in low concentrations as an indicator of intracellular glucose uptake [80].

Fluorescently labelled 2-deoxyglucose 2-NBDG was added to the cell culture medium at a concentration of 50 μM so that cells were treated with both indicated agents and the labelled 2-DG simultaneously. After 3 hours cells were washed once with PBS, trypsinized, pelleted (200x g, 3 minutes) and re-suspended in DMEM without phenol red (colourless), round-bottom 96 well plate and analysed. The 2-NBDG green fluorescence was then quantified (mean-value of the sample population) and plotted.

Assessing ROS levels using dehydroethidium DHE

Dehydroethedium DHE, is a RedOx probe that interacts to reactive oxygen species, including superoxide, forming fluorescence ethedium and other derivatives thereof that chelate the DNA and hence generate a stable red

fluorescence signal proportional to the amount of intracellular ROS [81].

Following the intended duration of treatment, cells were washed once with PBS, trypsinised, pelleted (200x g, 3 minutes) and re-suspended in full DMEM with 30 μg/ml dehydroethidium DHE (Biomol, Germany) and incubated for 15 minutes. Subsequently cells were pelleted again, and resuspended in DMEM without phenol red (colourless), transferred into round-bottom 96 well plate and analysed. The DHE red fluorescence was then quantified (mean-value of the sample population) and plotted.

Assessing mitochondrial mass using MitoTracker® Green

MitoTracker® Green To compare assess the variations in mitochondrial mass between cells with different Fbp1-expression status. MitoTracker Green is a fluorescent dye that localises to the mitochondria independent of mitochondrial inner-membrane potential, making it suitable for assessing mitochondrial mass independent of mitochondrial function. For measuring mitochondrial mass, treated cells were washed once with PBS, trypsinized, pelleted (200x g, 3 minutes) and re-suspended in DMEM without FCS with MitoTracker Green (2nM) (Thermo-Fischer Scientific, Weltham, MA) and incubated for 30 minutes. Subsequently cells were pelleted again, and resuspended in DMEM without phenol red (colourless), transferred into round-bottom 96 a well plate and analysed. The mean values of green fluorescence of each population were calculated as an indicator of the mitochondrial mass was.

Determining mitochondrial inner-membrane potential using JC-1

JC-1 is a cyanine dye suitable for the fluorescent assessment of mitochondrial function by measuring the mitochondrial inner membrane potential. Healthy and active mitochondria maintain high levels of inner-membrane potential as a result of an active respiratory chain. The JC-1 dye concentrates on the inner-side of the polarised mitochondrial membranes undergoing a fluorescent shift from green (free monomeric dye) to red (aggregated JC-1). Therefore, the ration of red/green fluorescence signals of JC-1 dye enables the assessment of the mitochondrial membrane polarisation and function[82].

For measuring mitochondrial membrane potential with JC-1, treated cells were washed once with PBS, trypsinized, pelleted (200x g, 3 minutes) and re-

suspended in full DMEM with 2μM JC-1 (Biomol, Germany) and incubated for 15 minutes. Subsequently cells were pelleted again, and resuspended in DMEM without phenol red (colourless), transferred into round-bottom 96 a well plate and analysed. The mean values of red and green fluorescence of each population were calculated and the mitochondrial inner membrane potential was then quantified as a ratio of mitochondrial aggregated to free (cytosolic) JC-1 red/green fluorescence.

SRB Survival and growth assays

The total-protein based SRB colourimetric assay was used to assess cell survival and growth upon genetic alterations, small molecule treatments and medium conditions alterations. SRB sulforhodamin-B, is a water-soluble dye that stoichiometrically binds to proteins in weak acidic conditions. In alkaline conditions, this SRB-protein bond is destabilized and the dye is released and dissolved into the solution allowing colourimetric determination of the amounts of bound SRB, and thus the correlating amount of total proteins reflecting cell density. These properties are exploited in the SRB growth/survival assay, in which viable adherent cells are first fixed onto the cell-culture modified surface and then measured using the following protocol derived from Vichai and Kirtikara 2006 [83].

Cells were cultivated in 96 well plates at a density of 5000 or 10000 cells/well with 150 μl medium per well, unless otherwise indicated. In case of small-molecule treatments, cells were incubated for 24 hours following seeding and then treated with a 1:1 serial dilution using the VIAFLO ASSIST automated system (Integra Biosciences, Biebertal, Germany). Treatments were performed in triplets or quadruplets. Co-treatments were performed at a constant concentration combined with the ascorbate gradient. At the indicated time intervals, cells were fixed by adding half a volume (75 μl) of pre-chilled 10% tricholroacetic acid TCA and incubating at +4° for 1 hour at least. Subsequently, the plates were washed with deionised water three times and then dried for 20 min at 60°c. Afterwards, 75 μl of SRB and 1% acetic acid solution was added into each well and incubated for 30 minutes in the dark. Subsequently, all wells were washed twice with 1% acetic acid solution and plates were then dried for 20 min at 60°c. Finally, 150μl of 10 mM Tris (pH=10.5) were added and plates were shaken at 450 rpm for 5 minutes to dissolve the SRB

dye. The absorption of SRB was measured at 535 nm using the Tecan-Ultra microplate reader. Optical-density reads were then normalized to the non-treated and the resulting survival curves were plotted using GraphPad Prism.

LC-MS Metabolic flux analysis of MCF-7 cells:

Cells were seeded in 6 well-plates at 300.000 cells/ well. After 24 hours, media were replaced and cells were further incubated for 16 hours. Subsequently, media was replaced with fresh media. After 4 hours, cells were washed with ice cold PBS and metabolites were extracted in 1 mL of methanol/acetonitrile/H_2O (2:2:1). Samples were shaken for 10 minutes, centrifuged for 15 minutes at at 4 °C and supernatants were collected for LC-MS analysis.

LC-MS analysis was performed on an Exactive mass spectrometer (Thermo Scientific) coupled to a Dionex Ultimate 3000 auto-sampler and pump (Thermo Scientific). Metabolites were separated using a Sequant ZIC-pHILIC column (2.1 x 150 mm, 5 mm, guard column 2.1 x 20 mm, 5 mm; Merck) using a linear gradient of acetonitrile (A) and eluent B (20 mM (NH4)2CO3, 0.1% NH4OH in ULC/MS grade water (Biosolve)). Flow rate was set at 150 ml/min and the gradient ran from 20% B to 60% B, followed by a wash step and equilibration at 20% B. The MS operated in polarity-switching mode with spray voltages of 4.5 kV and -3.5 kV. Metabolites were identified on the basis of exact mass within 5 ppm and further validated by concordance with retention times of standards. Quantification was based on peak area using LCquan software (Thermo Scientific) Peak intensities were normalized based on median peak intensity.

Extraction of mRNA from cultured cells

Cells were seeded in full DMEM in six-well plates at a density of $2x10^5$ cells/well. After 1 day cells were treated, or transfected as indicated, and after the indicated duration of treatment mRNA was extracted using the following triazole/chloroform protocol:

- Medium was aspirated and cells were washed with 2 ml PBS.
- 200 μl Triazole (Sigma-Aldrich) were added directly onto the cells, and cells

were thoroughly scratched.

- The triazole was incubated on top of the cells for 5 minutes at room temperature.
- The Triazole lysates were aspirated and transferred into fresh Eppendorf tubes.
- 40 µl of chloroform were added to each tube.
- Tubes were vortexed for 15 seconds each, and then incubated for 15 minutes on ice.
- Tubes were centrifuged at 12000 x *g* for 15 minutes at 4°C to fully separate the aqueous and chloroform phases, with the genomic DNA condensed on the interface.
- The RNA-containing upper aqueous layer was transferred into fresh Eppendorf tubes.
- 100 µl of isopropanol were added to each tube to precipitate the RNA.
- Tubes were incubated for 10 minutes at room temperature.
- Tubes were centrifuged at 12000 x *g* for 4 minutes at room temperature, washed twice with 500 µl 70% ethanol.
- RNA was pelleted by centrifugation at 7500 x *g* for 5 minutes at 4°C.
- Pellets were air dried under laminar flow bench and the RNA was dissolved in 20 µl of nulcease-free water.

Complementary DNA (cDNA) synthesis

The synthesis of cDNA from the isolated RNA was carried out using the ProtoScript® First Strand Synthesis kit from NEB®.

The cDNA was synthesised using the protocol provided with the kit. To ensure that the mRNA is exclusively reverse-trscribed without other RNA types in the mixture, the reverse transcription was performed using poly-t primers that anneal specifically to the poly-A tails of the mRNA transcripts.

Real-time quantitative PCR rt-qPCR

For the quantitative PCR the LightCycler® Sybr Green (Roche®) reaction mix was utilized. The reactions were prepared according to the following protocol:

The following master-mix was prepared for each primer pair (target gene) to

be tested. Quantities are giver for 1 reaction:

- Cybr Green®: 2.5 μl
- Primer Mix: 1 μl
- Nuclease free water: 0.5 ml

Pipetted onto 1 μl of cDNA (concnetration≈30 ng/μl)

The tested cDNAs were pipetted in Microplate 96 LP (Analytik Jena AG) compatible to the qTOWER real-time PCR thermal cycler (Analytik Jena AG).

4 μl of the master-mix were pipetted in triplets on each type of the tested cDNAs. Subsequently, the plates were fed into the qTower real-time PCR thermal cycler, where the reactions occurred and the results were obtained.

Quantitative interpretation of the qPCR data

The mean values of the yielded CT of each triplet or reactions were calculated, including the mean-values of each tested cDNA with the reference genes. Then using these mean values of the CT of each target and reference genes, relative expression of the target genes was compared for the different cDNAs (treated vs non-treated or transfected vs empty vector) using the ΔΔCT equation to yield the relative expression values:

$\Delta Ct = Ct_{(target\ gene)} - Ct_{(reference\ gene)}$ for a given sample.

$\Delta\Delta Ct = \Delta Ct_{(treated\ sample)} - \Delta Ct(control\ sample)$

Relative expression (Fold change)$= -2^{\Delta\Delta Ct}$

Transcriptional profiling of MDA-MB231 cells

RNA was extracted from 500.000 cells. RNA concentrations were adjusted to 100ng/μl and samples were sent to collaborators in the Functional Genome Analysis Devision in DKFZ (Lab of Professor Jörg Hoheisel), were they were analysed using the Illumina RNA microarray system. The utilised method was described in previously published research from the group [84]and is summarised below:

- RNA-integrity of the samples was verified using Agilent 2100 Bioanalyzer (Agilent Technologies, Palo Alto).
- The analysis of the total RNA in the samples was performed using Sentrix Human-6v3 Whole Genome Expression BeadChips (Sentrix Human WG-6; Illumina).

- Following hybridisation to the chips according to the manufacturer's instructions, the arrays were scanned with a BeadArray Reader (Illumina).

Colony forming assay

Yeast

In yeast this assay was used to assess the intact cell-fractions upon long term MMS treatment by assessing the percentage of cells capable of giving rise to a colony upon MMS exposure.

Overnight cultures in SD-Ura were first diluted to an OD_{600} of 0.2 and incubated for 5 hours till it reached mid-log phase. Each culture was then split into three parts, non-treated and treated with 0.02% and 0.03% MMS. Following 12 h of shaking at 30°C, cultures were diluted and cell density of all samples was adjusted to OD of 0.5. Subsequently, the adjusted suspensions were used for both PI-staining and colony formation assay. The adjusted cell suspensions of non-treated samples were diluted 1:1000 (three step serial dilution 1:10) then 50 μl of each diluted sample were spread on an SD-Ura agar plates. Adjusted suspensions of cells treated with 0.02% MMS were diluted 1:10 and then 50 μl of each diluted sample was spread on an SD-Ura agar plate. The agar plates were incubated for 48 h at 30° then colonies were manually scored. This experiment was repeated three times independently.

Cell culture

Cells were seeded in 6 well plates at the extra-low density of 300 cells/well in 2 ml full DMEM. Any treatment, if included, was started 3 days after seeding. After 2 to 3 weeks of incubation colonies were fixed, stained and visualised according to the following protocol.

- The culture medium was aspirated and cells were washed in 2 ml PBS.
- Colonies were fixed and stained using a PBS solution containing 0.021% *(v/v)* formaldehyde and 0.5% *(w/v)* crystal violet.
- Following 30 minutes of incubation in the dark at room temperature, the staining solution was aspirated and all wells were rinsed 3 times in sterile water.
- Stained colonies were imaged using a regular camera.

III Results

"There is nothing like first-hand evidence". Sherlock Holmes (Arthur Conan Doyle)

III-I Investigating the mechanism behind FBP1 MMS-sensitizing effect in *S.cerevisiae*

It has already been shown that FBP1 is transcriptionally induced upon MMS treatment. Several FBP1-related aspects can affect the response of yeast cells towards MMS-induced DNA-damage. These include the catalytic activity of the expressed enzyme, the altered RedOx balance as reflected by decreased post-MMS ROS accumulation in absence of FBP1, in addition to a plethora of possibilities including the potential non-catalytic interactions and effects of metabolic by-products.
To further probe this relationship between Fbp1 and MMS-sensitisation I screened a library of Fbp1-analogues with point mutations targeting evolutionary-conserved residues of functional and mutational relevance. Each mutant had one amino acid replaced for alanine (alanine screening). The evolutionary conservation over long phylogenic distances points out to functional constraints preserving the conserved residues. Enzymes catalysing the same reactions exhibit much higher conservation on the level of amino-acid sequences compared to the nucleotide sequence. This is because silent mutations within evolutionary conserved codons are tolerated.

III-I-1 Selection of amino acid residues for mutational analysis

"This passage is based on my publication in Microbial Cell ˝ 2017 Ghanem et al." [85]

To investigate the relevance of evolutionary conserved residues to the catalytic and MMS-sensitiing activities of Fbp1, we prepared fbp1 over-expression vectors, each containing a single mutagenised codon of a conserved residue. The global alignment of primary amino-acid sequences of Fbp1 orthologues from several species including *Homo sapiens* and *Saccharomyces cerevisiae* revealed 46% identitiy Fig.1 [86, 87]. We therefore were confronted with a large choice of conserved residues as candidates for our mutagenesis screen. Hence we relied upon previous evidence from various structural and functional studies on yeast

and mammalian Fbp1 orthologues to define the residues with the highest likelihood of participation in the dual role observed in yeast.

An overall glance at the aligned sequences of yeast *vs* human FBP1 amino-acid sequences reveals a fully heterologuos N-terminus that extends in the yeast orthologue for 9 additional residues, for which no counterparts are present in the mammalian protein [87]. This “overhang” has been implicated in the glucose-triggered post-translational degradation “catabolite inactivation” of FBP1 in yeast, the N-terminal Pro1 residues is involved in recruiting specific proteases to the ubiquitinated protein according to the N-end rule [88, 89]. The phophorylation of Ser11 by cAmp mediates the loss of FBPase activity upon glucose replenishment. [90]. The residues 52-72 in the mammalian orthologues, homologues to 63-82 in yeast participate in the formation of a loosely structured loop with a crucial effect on the finally tertiary structure of the FBP1 homo-tetramer. The interaction to AMP disrupts the interaction between the loop and the active site and thus leads to the inactive T-state confirmation, while in absence of AMP from the structure this loop orients towards the active site permitting the participation of Asp79 (yeast) Asp68(mammals) in the catalytic activity. This mechanism allows the energy regulation of gluconeogenesis [91] (Fig 1.I c) The above mentioned loop contains two evolutionary conserved residues. The first, Asn(64 mammals, 75 yeast) participates in the formation a water-water binding pocket along with two other evolutionary conserved residues Asp (74 mammals 85 yeast) and, Glu (98 mammals, 109 yeast). The water molecule bound to this pocket facilitates the nucleophilic attack of another neighbouring water molecule on the phosphate-group at 1`position of the substrate F1,6bP, which eventually splits the substrate into Fructose-6-phosphate F6P and inorganic phosphate group iP. The second, Asp(68 mammalis, 79 yeast), aligns towards the active site and promotes the movement of a proton from the phosphate group at 1` towards an OH group in the product F6P [91].

A stretch of evolutionary conserved residues Asp118 to Ser 123 in mammals and Asp128 to Ser133 in yeast forms a divalent-cation binding site essential for the enzymatic catalysis (Fig 1.I b). This metal binding pocket is conserved through all Fbp1 orthologues. Moreover, a homologues metal bindings site is encountered in various other phosphatases similarly requiring metal cationic co-factors [92].

Mammalian and yeast Fbp1 orthologues share the exact same sequence comprising this metal binding pocket Asp-Pro-Ile-Asp-Gly-Ser [92].

Phe(185 mammals, 194 yeast) is an evolutionary conserved residue within a conserved stride of other amino-acids. Due to the bulkiness of phenyl-alanine in addition to its middle position in Fbp1, we considered a key-effect of this residue on protein folding plausible and included it in our mutagenesis screening.

The c-terminal region of FBP1 comprises the largest evolutionary conserved regon of this protein, exhibiting 66% identity between yeast and mammalian orthologues. This region extends between Asp 243 and Ser321 in mammals and Asp254 and Ser333 in yeast and it also contains the catalytically active site (substrate-binding pocket), this knowledge has been recently harnessed in studies on human cancerous cells as well [61, 93]. The c-terminus includes two evolutionary-conserved histidines His265 (yeast) and His324 (yeast). Due to their amphephilic nature, and presence near the active site, these two residues are likely to contribute to catalysis.

Based on the summarised structural and functional knowledge we chose 9 candidates for out alanine-screening, in which we mutagenised the targeted residues by introducing point mutations converting their respective codons to those of alanine.

In the results and discussion pertaining to this mutational screening, I will refer to each mutation by the three-letter symbol of the mutagenised (alanine-replaced) amino-acid and its respective number in the amino-acid chain of the yeast orthologue.

Based on the summarised knowledge, 9 residues were chosen for the alanine screening. A point mutation was introduced to alter the codon of each targeted residue into an alanine codon. In the following results and discussion pertaining to this mutagenesis screen, each mutation was referred to using the three-letter symbol of the amino-acid and its respective number in the amino-acid chain of the yeast homologue. Table 9 features the screened mutations, along with their abbreviations and the utilised mutagenesis primers.

Table 9: Summary of the analyzed yeast fbp1 mutations and the utilized mutagenesis primers

Mutations (Altered residue)	Mutagenesis primers	Abbreviation of the mutated FBP1 form
Pro1→Ala1	fw: GGATTCTAGAACTAGTATGGCAAC TCTAGTAAA TGGACC rev: GGTCCATTTACTAGAGTTGCCATACTAGTTCTAGAATCC	Pro1
Asn75→Ala75	fw: GTTAGCAGGCGCTTCCGCCTTCACTGGTGACCAGC rev: GCTGGTCACCAGTGAAGGCGGAAGCGCCTGCTAAC	Asn75
Asp79→Ala79	fw: GCTTCCAACTTCACTGGTGCCCAGCAAAAGAAGTTGGAC rev: GTCCAACTTCTTTTGCTGGGCACCAGTGAAGTTGGAAGC	Asp79
Glu109→Ala109	fw: GGTCCTTGTATCTGAAGCACAGGAAGATTTGATCG rev: CGATCAAGTCTTCCTGTGCTTCAGATACAAGGACC	Glu109
Asp131→Ala131	fw: GTGTGTTGTGATCCTATTGCTGGCTCCTCAAATTTGGAC rev: GTCCAAATTTGAGGAGCCACGAATAGGATCACAACACAC	Asp131
Ser133→Ala133	fw: GTGATCCTATTGATGGCGCCTCAAATTTGGACGCCGG rev: CCGGCGTCCAAATTTGAGGCGCCATCAATAGGATCAC	Ser133
Phe194→Ala194	fw: GGTGATGGAGTTGATGGGGCTACCTTAGACACAAACTG rev: CAAGTTTGTGTCTAAGGTAGCCCCATCAACTCCATCACC	Phe194
His65→Ala265	fw: CCATGGTTGCTGATGTTGCCAGGACGTTTCTTTACGG rev: CCGTAAAGAAACGTCCTGGCAACATCAGCAACCATGG	His265
His324→Ala324	fw: GATTTGGTGCCAAGTCATACCGCTGACAAATCTTCTATT rev: AATAGAAGATTTGTCAGCGATATGACTGGCACCAAATC	His325

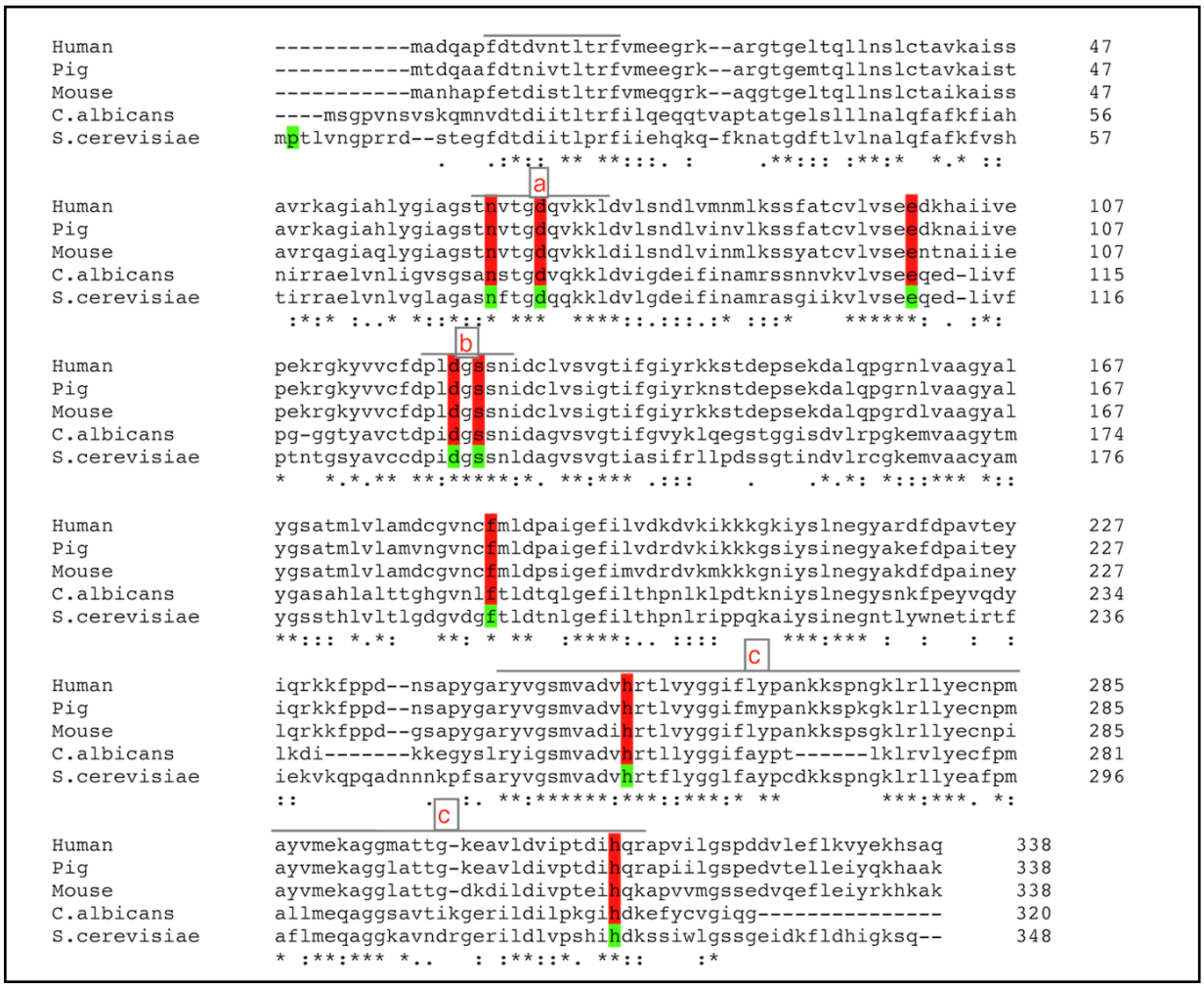

Figure 1 featured in my publication in Microbial Cell ˝ 2017 Ghanem et al.“ [85]

Figure 1: multiple global-alignment of *FBP1* amino-acid sequences of *Saccharomyces cerevisiae* and several species using the online-available ClustalW2 multiple sequence alignment tool, provided by EMBL-EBI.

Identical residues are marked with (l) ; similarities (:) and totally different ones with (.)

Residues included in the mutational analysis are highlighted.

Three regions (a, b and c) of sequence homology are indicated: (a) representing the mostly conserved part of the regulatory loop, (b) the conserved metal binding site, and (c) the largest homology domain on the c-terminus containing the active site.

Mutated residues highlighted.

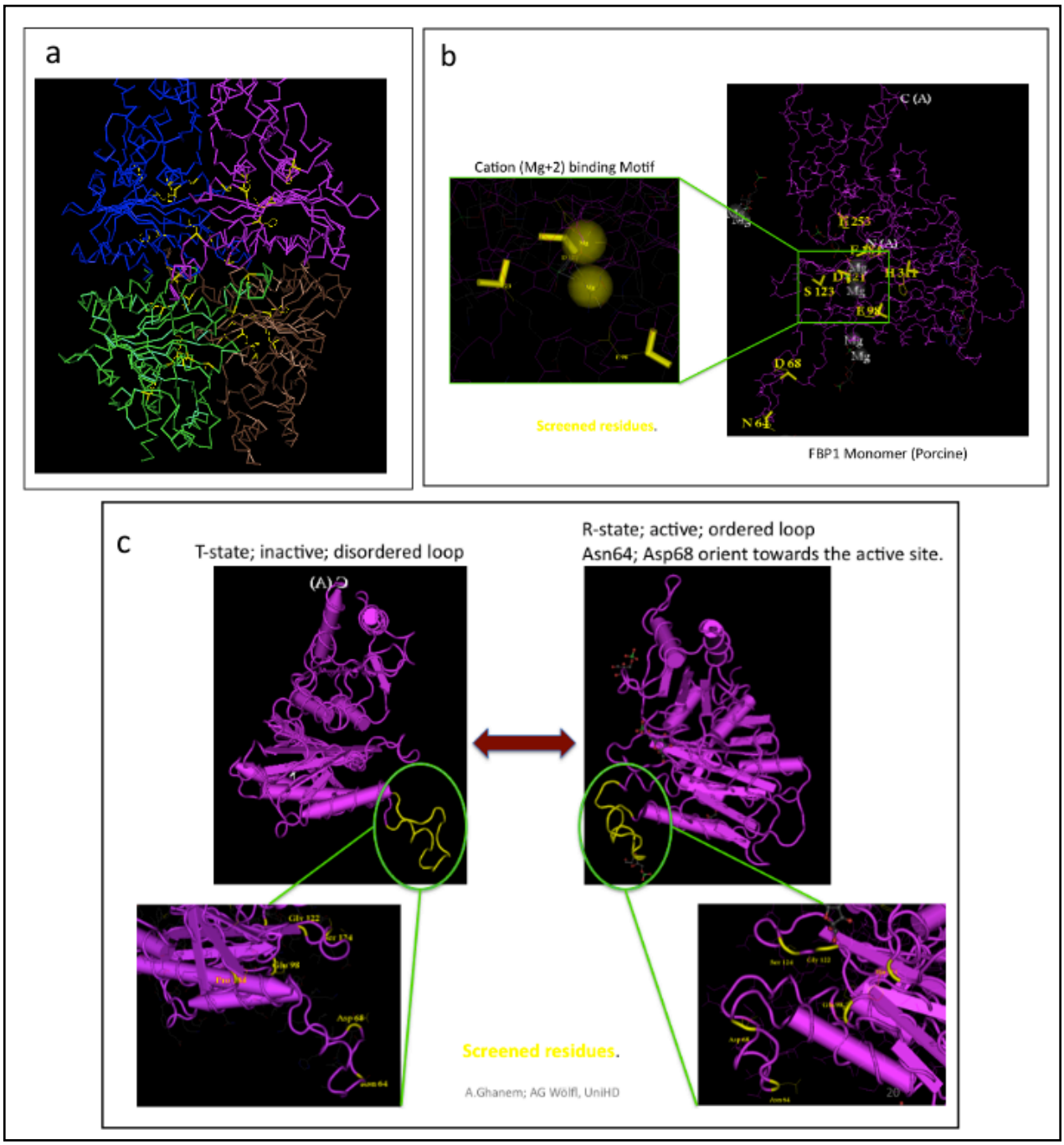

Figure 1.I: Structural relevance of the mutated residues.
a) The FBP1 tetramer with the mutated residues annotated. b) FBP1 monomer featuring the mutated residues, with focus on the cation binding motifs and the adjacent targeted residues. c) Monomeric structure of FBP1 and the oscillation between the t and r states. This figure was created based on se from the NCBI Structure Database and the Structure Cn3D software tool was used to render the structures and label the mutated residues.

III-I-2 Detection of expression of Fbp1p mutants from expression cassettes

"This passage is based on my publication in Microbial Cell ˝ 2017 Ghanem et al." [85]

The protein expression of 6 out of the 9 tested mutants was successfully detecgted in both the cytosole and the nucleus of the Fbp1-deficient strain *fbp1*Δ. Meanwhile, the two Phe194 and His 265 mutants were only present in the nucleus. Only one mutant Asp79 remained undetected in either the cytosolic or nuclear fractions (Fig2 a) The semi-quantification of western-blot band-intensities indicated an effect of some of the mutagenised residues on the nuclear/cytosolic sub-cellular localisation of FBP1 (Fig.2 b). Beside Phe194 and His265 leading to exclusive nuclear sub-localisation, three mutants (Asp131, Ser133 and His324) also tilt the balance towards the nuclear localisation. In contrast, Pro1 and Glu109 favour cytosolic sub-localisation of FBP1.

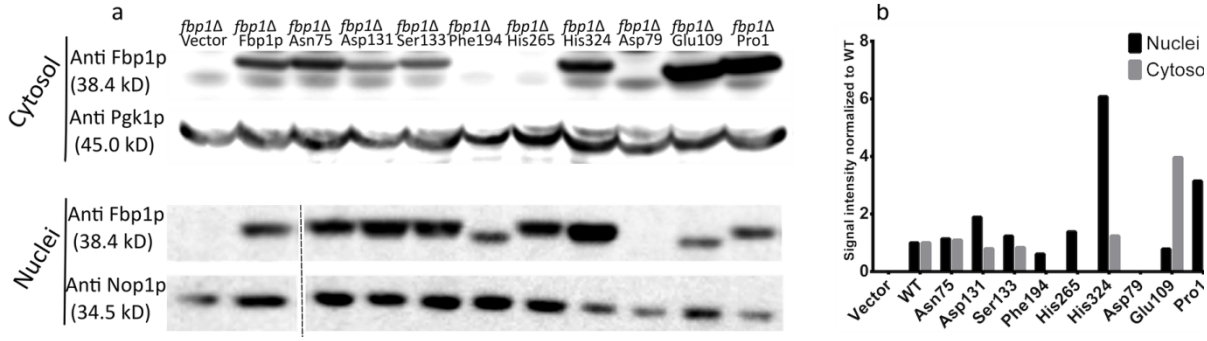

This figure featured in my publication in Microbial Cell ˝ 2017 Ghanem et al." [85]
This immunoblot was performed by Jinda Holzwart as part of her Diploma thesis.
Figure 2: Immuno-detection of the over-expressed Fbp1p mutants.
a) Western-blot showing the levels of the over-expressed mutants in both cytosolic and nuclear fractions. Over-expression was verified in absence of endogenous Fbp1p expression in *fbp1*Δ strains. PGK1 and NOP1 were utilized as cytosolic and nuclear loading controls, respectively. b) Quantification of the western-blot signals, each band was normalized to the intensity of its loading control, resulting values where then normalized to those of the wt.

III-I-3 Catalytic activity of the Fbp1p mutants

"The following passage based on my publication in Microbial Cell ˝ 2017 Ghanem et al." [85]

To assess the effect of altered residues on the catalytic activity of Fbp1 we over-expressed the mutated proteins in a haploid wild-type BY4741 strain and quantified the resulting increase in the FBPase catalytic activity in the crude native protein lysates of the mutant-expressing strains compared to the strain harbouring the corresponding empty vector. This revealed that the screened mutants clustered into three distinct groups in relation to their catalytic activity (Fig. 3):

- Pro1 and Asn75 bestowed similar increase of the FBPAase activity to that seen with the wild-type FBP1.

- Phe194, His265 and His324 all show partial increase in the enzymatic activity of around 50% of that of the wild-type enzyme.
- Asp79, Glu109, Asp131 and Ser 133 all resulted in no increase in the FBPase activity, and the strains harbouring these mutants had similar FBPase activity to the wild-type.

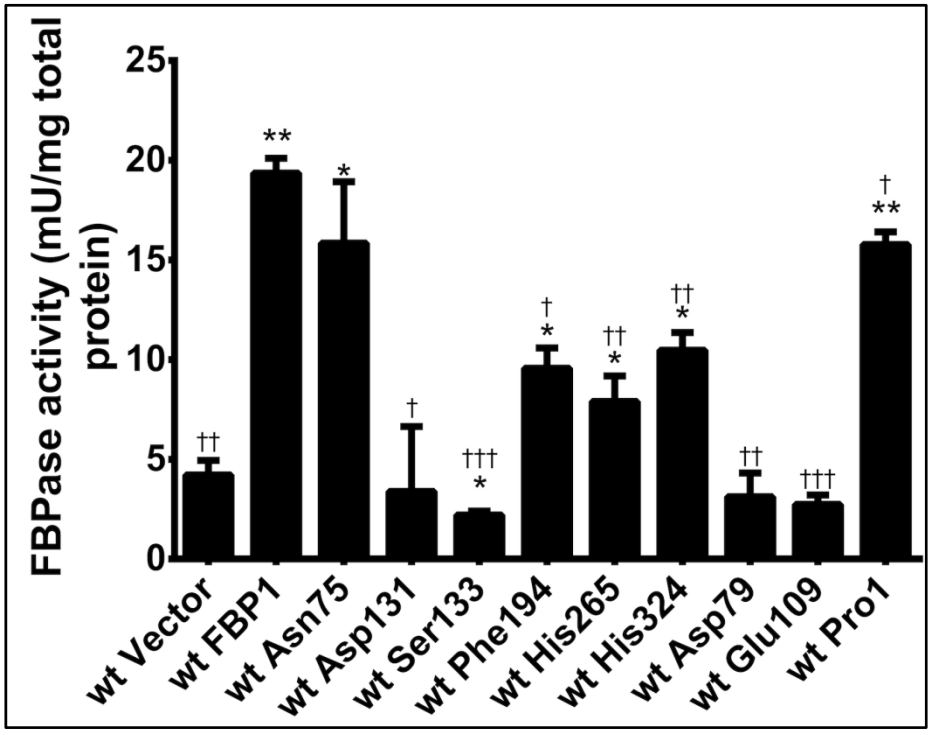

Figure 3 featured in my publication in Microbial Cell ˝ 2017 Ghanem et al.“ [85]
This figure is based on enzymatic activity measurements of mutated Fbp1 performed by Jinda Holzwarth as part of her Diploma thesis.
Figure 3: Enzymatic activity of the utilized *FBP1* mutants:
FBPase catalytic activity was measured in native lysates of wild-type BY4741 strains with over-expression of wild-type and mutated *fbp1* cassettes. Measurements were performed in triplets, and error bards represent SD.
Statistical significance was determined using student t-test for each of the mutants compared to both cells with control vector and those with over-expression of the wild-type Fbp1p. (*) Indicates statistically relevant difference compared to empty vector and (†) compared to the wild-type Fbp1p.

III-I-4 Rescue of growth on non-fermentable medium (Spot-assay on SDEG)

“The following passage based on my publication in Microbial Cell ˝ 2017 Ghanem et al.“ [85]

To probe the capacity of the screened mutants to replace the deleted endogenous expression of FBP1 and rescue gluconeogenesis in *fbp1Δ* cells was assessed. This was done by assessing the growth of fbp1Δ strains over-expressing individual mutatagenised cassettes on a non-fermentable medium. The non-fermentable medium SDEG contains ethanol and glycerol as exclusive carbon sources and thus

only permits the growth of cells with a functional gluconeogenesis pathway. The spot assay on SDEG-agar yielded the predictable observation that Fbp1 catalytic activity is indispensible for proliferation on non-fermentable carbon sources. The four mutations that completely attenuate the catalysis; Asp79, Glu109, Asp131 and Ser133, also abrogated growth on SDEG (Fig.4 a). In contrast mutants partially or fully spraining the FBPase activity; Pro1, Asn75, Phe194, His265 and His 324, were able to rescue the growth on SDEG in the absence of endogenous (Fig.4 a).

III-I-5 Sensitivity to low doses of MMS

"The following passage based on my publication in Microbial Cell ˝ 2017 Ghanem et al." [85]

Since it had been demonstrated that MMS-exposure induces fbp1 transcription, and that the presence of the endogenous Fbp1 is decisive for the sensitivity towards low doses of MMS [94], I used the established mutant library to screen probe the connections of the additional MMS-sensitisation role to the mutated evolutionary conserved key-residues of this enzyme. For this purpose, the mutagenised proteins were expressed in both wild type and *fbp1*-deficient (*fbp1Δ)* BY4741 genetic backgrounds. The resulting strains were cultivated in liquid media, then serially diluted and spotted on SD-Ura agar containing low concentrations of MMS increasing from 0.01% to 0.0175%. The spot-assay agar plates were surveyed following 48 hours of incubation. Predictably, the inactivating mutations Asp79, Glu109, Asp131, Ser133 and His324 also attenuated the additional FBP1-induced MMS-sensitisation, yielding strains with similar growth on MMS to that of wild type stain with an empty vector (Fig. 4 b to i). In contrast, three enzymatically active mutants maintained the MMS-sensitising effect as they correlated to further growth inhibition on MMS-agar similar to ectopically expressed non-mutated FBP1 (Fig. 4 b to i). Intriguingly, mutagenising Asn75 abrogated the MMS-sensitisation (Fig. 4 b to i) despite maintaining almost the full catalytic activity of the non-mutated enzyme (Fig.3). Hence this mutant seems to decouple the catalytic activity of FBP1 from its ascribed role in increasing sensitivity towards low MMS concentrations. Similar growth tendencies were observed for the mutant-harnouring strains with wild type and *fbp1Δ* genetic backgrounds. Importantly, the *fbp1Δ* strains exhibited less sensitivity to all tested MMS concentrations in contrast with their wild type counterparts. Hence

confirming earlier findings that fbp1 deletion bestows cells with increased resistance towards MMS [94]. The direct observations from the spot-assays were further confirmed using spot-intensity quantification (Fig. 4 f, g, h and i).

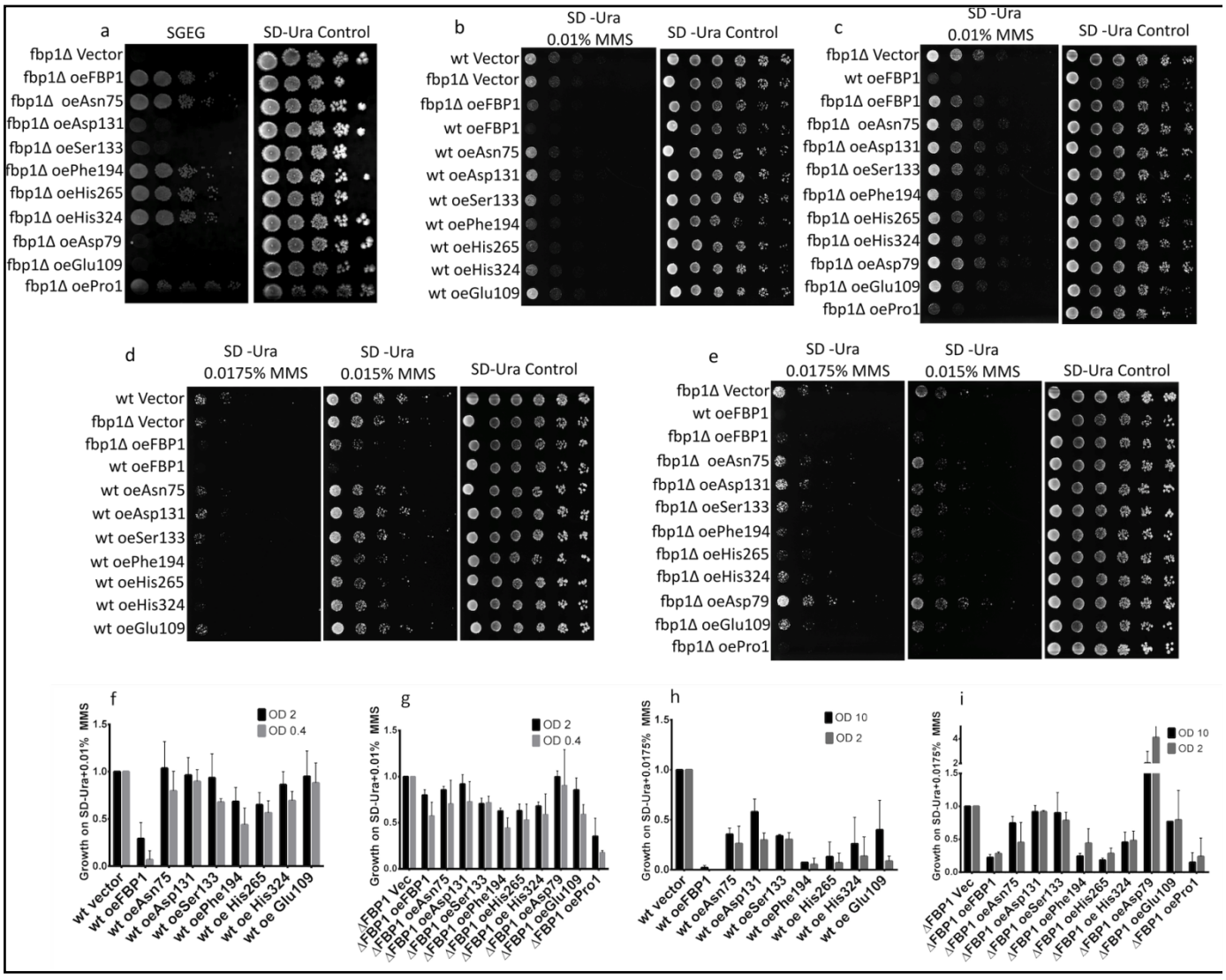

Figure 4 featured in my publication in Microbial Cell ˝ 2017 Ghanem et al.“ [85]

Figure 4: Drop-tests on Non-fermentable (SDEG) and MMS-containing agar-media.

a) Drop-test on SDEG non-fermentable medium. WT and mutated *FBP1* cassettes were introduced into BY4741 *fbp1*Δ cells lacking endogenous *FBP1*, the resulting strains were grown in liquid SD-Ura medium, diluted and spotted on SDEG, same suspensions were spotted on SD-Ura agar as a control. Agar-plates were incubated for 48 hours at 30°

b&c) Drop tests on SD-Ura agar with 0.01% MMS. Mutants and wild-type cassettes were introduced into both WT (a) and Δ*fbp1* (b) BY4741 cells. The resulting strains were grown in SD-Ura and then diluted (1:5) and spotted on freshly prepared SD-Ura containing 0.01%, and on SD-Ura as non-treated control. Agar plates were incubated for 48 h at 30° for 48 h.

d&e) Drop tests on SD-Ura agar containing 0.015% and 0.0175% MMS. Plates were incubated for 72 h at 30°.

f to i) Quantifications of the spot-intensities of the drop tests on SD-Ura 0.01% MMS second and third spots (OD_{600}: 2 and 0.4 respectively) and 0.0175% first and second spots (OD_{600}: 10 and 2 respectively). Featured results are taken from three biologically independent replicates, (error-bars: SD; N=3)

III-I-6 Over-production of Fbp1p sensitises cells to MMS in liquid medium

"This passage is based on my publication in Microbial Cell ˝ 2017 Ghanem et al." [85]

To further address the MMS-sensitising effect of Fbp1, the growth of yeast strains with variable Fbp1 contexts was evaluated in MMS-containing liquid SD-Ura. Pre-cultures of the tested strains were incubated over-night in SD-Ura, following dulitions, cultures were then preincubated for 3 hours prior to treatment. The treatments were performed in triplets in a 96 micro-titer plate format, with 0.01% and 0.02% MMS. Upon treatment OD_{600} was measured over the course of 24 hours in a microtiter plate reader. The exposure to 0.02% MMS had a uniform severe growth inhibitory effect on all tested strains. Meanwhile, the effect of the lower concentration 0.01% was largely determined by the context of Fbp1 expression in the cells. The ectopic introduction of a catalytically active form of Fbp1 (wild type or active mutant) increased the sensitivity towards 0.01% MMS and correlated to a lower growth over time (Fig 5, a to g). The wild type enzyme and active mutants Asn75 and His265 all significantly obstructed growth when ectopically expressed in a wild type genomic background (Fig. 5, a e and g). The inactive mutant Asp131 lacked this effect, and cells still achieved a similar growth to those harbouring an empty vector (Fig. 5, a and F). Also noteworthy is the contrast in the outcome of Fbp1 ectopic expression according to the presence of endogenous Fbp1. Predictably, the presence of endogenous Fbp1 potentiated the MMS-sensitising effect seen with over-expressed catalytically active Fbp1. And while cells with wild type background and over-expression of Fbp1 seemed to undergo permanent inhibition of growth, those with an *fbp1Δ* genotype, only suffered growth retardation upon 0.01% MMS treatment, and still matched the OD_{600} of the non-treated cells at a later point (Fig.5 A to D).

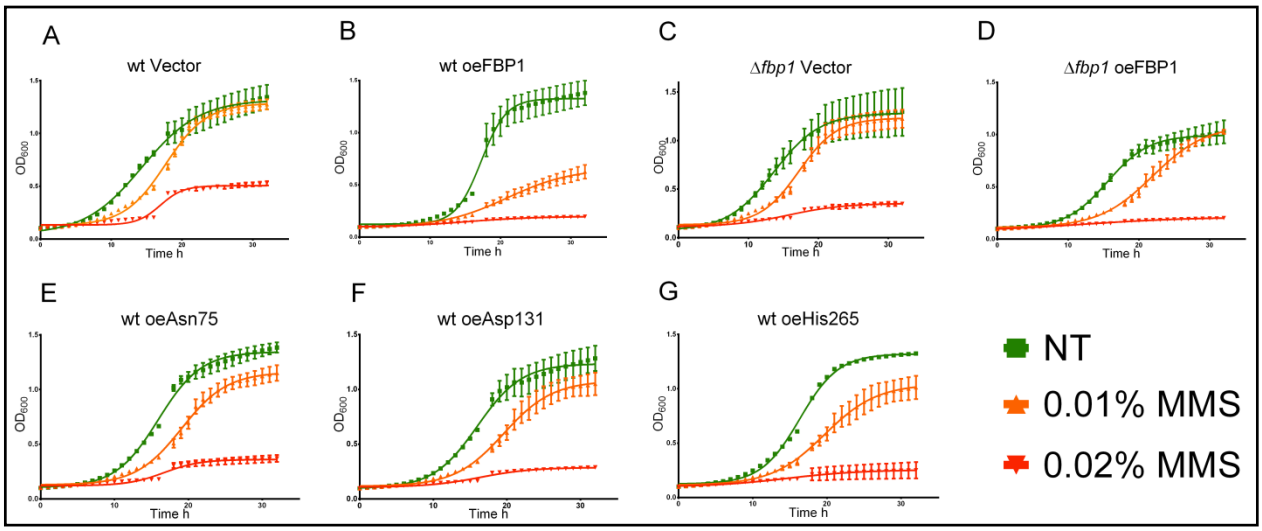

Figure 5 featured in my publication in Microbial Cell ˝ 2017 Ghanem et al.“ [85]

Figure 5: Growth curves upon MMS treatment:

Figures a to g feature the growth curves of the non-treated and MMS-treated (0.01% and 0.02%) yeast strains in liquid SD-Ura medium. Curves feature the increasing OD_{600} values over-time at 30° with intermittent shaking, error bars represent SD, N=3.

III-I-7 The effect of Fbp1p over-production on cell survival depends on its genomic context of *fbp1*

“The following passage based on my publication in Microbial Cell ˝ 2017 Ghanem et al.“ [85]

To determine the effect of Fbp1 on cell survival upon MMS treatment I used FACS of propedium-iodide PI stained cells. Log-phase liquid cultures in SD-Ura medium were treated with MMS for 12 hours. The FACS analysis showed an increase in dead cell fractions upon 0.02% and 0.03% MMS treatment in all tested strains (Fig.6 a and b).

The effect of ectopic Fbp1 was completely dependent on the presence of endogenous expression. Only in wild-type cells did the over-expression lead to decreased survival upon MMS treatment, seen as increased in PI-positive dead-cell fractions of treated populations. Over-expressed Fbp1 lacked this sensitising effect in absence of its endogenously expressed counter-part (in *fbp1Δ* cells). Both the Asn75 and His265 mutants failed to reproduce the effect of the ectopically introduced wild type enzyme in increasing cell death upon MMS-exposure (Fig. 6 a).

Interestingly, the ectopic over-production of Fbp1 correlated to improved cell survival and diminished PI-staining both in absence and presence of endogenous expression. This side observation consists with previous findings of an improved chronological life span associated to Fbp1[94].

III-I-8 Over-production of Fbp1p hampers colony-forming capacity upon MMS treatment

"The following passage based on my publication in Microbial Cell ″ 2017 Ghanem et al." [85]

To further investigate cell survival upon MMS treatment, we tested the impact of wild type and mutated forms of Fbp1p on the colony forming capacity of cells following MMS treatment. Generally, 12 hours of 0.02% MMS treatment lead to a two to three orders of magnitude decrease of the colony forming units CFU/μl (Fig. 6, c and d). In the context of WT cells with endogenous Fbp1p expression, this decrease was strongest when wild-type Fbp1p or the active mutant His265 were over-expressed (Fig. 6 c). In contrast, over-expression of wild-type Fbp1p in cells lacking the endogenous gene (*fbp1*Δ) had no further inhibitory effect on colony forming capacity (Fig. 6 D). It is also worth noting that in the WT strain, over-expression of Fbp1p or its active mutant His265 lead to significant decrease in CFU/μl in the non-treated samples as well, compared to non-treated cells harbouring the control vector.

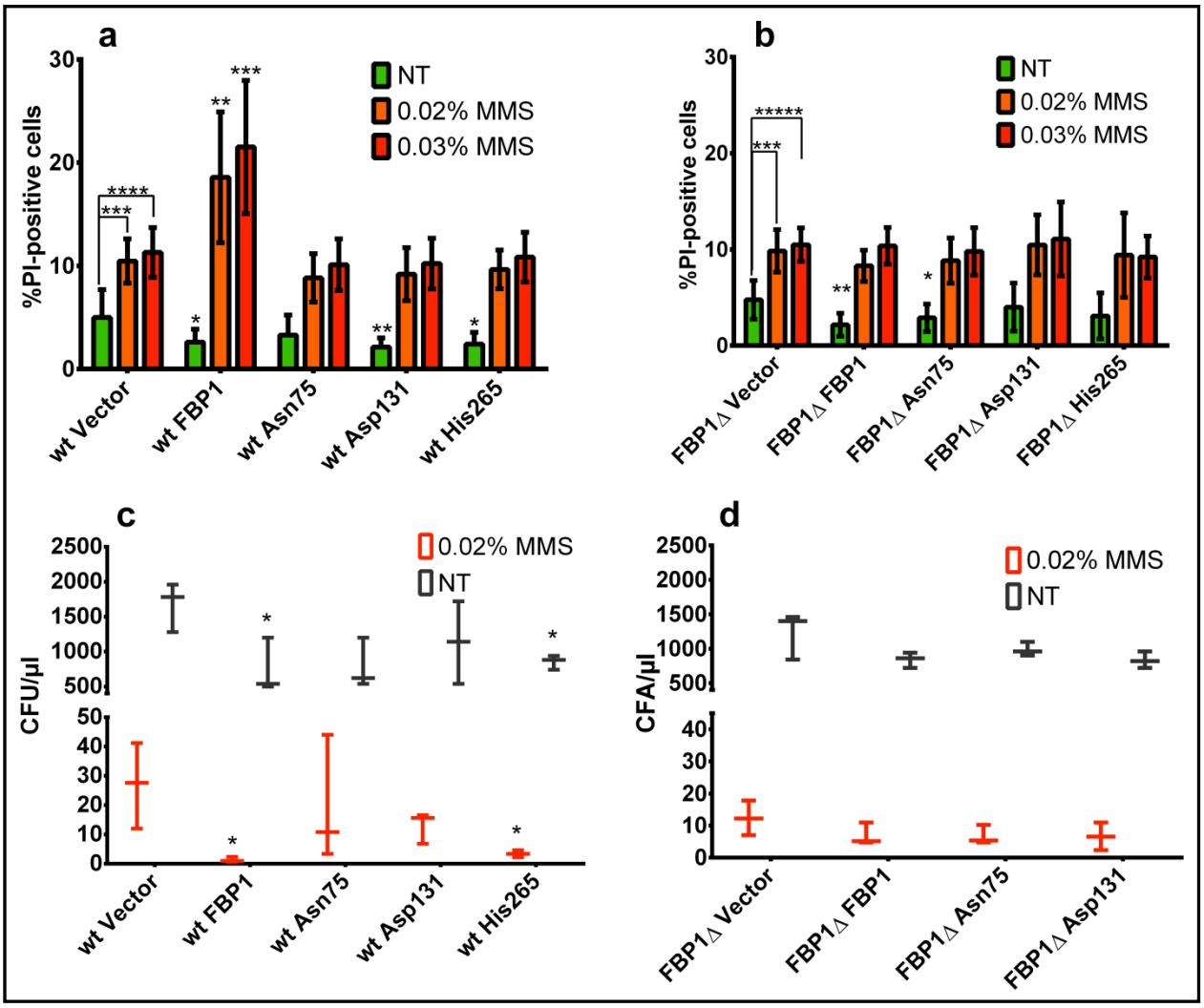

Figure 6 featured in my publication in Microbial Cell ˝ 2017 Ghanem et al.“ [85]
Figure 6: Cell survival and colony formation upon MMS treatment.
a&b) FACS analysis of PI staining following 12 hours of MMS treatment.
Bars represent the PI-positive percentage fractions of cells as measured using FACS.
Results feature three biologically independent replicates with three technical replicates each. Error bars show the standard deviation.
Statistical significance was determined using unpaired student t-test assuming equal variance.
(*: p<0.05; **: p<0.01; ***: p<0.001; ****: p<0.0001)
The brackets over the wt Vector ,*fbp1*Δ Vector strains and the control vector strains show the significance difference between treated and non-treated samples within the same strain. While asterisks over the mutants represent statistical significance when comparing the results of these strains with those of the control vector.
c&d) colony formation on SD-Ura agar following 12 hours of MMS treatment in liquid SD-Ura. Results are from 3 independent experiments. Error bars show the standard deviation. Asterisks indicate statistically significant differences compared to the control vector strains. Significance was assessed using student t-test (*: p<0.05)

III-I-9 FBP1 loss curtails ROS induction and correlates to an induced anti-oxidant capacity

Previous reports demonstrated that FBP1 absence reduces post-MMS ROS-accumulation. This was shown to occur one hour after treatment (Reference ??). To further verify and extend this finding, ROS levels were measured following longer-term treatments (18 hours) with a lower dose (0.01%) of MMS. Fluorescent images of DHE-stained cells showed that the ectopic over-expression of FBP1 clearly correlated to higher levels of ROS upon MMS treatment. That was the case in the presence or absence of endogenously expressed Fbp1 (wild type and Δ*fbp1* cells) (Fig.7 i). Moreover, Fbp1 over-expression induced ROS accumulation in non-treated cells following the 18-hour incubation. This effect was stronger in wild type cells over-expressing Fbp1 compared to Fbp1 deficient cells. To further quantify similar observations related to Fbp1 effects on ROS accumulation, I used microtiter plate reader to quantify DHE fluorescence. Since long incubation time would allow for big differences in cell density due to unequal proliferation rates. I used GFP fluorescence to set DHE signals to the scale of different cell densities of strains harbouring either free GFP or in fusion with Fbp1 (Fig. 7 ii).

The Fbp1-deficient cells exhibited lower DHE fluorescence compared to wild-type, and this was the case for both non-treated and long term (18-hours) MMS treatment. Ectopic over-expression of Fbp1 in the Δfbp1 cells correlates to an increase in ROS to levels higher than those of the wild-type strain. Long-term MMS treatment induced ROS accumulation in all three different contexts. However, the absence of Fbp1 partially mitigated the ROS increase upon MMS treatment. Basal ROS levels in the wild-type are also lower than those of the fbp1Δ cells, while they were highest upon over-expression of Fbp1. This indicates an impact of Fbp1 on the RedOX homeostasis independent of the genotoxicity of MMS. Due to its correlation with higher ROS accumulation, I speculated an impact of Fbp1 on the cytosolic anti-oxidant capacity. Glucose-6-phsophate dehydrogenase G6PD catalyzes the oxidation of glucose-6-phosphate to 6-phosphogluconolactone gluconalactone with NADP+ as a co-factor that gets reduced into NADPH. Additionally, this reaction is the first committed step in pentose phosphate pathway PPP, which generates one more NADPH in its last oxidative step. This makes G6PD the major cytosolic source of

NADPH. NADPH plays a pivotal anti-oxidant role in the cytosol via providing the reducing equivalents required for maintaining glutamine in a predominantly reduced form. By measuring G6PD activity in native protein lysates, Fbp1-deficient cells exhibit increased base-line G6PD activity, and also a stronger induction of G6PD catalytic activity in response to MMS. This increased G6PD induction gives the Fbp1 deficient cells an edge over the wild-type cells due to the induced flux through PPP. In addition to the aforementioned anti-oxidant capacity the PPP is also the only intracellular source for ribose synthesis needed for DNA repair pathways, including base-excision repair thought to be of importance following MMS-exposure.

This points out a contribution of excess (raised) G6PD in increasing tolerance towards MMS in the Fbp1-deficient cells.

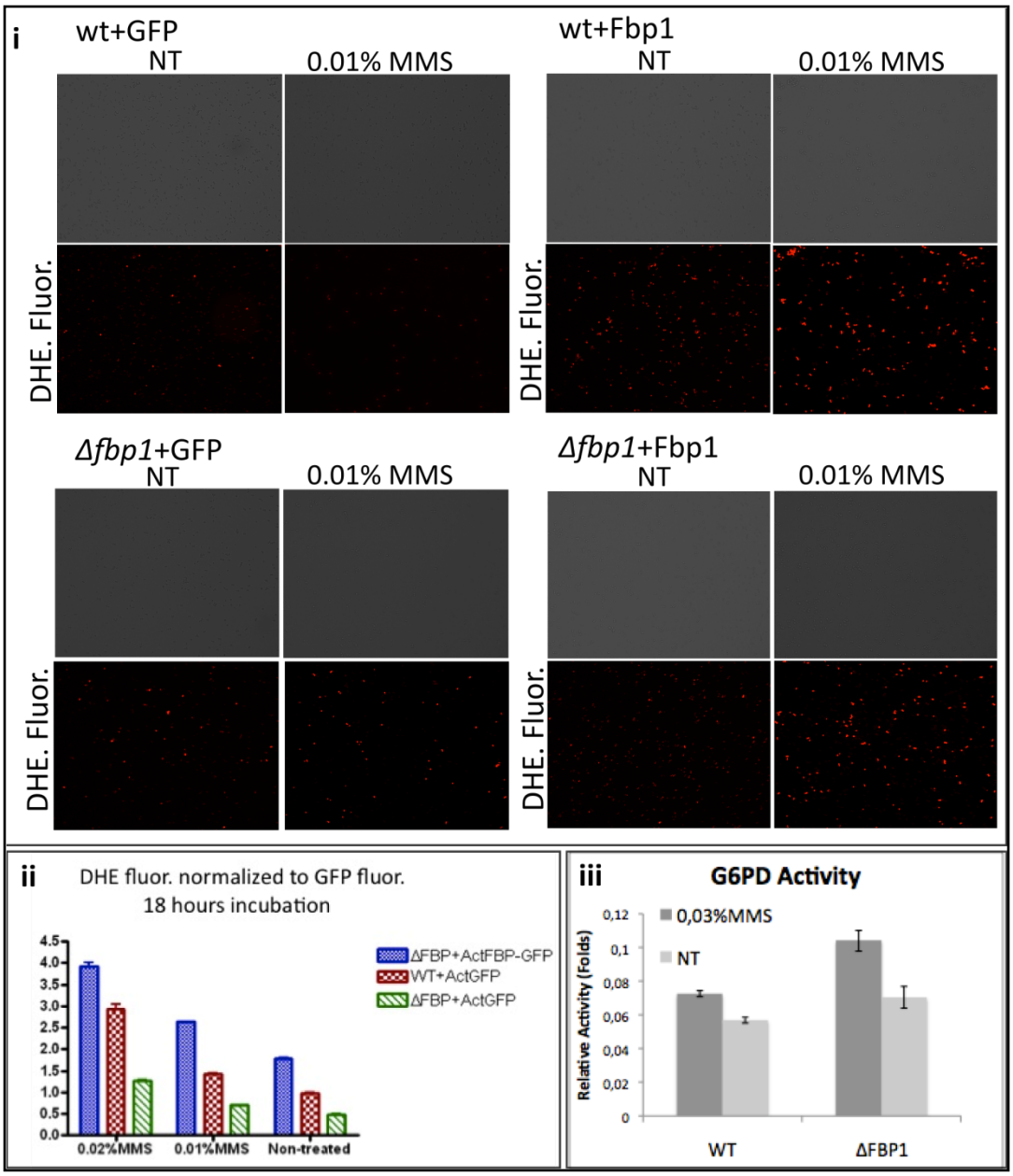

Figure 7: Fbp1 induces increased ROS accumulation upon MMS exposure:
i) Fluorescent microscopy images depicting DHE red fluorescence of yeast strains with varying Fbp1 expression 20 hours following MMS exposure. ii) Bar charts depict the fluorescence levels of DHE of GFP-harbouring yeast strains with various Fbp1 expression. DHE signals were normalized to measured GFP fluorescence (correlating to the cell density). iii) G6PD activity measured in wild-type and Fbp1-deficient strains 4 hours following MMS treatment.

III-II The Effects of Fbp1 in Cancers

Emphasis on the importance of increased glycolytic flux had been defining our understanding of tumour metabolism. Only recently, light had been shed on the aberrant regulation of gluconeogenesis as a contributing factor to the metabolic reprogramming that allows malignant transformation. Increasing evidence from

different types of tumours points out to the repression of FBP1 in tumours compared to adjacent normal tissues. Epigenetic silencing of Fbp1 occurs as part of tumerigenesis in liver, colon, gastric, pancreatic and renal cancers. These tumours show an overall repression of FBP1, while breast cancers are heterogeneous in regards to their expression of Fbp1. On the direct enzymatic level, the loss of Fbp1 in cells confers a metabolic advantage onto the cells by allowing the uncontested flux of metabolites through the glycolytic pathway. Additionally, several reports also indicated non-catalytic ways through which Fbp1 loss indirectly contributes to tumour metabolic reprogramming or further gain of aggressiveness and invasiveness. An inhibitory interaction of Fbp1 with Hilf1α in the nucleus has been observed, which is independent of the catalytic function. Consistently, Fbp1 expression has been relatively correlated to Hif1α levels in breast cancer cell lines [61]. The benefits bestowed upon tumours via Fbp1-loss are experimentally reversible by ectopic replenishment of the silenced FBP1, or by epigenetically repressing it as very recently reported in hepatocellular carcinoma cells [95].

III-II-1 The significance of FBP1 in the context of Breast Cancer (Back-ground)

Breast cancers make an interesting model for understanding the effects of FBP1 on cancer metabolism and aggressiveness in general. This is because breast tumours are heterogenous in regards to their FBP1 expression [96]. Broadly speaking, breast tumours fall into two major categories; ductal breast cancers DBC, and basal like breast cancers BLBC. The former are primary tumours, of epithelial morphology and are hormone driven exhibiting positive estrogen receptor ER and progesterone receptor PR and human epidermal growth factor 2 HER-2 receptors expression[97]. The latter are also often called triple-negative-breast cancers TNBC. They are distinguished by the lack of the three hormone receptors ER, PR, HER-2, in addition to the absence of epithelial markers including E-Cadherin[97]. Compared to ductal breast cancers, basal-like breast have a markedly worse prognosis, attributed to their invasiveness and metastatic nature. Interestingly, the relationship between the two types is a dynamic one. In contrast with the non-metastatic Breast carcinoma in-situ BRIC some ductal breast cancers display the capacity of gaining invasive and

metastatic features. Eventually this results in metastasis having similar markers to BLBC and TNBC, the lack of hormonal receptors and E-Cadherin. To gain invasiveness, ductal breast cancers have to undergo a morphological change called the epithelial-mesenchymal transition EMT. Simultaneously, further metabolic reprogramming occurs to support the requirements of invasiveness and flourishing in a new microenvironment, and independently of hormonal stimulation. FBP1 is central in this metabolic reprogramming. Primary ductal breast tumours have high levels of FBP1, while basal-like tumours and metastases lack it. Furthermore, FBP1 has been proven as a target of epigenetic repression during experimentally induced EMT, along with the hormonal receptors ER, PR and HER-2 in addition to E-Cadherin [60]. Indeed, the ectopic replenishment of FBP1 (under a constitutive promoter) was enough to block the EMT progression, maintain detectable levels of the hormonal receptors, and rescue the epithelial markers and morphology. In other words, *fbp1* is silenced as part of EMT, and when rescued FBP1 seems to mitigate the whole EMT program and preserve the epithelial morphology [60].

III-II-2 The breast-cancer cell-culture model to evaluate the effects of FBP1

As mentioned earlier, my choice of breast cancer cell lines as a model to investigate the effects of FBP1 mainly relates to the heterogeneity of breast tumours in respect to FBP1 expression, and also to the dynamic changes that occur on FBP1 in the contexts of EMT and metastatic events. I therefore started with two breast cancer cell lines MCF7, and MDA-MB231. The former a representative of ductal breast cancer, while the latter of distant metastatic origin. These two cell lines represent the contrast between ductal and primary tumours on the one hand, and basal-like and metastatic one on the other. FBP1 is highly expressed in MCF7 cells, while it is completely silenced in MDA-MB-231. The same applies to the hormonal receptors ER, PR, and HER-2 and also to the epithelial marker E-Cadherin. Indeed, the morphological differences between the two cell lines are simply observable under the microscope, as figure 8 clearly depicts.

To investigate the effects of FBP1 in these cell lines, I cloned the coding sequence of the FBP1 gene and established several stable constitutive over-expressions. In

addition, I used CRISPR-Cas9 gene-editing to establish deletions of FBP1 in MCF7 cells.

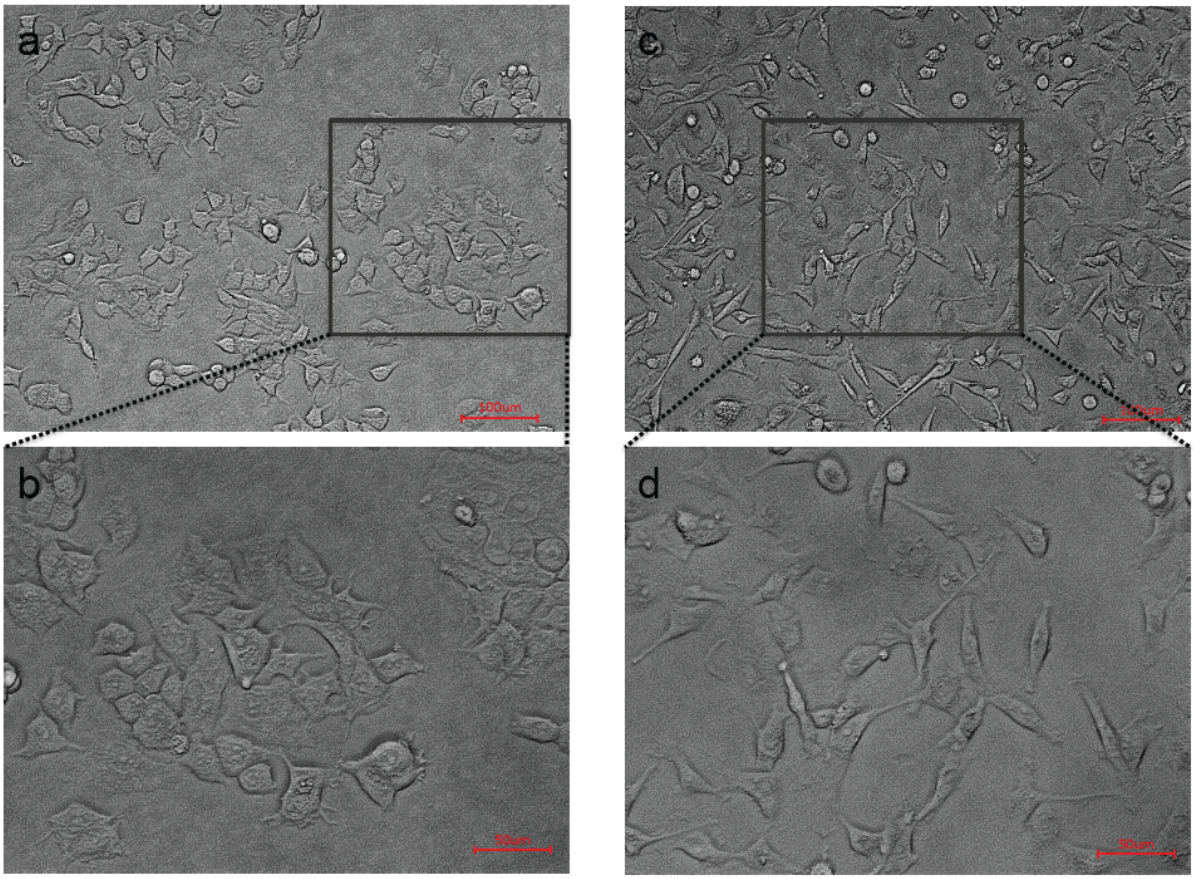

Fig 8: Microscopic features of the breast cancer cell lines used in this work:
A and b) MCF-7 cells. C and D) MDA-MB231 cells.

III-III The impact of altered FBP1 expression in breast cancer cell lines

III-III-1: The verification of the established over-expression and deletion in MCF7 cells

Both the over-expression and deletion of this enzyme were established in MCF7 and their basal effects on cells were characterized. The stable over-expression and deletion were achieved using antibiotic selection and the resulting cells were tested for the presence of FBP1 protein and its catalytic function. The tests repeatedly

verified the stable alterations in FBP1 levels and catalysis as shown in figure 9. The correlation between the increased protein levels in the over-expression cells and the increase in FBPase activity, in addition to the complete absence of FBP1 and its activity from the deletion cell-type further verifies the reliability of the established system for drawing conclusions in regards to the effects of FBP1 and its function on the metabolic, proliferative and other addressed parameters.

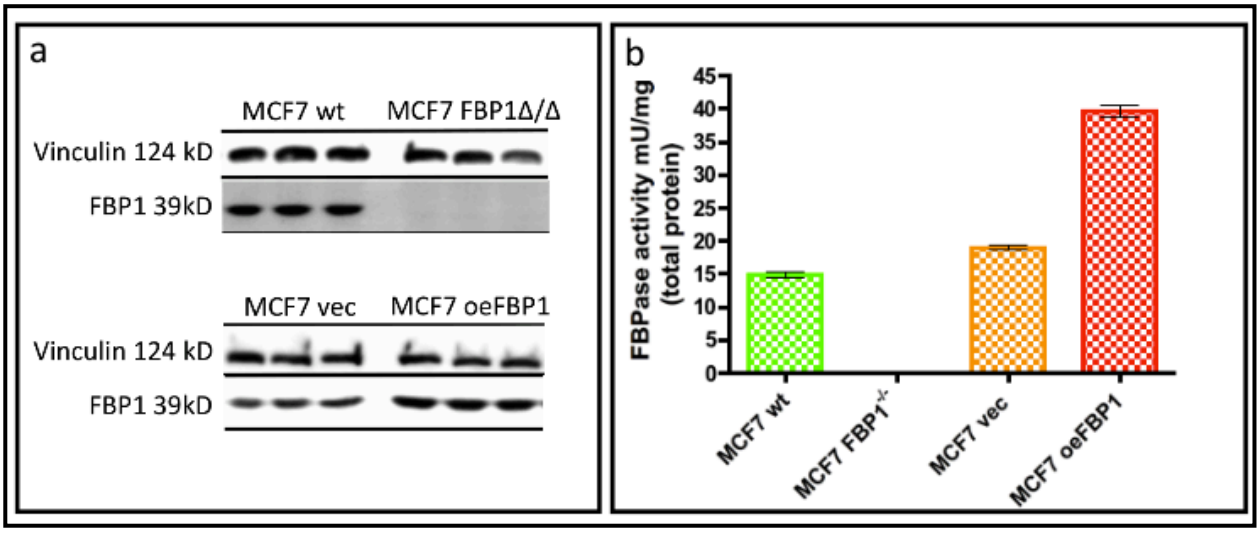

Figure 9: Verification of FBP1 over-expression and deletion in MCF7 cells.
a) Western-blots comparing the established stable FBP1 deletion and over-expression cell types to the wild type and empty-vector cells, respectively. The blots feature biologically independent triplets of each cell type. b) The measured FBPase catalysis in native protein extracts of the stably modified cell types-.

III-III-2 FBP1 over-production slows down MCF7 proliferation; the lack thereof attenuates proliferation in glucose low/deprived conditions. No visible effect of FBP1 on MCF7 capability of colony formation

I used SRB assays at several time-points to measure the impact of FBP1 on growth and proliferation rate of MCF7. The over-expression of the enzyme clearly reduced proliferation rate, while the deletion slightly induced it. This was expected due the antagonizing effect of FBP1 towards glycolysis in addition to the potential futile cycling arising from increased FBPase activity in a glucose rich environment, where gluconeogenesis is not required.

On the other hand, FBP1 is essential for survival in glucose-deprived media. To verify this speculation, I measured the growth and proliferation rate of MCF7 cells with different FBP1 expression in DMEM media with varying initial glucose concentrations.

As figure 10 b clearly shows, the unmodified (WT) MCF7 cells can survive and continue to proliferate even after 7 days in DMEM media with reduced (2mM) or annulled glucose content. Whilst the FBP1-deficient cells $FBP1^{\Delta/\Delta}$ seize to proliferate following 5 days in 2 mM glucose and as soon as 3 days in glucose-deficient DMEM. In both cases (0 and 2 mM glucose) FBP1-deficient cells perished following one week of incubation. The over-expression of FBP1 only leads to a very marginal increase in proliferation in glucose reduced or deficient media. Contrary to my initial expectations, FBP1 over-expression or depletion had no visible effect on the capacity of MCF7 to form colonies in full DMEM medium.

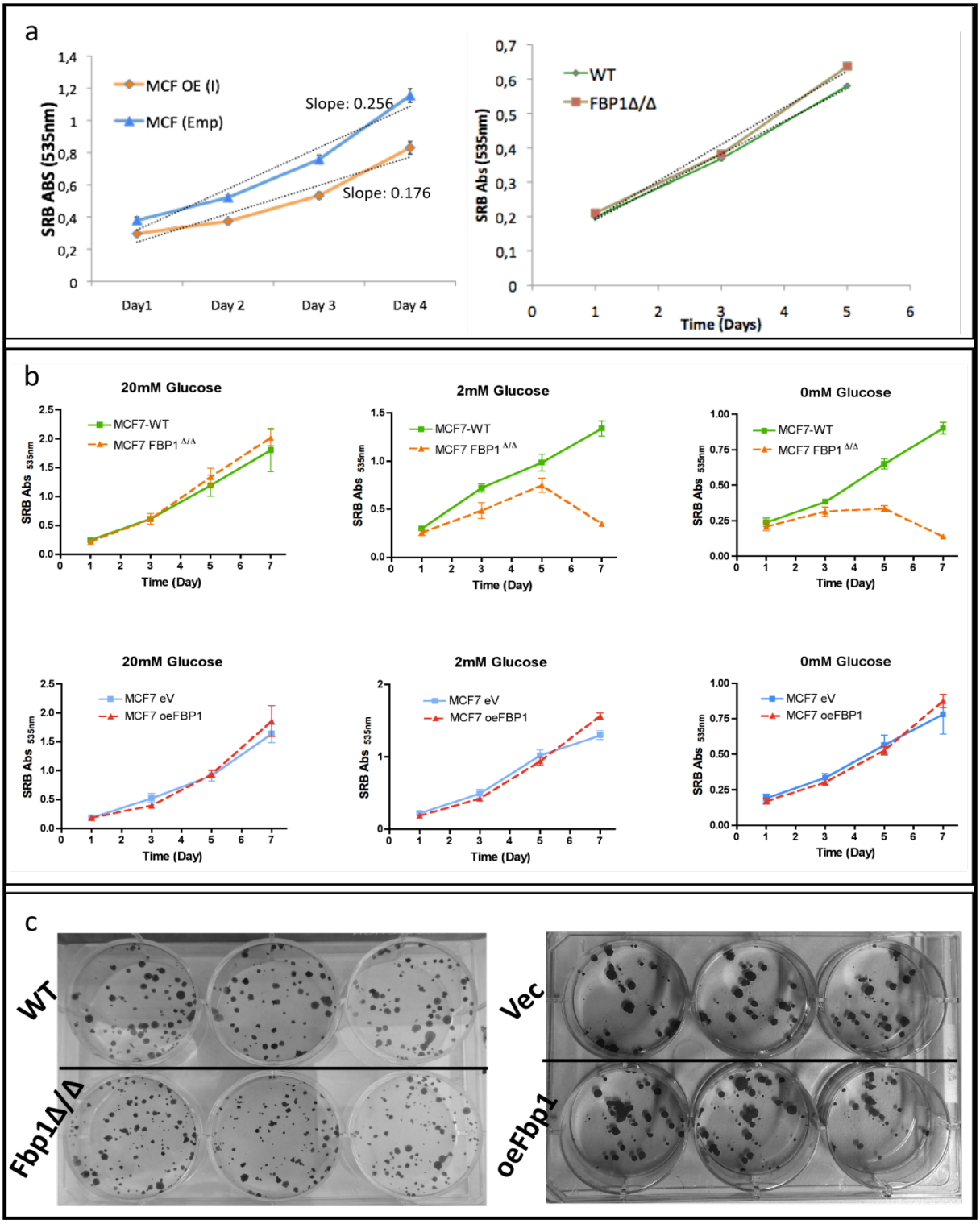

Figure 10: FBP1 effects on proliferation and colony formation:
a) SRB proliferation assays of the oeFBP1 vs empty-vector cells (left) and of the FBP1$^{\Delta/\Delta}$ vs wild-type (right). All measurements were performed with at least 6 replicates with error bars showing SD.
b) SRB proliferation assays with varying glucose concentrations c) colony forming assay in full DMEM (3 weeks).

III-III-3 The over-production of FBP1 limits glucose sensitivity and uptake in MCF7 cells, while the deletion of FBP1 winds up the flux through glycolysis and pentose phosphate shunt

It has been postulated that FBP1 slows down glycolysis both by enzymatically competing with glycolysis and also by other non-catalytic mechanisms. Therefore, I used fluorescence-labelled glucose (2-NBDG) to probe the effects of FBP1 on glucose uptake in MFC7 cells. The over-expression of FBP1 clearly inhibits glucose uptake in full DMEM. In contrast the deletion of FBP1 does not affect glucose uptake (Fig 11 a). To test the effect of FBP1 over-expression on dynamic glucose sensing in MCF7 cells, I compared glucose uptake in MCF7 cells over-expressing FBP1 to cells harbouring the control vector following glucose starvation/replenishment and also in glutamine-free DMEM (Fig. 11 b). Glucose depletion induces metabolic stress in cells and consequently activates AMPK. This in turn leads to a shift from glycolysis to TCA and oxophos fuelled by glutamine. Upon glucose replenishment, cells sense and take-up glucose eventually reducing the metabolic stress, and cells shift back to glycolysis. Glutamine depletion in turn, deprives the TCA from an important precursor, leading to increased reliance on glucose. Indeed, glutamine deprivation induced glucose uptake in both oeFBP1 and vector control cells. Comparing the two cell types, FBP1 over-expression correlates to decreased glucose uptake in all three conditions; full DMEM, glucose deprivation followed by 4 hours replenishment and glutamine-free DMEM (Fig 11 b). This points out to a general inhibitory effect of FBP1 on cellular glucose uptake. Especially in glutamine-deprived media, FBP1 seem to limit the cells' compensatory capacity to maximise glucose uptake. Due to the increased difference in glucose uptake rate between oeFBP1 and control vector cells upon glucose replenishment, I speculated that FBP1 should alter glucose sensitivity in cells. To test this, I used the theoredoxin-interacting protein (TXNIP) as a marker of glucose sensitivity and uptake. TXNIP is a pro-oxidaton protein that also functions as a glucose sensor and eventually mediates a negative feedback loop that slows down and regulates glucose uptake. TXNIP expression is mediated by glycolytic intermediates on a transcriptional level, and energetic stress leads to TXNIP ubiquitination and degradation. Therefore, the more glucose is taken up and funnelled towards glycolysis, the higher the resulting TXNIP expression. Following

glucose starvation, TXNIP is completely depleted form the cells. In contrast, glucose presence in DMEM is enough to maintain a medium level of TXNIP expression whereas 2-Deoxyglucose is a potent inducer of TXNIP due to its phosphorylated analogue which cannot be further isomerised, and therefore accumulates in the cells and drives TNXIP expression (Fig. 11 c and d). Glucose replenishment restores TXNIP expression to a level that corresponds to the amounts of glucose taken up and phosphorylated. Therefore, TXNIP level makes a suitable marker for glucose sensitivity following depletion and replenishment. Compared to unmodified MCF7, FBP1 deficient MCF7 cells exhibit higher levels of TXNIP expression both in base-line conditions (full DMEM) and following glucose starvation/replenishment with different glucose concentrations (Fig. 11 c and d). In contrast, the over-expression did not lead to as clear and reproducible differences in TXNIP induction following glucose deprivation/replenishment. This might in part be due to the fluctuations in the levels of FBP1 over-expression as clearly seen when comparing the western blots in figures 11 c (lower panel) and 11 e. Consistent with its effects on glucose uptake and sensitivity, the absence of FBP1 induces the glycolytic flux. It also leads to clear induction of the pentose phosphate pathway whose effects are clearly reflected in the increase in reduced/oxidized glutathione ratio. Moreover, the increased lactate levels combined with decrease in most TCA intermediates signify an increase in aerobic fermentation.

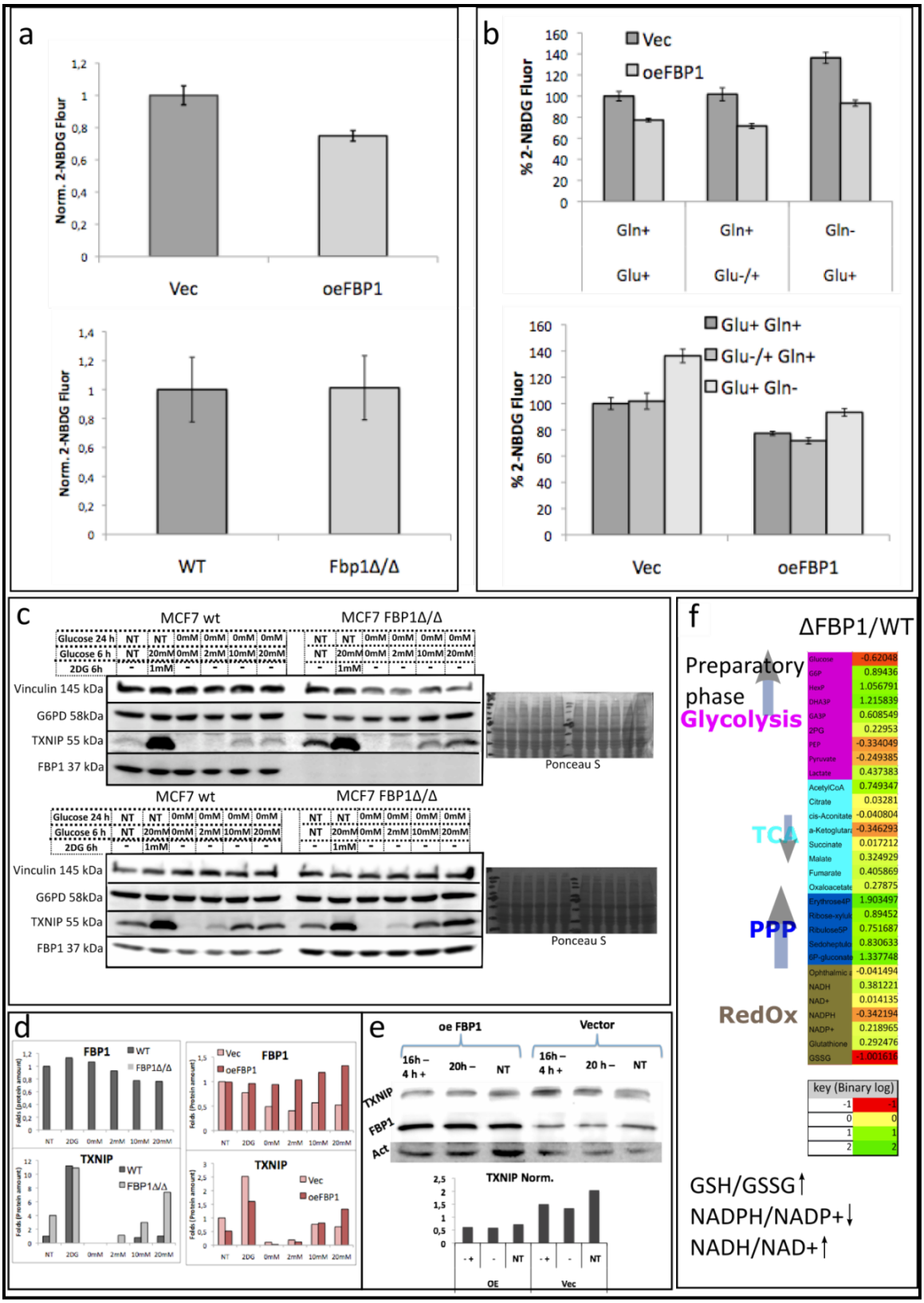

Figure 11: The over-production of FBP1 slows down glucose uptake, the deletion thereof induces glycolytic flux. a) Glucose uptake in full DMEM (20mM glucose, 2mM Glutamin) measured by FACS analysis of cells incubated with 2-NBDG for 4 hours. 5000 cells were analyzed, data represents mean-values (n≥4) error-bars (SD). b) Glucose uptake in glutamin-depleted DMEM and following depletion and replenishment of Glucose. Glucose depletion (Glu-/+) was done for 16 hours,

followed by 4 hours with replenishment at 20mM Glucose accompanied by 2-NBDG. Glutamin depletion (Gln-) was done for a total of 20 hours, including the 4 hours of incubation with 2-NBDG. c) Western blot of cells lysed following glucose starvation and replenishment. d) Quantifications of the western blot bands in (c). Signal intensity of each band was normalised to the corresponding loading control (Vinculin) band. e) Western blot of cells lysed following glucose starvation/replenishment. f) Heat map featuring metabolomics flux analysis of FBP1-deficient MCF7 cells compared to unmodified (WT) MCF7 cells. The data features the binary-logarithmic fold changes in the levels of individual metabolites in FBPΔ/Δ compared to WT cells.

To further verify the correlation between FBP1 expression and glucose sensitivity in altered TXNIP levels, I performed western-blots on independent triplets of each glucose starvation/replenishment condition discussed above. TXNIP was immunoblotted along with FBP1, in addition to pACC and pAMPK as sensors of energy stress and mediators of adaptation to nutrient scarcity. In complete glucose starvation for 20 hours, AMPK is phosphorylated in both wild type, and FBP1-deficient MCF7 cells. Acetyl co-enzyme A carboxylase is a direct phosphorylation target of phosphorylated (activated) AMPK. Compared to unmodified MCF7 cells, BP1-deficient MCF7 show stronger phosphorylation of pACC (Fig 12. A) and very slight increase in AMPK phosphorylation. This reflects increased sensitivity to glucose deprivation in absence of the FBP1 due to inhibited gluconeogenesis. In contrast with glucose abundance, TXNIP expression is diminished upon glucose deprivation due to both the absence of glycolytic metabolites and AMPK activation. In the glucose-replenished condition, 4 hours of 20 mM glucose following 20 hours of glucose deprivation, FBP1-deficient cells exhibit much higher TXNIP levels than unmodified cells. This indicates faster response to glucose replenishment in the absence of FBP1. In glucose abundant condition, constant incubation with 20 mM glucose, FBP1-deficient cells also have higher levels of TXNIP expression compared to wild-type cells. This can stem from the increased glycolytic flux in the FBP1Δ/Δ, especially the accumulation of glucose-6-phosphate G6P which indirectly induces TXNIP expression via interaction to its transcription factors.

IN other words, knocking out FBP1 renders the cells more sensitive to glucose deprivation, as seen by increased AMPK and ACC phosphorylation. However, the FBP1-deficient cells also become faster at sensing and taking up glucose upon replenishment. Further repetition of these western-blot is required to statistically

consolidate these findings, the use of multiple controls and general protein staining of membranes should be included to overcome the large deviation in these results.

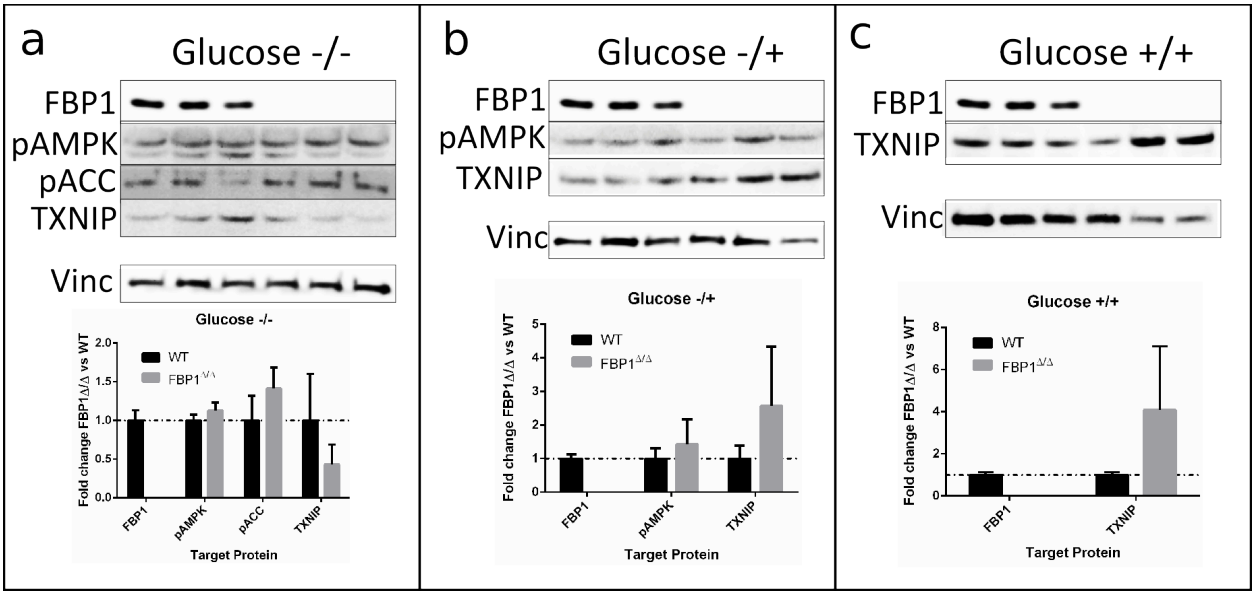

Figure 12: Western-blots showing the FBP1-related alterations in glucose sensitivity and response to glucose starvation in MCF7 cells. a) Full glucose deprivation 0 mM glucose for 24 hours. b) Glucose replenished condition, 20 hours of glucose starvation followed by 4 hours of glucose replenishment 20 mM. c) Full medium 20 mM glucose. All western-blots feature biologically independent, simultaneously treated triplets of wild-type and FBP1-knockout MCF7.

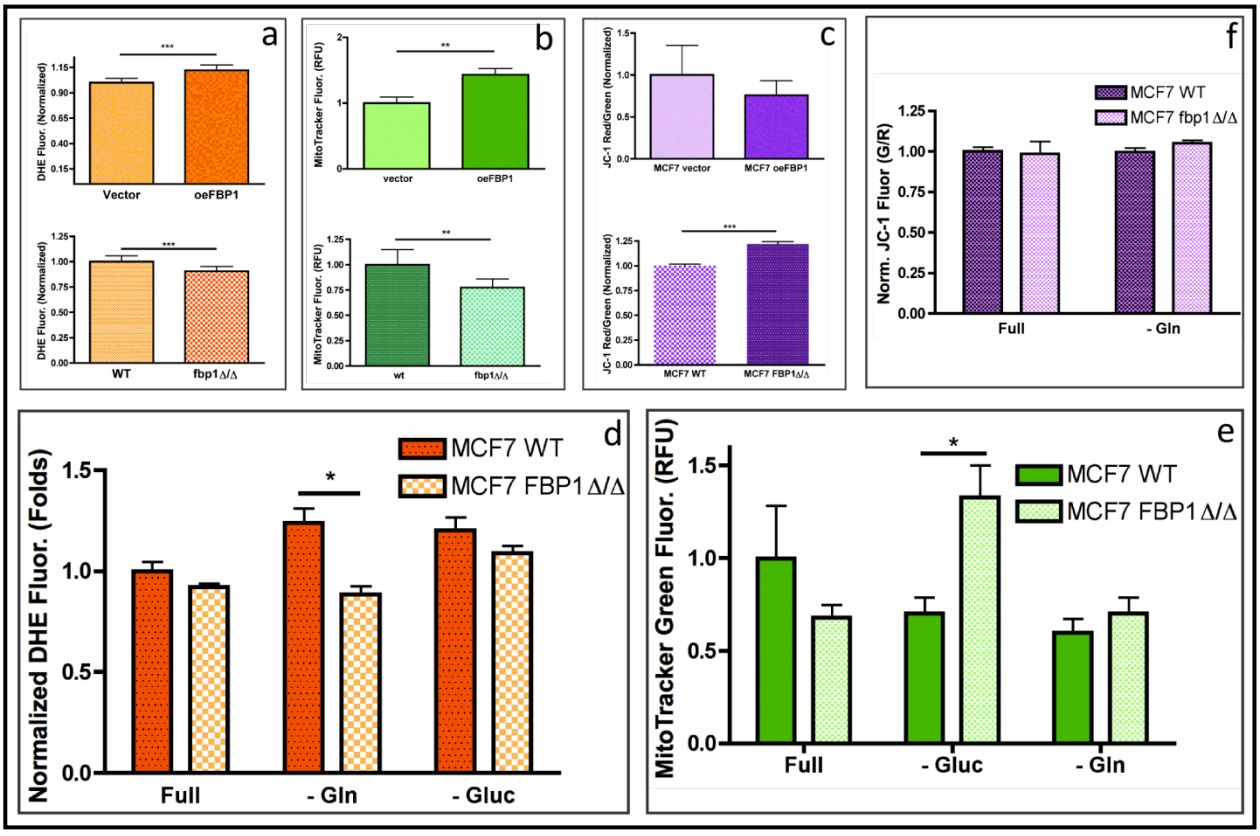

Figure 13: FBP1 increases oxidative stress and mitochondrial biomass.
a) ROS accumulation in cells cultivated in full DMEM measured using DHE fluorescence. b) Mitochondrial mass in full DMEM measured using the MitoTracker® green probe. c) Mitochondrial

inner-membrane potential MIMP measured using JC-1 in cells cultivated in full DMEM. In a,b,c cells were analyzed using FACS analysis, the bar-plots feature the fluorescence mean-values of at least 4 completely independent replicates of 5000 cells each normalized to the non-treated wild-type or control vector cells, and error bars represent the SD. d) ROS accumulation in cells deprived of glucose or glutamine compared to full medium. DHE-labelled cells were analyzed using FACS (5000 cells measured). The bar-plots feature the mean-values of 3 biologically independent parallel replicates and error bars represent the standard deviation. e) Mitochondrial mass in cells deprived of glucose or glutamine compared to full medium. MitoTracker Green labelled cells were measured using FACS, the bar-plots feature the mean-values of at least 3 independent replicates and the error bars represent the standard deviation. f) The mitochondrial inner-membrane potential measured using JC-1 in glutamine-deprived cells vs cells in full medium. 5000 labelled cells were measured using FACS. The bar-plots feature the mean-values of at least 3 independent replicates and the error bars represent the standard deviation.

III-III-4 Quantitative gene expression analysis upon transient FBP1 over-expression shows down-regulation of M-phase factors. Cell-cycle validation of these findings on a functional levels

To dynamically assess the FBP1-induced transcriptional alterations I measured the transcriptional levels of several genes after 4, 24, and 96 hours of transecting the cells with Fbp1. The examined genes were assigned based on predictions from observed functional roles of Fbp1, a full gene-expression analysis of MDA-MB231 with ectopic FBP1 (will follow in the upcoming part of this chapter) in addition to genes of interest based on the existing literature. The changes in expression of the target genes were quantified relative to the combination of three reference genes; beta-actin, vinculin and the ribosomal protein 30 RPL30. As predicted, a stark increase in the number of Fbp1 transcripts was observed in the cells harbouring the over-expression plasmids at all three time points following transfection. The most pronounced effects were found 4 days post-transfection, at which most of the examined genes were down regulated in response to Fbp1 over-expression (Fig.14 a). Exceptions to this were *Glutaminase1* and *UCH-L1*, both slightly up regulated, consistently with the findings in other cell-lines to be reported later in this chapter. In line with several reports of a multiplex antagonistic effect of Fbp1 towards the hypoxia induced factor 1 alpha, *hif1*α was down-regulated 96-hours post-transfection with Fbp1. *Fam38a*, a proto-oncogene linked to metastasis and poor prognosis [98], was also among the markedly down-regulated genes. Contrary to our expectations, *E-cadherin* was also down- regulated upon Fbp1 over-expression despite existing knowledge of a correlation of Fbp1 to epithelial phenotype and its reported counter-

EMT role (Fig. 14 a)[60]. The most prominently down-regulated target is the centrosome-associated protein e *CENP-E*, an essential pro-metaphase protein that promotes chromosomal segregation and also an activating factor for the spindle assembly checkpoint SAC [99]. In addition to the stark repression of *CENP-E* there is a clear down-regulation of aurora-kinase *AURKA*, a wide range serine/threonine protein kinase found in centrosome and essential for normal chromosome segregation (Fig. 14 a) [100]. Both suggest a slow down in the metaphase and possibly a slower cell cycle. Indeed, the DNA-content cell cycle analysis of the MCF7 cells with FBP1 over-expression compared to unmodified MCF7 exhibited significant increase of the G2-phase cell fraction on the expense of the G1-phase, which points to a slowed down meta-phase in accordance with the aforementioned transcriptional observations (Fig. 14 b).

A thorough interpretation and discussion of the remainder of the genes included in this expression in contrast with the results obtained from other cell lines will still follow after the characterisation of the behaviour of the other included cell lines in light of altered FBP1 expression is fully presented.

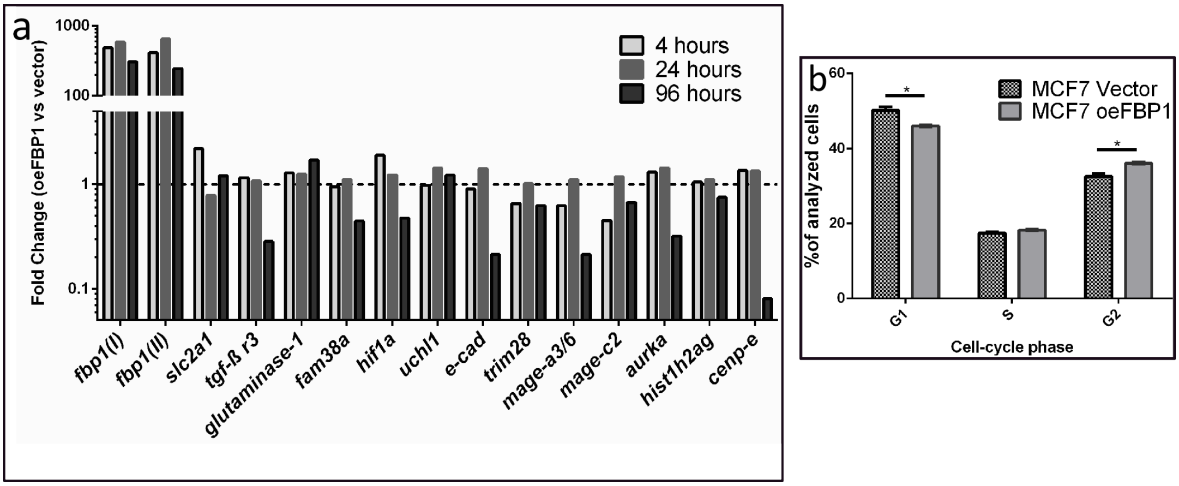

Figure 14: FBP1 over-expression induces variable transcriptional alterations and slows down mitosis.

a) relative expression values in MCF7 cells (oeFBP1 vs vector-control) from a qPCR at three time-points; 4, 24, 96 hours post-transfection. The bar-chart depicts relative expression values of the target genes calculated in comparison to a combination of three house-keeping control genes; beta-actin, ribosomal protein L30 RPL30, and vinculin. b) Cell-cylce analysis based on DNA-content measurement using FACS analysis of properly permeabilised and propedium-iodide stained cells. The charts feature the averages of three parallel technical replicates, (N=3) error-bars: SD.

III-III-5: MDA-MB-231 degrade the ectopically expressed FBP1, protease inhibitors can reverse the process and rescue the ectopic FBP1 expression

MDA-MB231 cells originate from a metastatic breast tumour. Lacking the hormonal receptors and featuring a mesenchymal morphology, these cells are representatives of the triple negative breast cancers. As mentioned earlier, this wide category of basal-like and metastatic breast tumours also exhibit repressed FBP1. To investigate the advantages bestowed on the cells via FBP1 repression, I sought to reverse this using stable ectopic over-expression of FBP1 in MDA-MB231 cells. Upon parallel transfection of both MCF7 and MDA-MB231 cells, transfected cells were selected using Geneticin. The established over-expressions were compared to the cells from the same type transfected with an empty vector as a control. Surprisingly, the MDA-MB231 cells harbouring the FBP1 over-expression vector showed a very minimal, almost negligible, amounts of FBP1 compared to the MCF7 cells (Fig 15 a). However, real-time PCR showed a clear increase in the level of FBP1 mRNA in the MDA-MB231 cells with the over-expression vector (Fig 15 b). Similarly, an increase in mRNA was also observed in the MCF7 cells, in which the stable over-expression of FBP1 was robustly verified on the protein level. This discrepancy between the detected mRNA and the almost absent FBP1 protein in the MDA-MB231 cells is suggestive of possible post-translational degradation of the protein, especially considering that the protein was successfully detected upon transient transfection. Therefore, I probed the levels of FBP1 protein in the MDA-MB231 upon proteasome inhibition. Indeed, following 48-hours of bortezomib treatment, FBP1 expression was clearly detectable in MDA-MB231 with FBP1 over-expression vector to levels comparable to those detected in MCF7, while unmodified MDA-MB231 containing the empty vector still lacked any FBP1 (Fig. 15 c9). To further confirm the complicity of the proteasome in degrading the ectopic FBP1 and eliminate the potential of non-proteasomal or indirect effects of bortezomib, I used the more specific MG132 proteasome inhibitor. A shorter treatment of 24-hour of MG132 or bortezomib was sufficient to rescue FBP1 over-expression (Fig. 15 d) and so was a 16-hour treatment with a gradient of MG132 concentrations (Fig. 15 d).

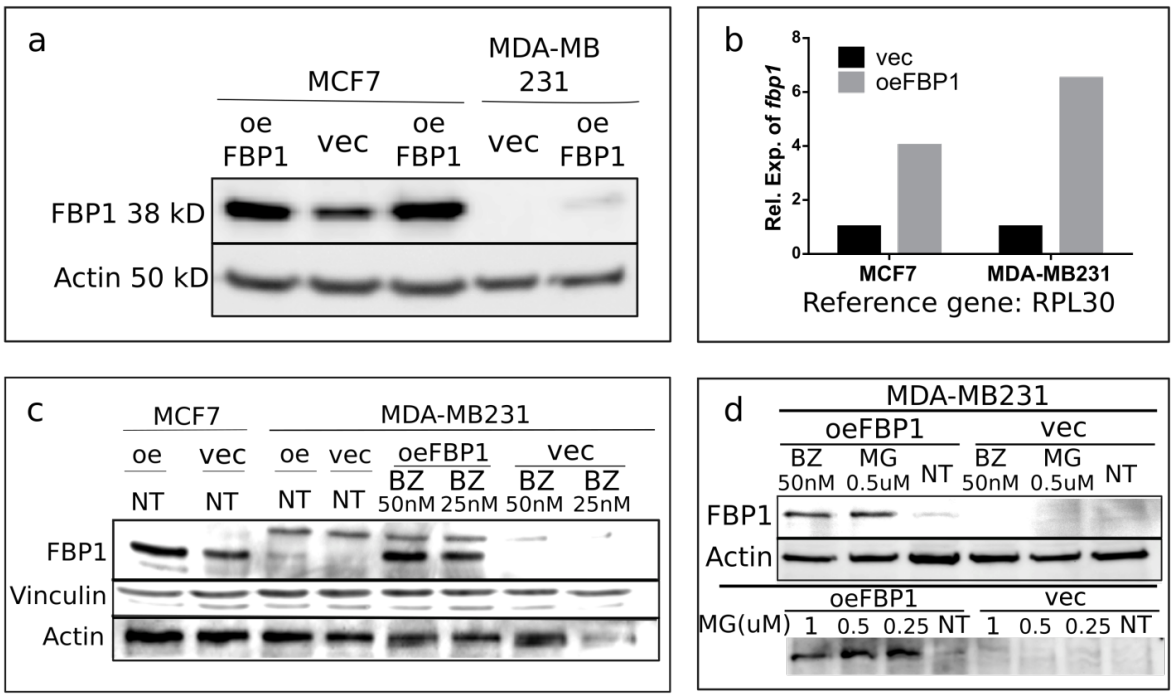

Figure 15: MDA-MB231 cells degrade the ectopically expressed FBP1. a) Western-blot showing the levels of over-expressed FBP1 in MDA-MB231 cells compared to those of MCF7 cells with FBP1 over-expression or with empty vector. Actin is used as loading control. b) qPCR showing the levels of fbp1 transcript in MCF7 and MDA-MB231 cells compared to cells carrying the empty vector. Rpl30 was used as a house-keeping reference gene. c) Western-blot featuring the levels of FBP1 in bortezobmib-treated (48 hours) MDA-MB231 cells with FBP1 over-expression plasmid compared to cells harbouring the empty vector. Non-treated MCF7 cells (oeFBP1, vector control) were used as a positive reference for FBP1. Vinculin and actin are used as loading controls. d) (up) Western-blot showing FBP1 levels in MDA-MB231 cells (oeFBP1 vs vector control) d) Western-blot showing FBP1 levels in MDA-MB231 cells (oeFBP1, vector control) following 24 hours of bortezomib (BZ) or MG132 (MG) treatments. Actin was used as a loading control. (Low) Western-blot showing the levels of FBP1 in MDA-MB231 cells upon 16-hour treatment with a concentration-gradient of MG132.

III-III-6: Analysis of the impact of FBP1 over-expression on the gene expression profile of MDA-MB231 cells

The post-translational elimination of ectopically introduced FBP1 in the FBP1-negative MDA-mb231 cells, implies that the metabolism of these cells is best adapted to the loss of this enzyme and the total absence of gluconeogenesis as a pathway. Thus, we assumed that Fbp1 expression should correlate to notable alterations in the gene expression programs of these cells. Additionally, we asked whether the capacity to degrade FBP1 is inherent to the MDAmb231 cells or rather an acquired trait gained through selection. To address these questions we compared the gene-expression profiles of the stably transfected MDA-mb231 cells with oeFBP1 to those harbouring the same empty expression vector.

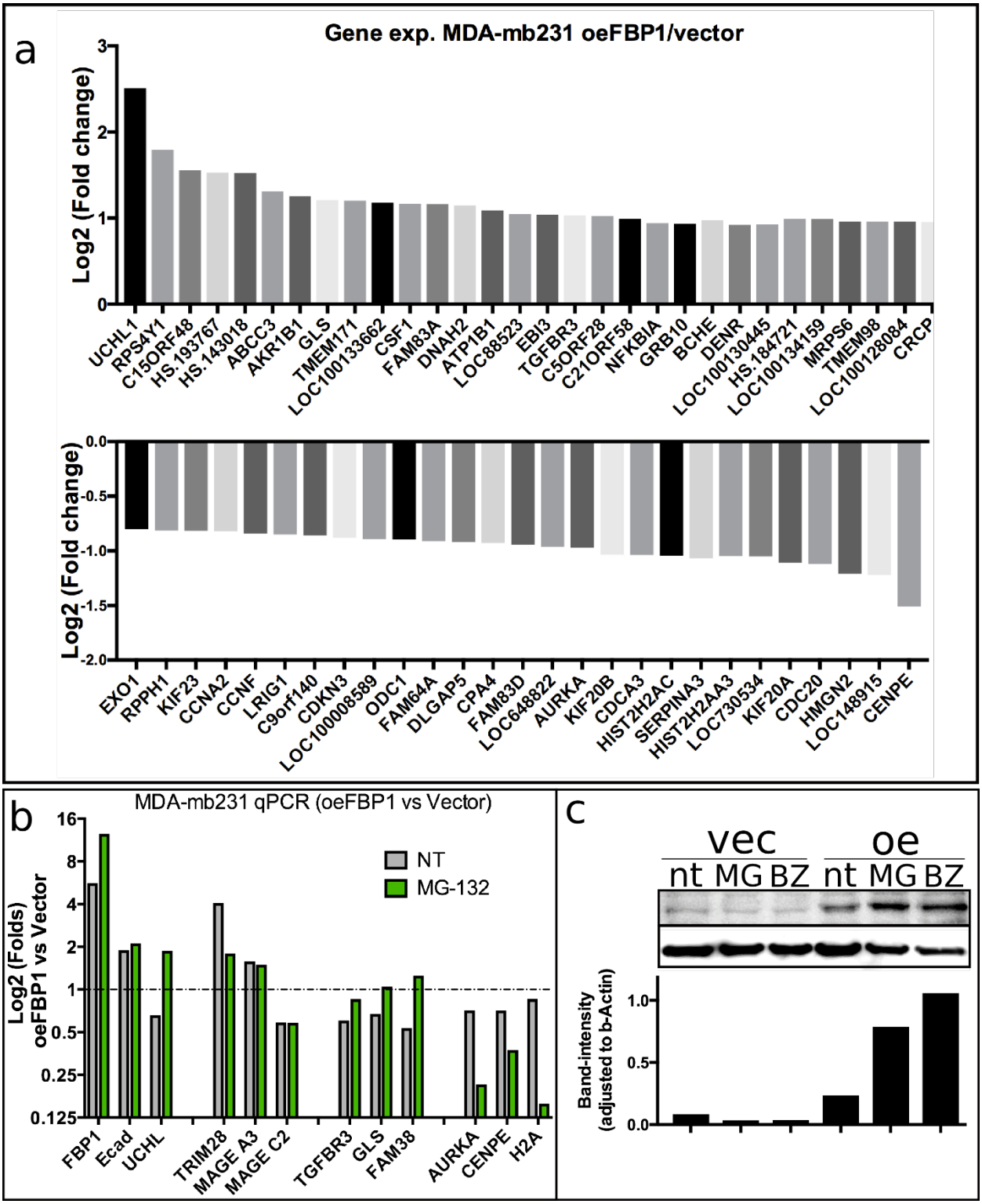

Figure 16: Discerning the effects of ectopic FBP1 on the over-all gene expression levels in MDA-mb231. a) As identified from a full transcriptome analysis: Upper-panel**:** The most up-regulated genes in the oeFBP1 compared to empty vector cells. Lower-panel: The most down-regulated genes in the oeFBP1 compared to empty vector cells. b) Quantitative rt-PCR featuring the relative expression (oeFBP1 vs vector) of a selection of genes (identified as top-regulated targets in the gene exp. profiling) in MDA-mb231cells. c) Western-blot depicting FBP1 levels in MDA-mb231 cells (oeFBP1 and vector) upon 4-hour treatment with one of the proteasome inhibitors MG-132 (0.5 μM) or Bortezomib (50 nM).

Among the most transcriptionally up-regulated genes (<2 folds induction) in FBP1 over-expression cells are those coding for several ribosomal proteins, proteins with an ATPase function, inflammation-related factors. Notable among these are also several individual proteins including UCH-L1, which plays a role in ubiquitin processing, glutaminase, the aldo-keto reductase (converting glucose to sorbitol as an initial step in the aldose pathway) and FAM83a, a proto-oncogene participating in the signal transduction from EGF-R to RAS/MAPk and PI3k/AKT/mTor. While the most up-regulated genes contribute to various functions and pathways, a majority of the most strongly down-regulated genes (<2 folds inhibition) are essential for the cell-cycle progression through the metaphase (M-Phase). Out of 23 top up-regulated genes, 15 are involved in cell cycle progression, vast majority of them involved in the initiation and progression of mitosis (M-phase) with two genes involved in the initiation and progression of DNA-replication (S-phase). Other most down-regulated genes are also indirectly involved in DNA-replication; these include two histone genes (H2AA3, H2AC), and a DNA-repair gene (*Exo1).* Other down-regulated genes include the key regulatory enzyme of the polyamine biosynthetic pathway ODC1 and the ubiquitination enhancer *LRIG1.* To confirm the link between the over-expressed FBP1 and the observed trends in gene-expression quantitative-PCR of a selection of the most differently regulated genes identified in the gene expression profiling. In addition to the normal (non-treated conditions) the levels of mRNA transcripts of the selected target genes were also compared upon treatment with MG-132, a proteasome inhibitor that stabilises FBP1 expression (as shown in sub-section II-III-6). Particularly for the 3 cell-cycle and/or DNA-replication related genes tested, slight down-regulation is seen in the non-treated condition. Meanwhile the proteasome inhibition further inhibited the expression of AURKA, CENP-E and HIST2H2AC in the cells over-expressing FBP1 compared to cells containing the empty vector. The mRNA levels of Fbp1 were clearly higher in the OE cells in both treated and non-treated conditions. The actual increase in the ectopically expressed FBP1 protein levels following proteasome inhibition was also verified using immuno-blotting (Fig.16 c).

Interaction network of the up-regulated genes upon FBP1 over-expression

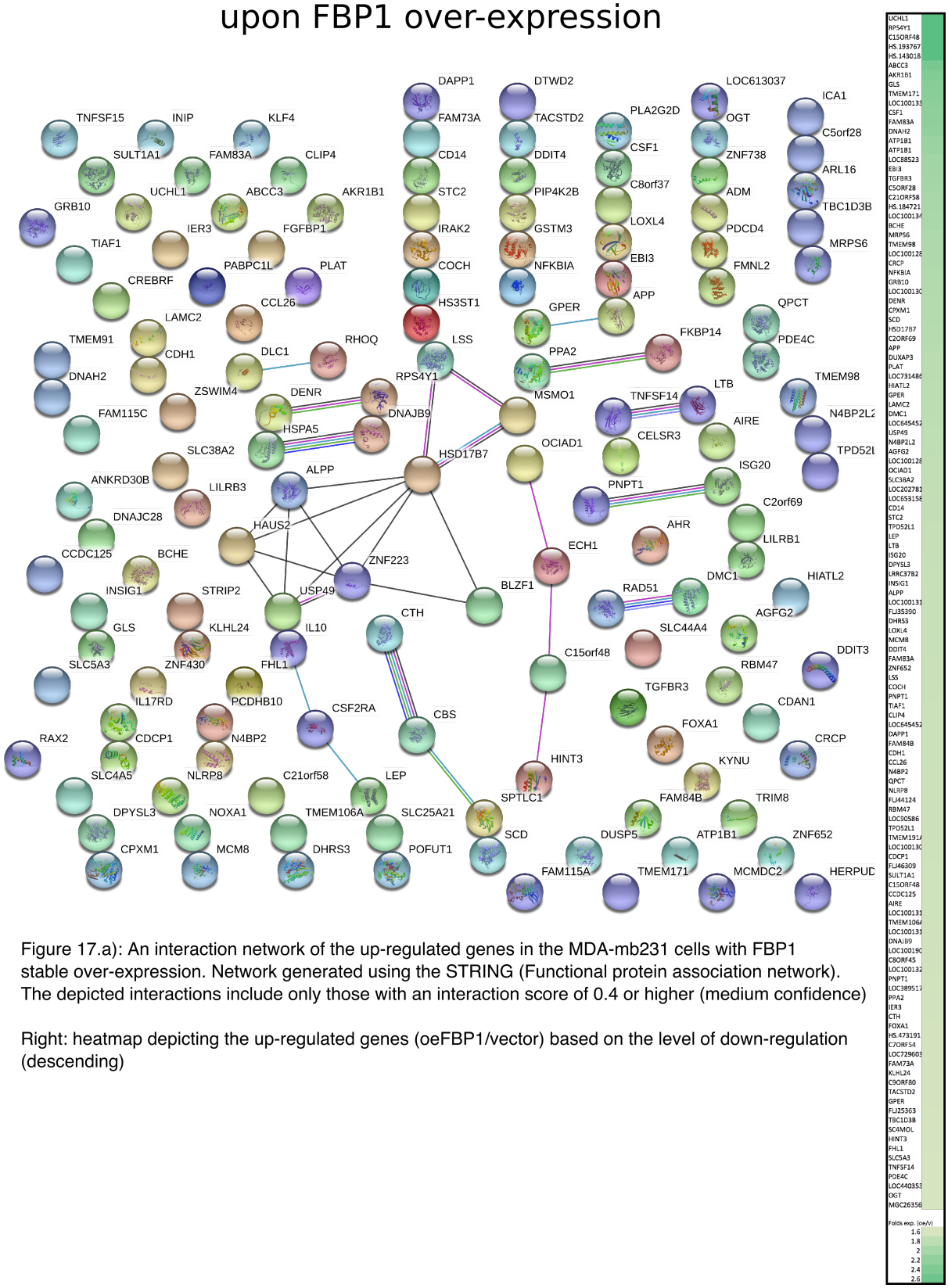

Figure 17.a): An interaction network of the up-regulated genes in the MDA-mb231 cells with FBP1 stable over-expression. Network generated using the STRING (Functional protein association network). The depicted interactions include only those with an interaction score of 0.4 or higher (medium confidence)

Right: heatmap depicting the up-regulated genes (oeFBP1/vector) based on the level of down-regulation (descending)

Interaction network of the down-regulated genes upon FBP1 over-expression

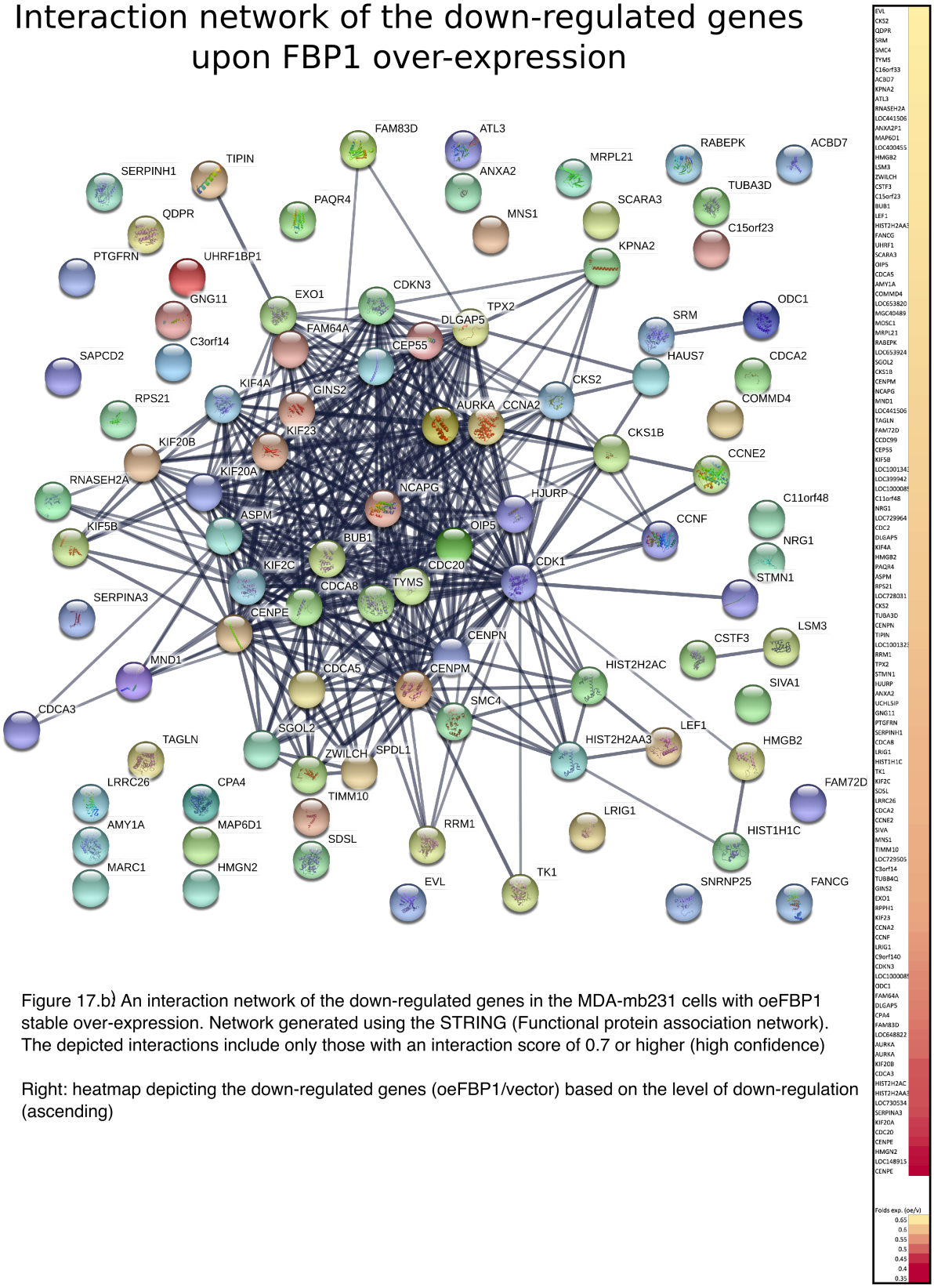

Figure 17.b) An interaction network of the down-regulated genes in the MDA-mb231 cells with oeFBP1 stable over-expression. Network generated using the STRING (Functional protein association network). The depicted interactions include only those with an interaction score of 0.7 or higher (high confidence)

Right: heatmap depicting the down-regulated genes (oeFBP1/vector) based on the level of down-regulation (ascending)

In order to assess the wider influence of FBP1 on cellular functions and pathways, more genes had to be included in the analysis than the initially discussed top regulated targets. Therefore, I performed a wider analysis of the impact of FBP1 over-expression on gene-expression patterns in MDA-mb231 including a larger pool of up-regulated (≥1.6 folds) and down-regulated (≤0.65 folds) genes (Figure 17 a and b). Using the STRING functional protein association network, two separate interaction networks of the proteins encoded by the up-regulated and down-regulated genes were made. Comparing the two interaction networks, the most noticeable difference is the clear arrangement of the down-regulated genes into an interaction-rich network (Figure 17 b). At the centre of this network are proteins associated with the cell cycle progression; the vast majority are proteins essential for mitosis and cytokinesis (M-Phase) these include the centrosome proteins CENP- A,E,M,N, aurora kinase A AURK-A and its activator TPX, the kinesin family members KIFs 2C, 4A, 20A, 20B, 23 and the centrosomal protein CEP55. Besides M-phase proteins, several other genes encoding for essential cell-cycle proteins are also seen within the aforementioned interaction network. These include, the Cyclin A2 essential for the cell cycle progression G1/S and G2/M transitions through activating CDK1 (also among the down-regulated genes) and CDK2. Other down-regulated genes include the histone cluster 2 (H2AC and H2AA3) in addition to Thymidilate synthetase essential for thymidine de-novo biosynthesis and the exonuclease 1 EXO1 essential for DNA-mismatch repair. In contrast with the heavy interactions observed between the down-regulated genes, the interactions among the up-regulated genes are scarce. Therefore no wider conclusions regarding the up-regulation of entire signalling pathways or cellular functions could be drawn.

I next sought to probe the transient effects of FBP1 over-expression on gene expression. Protein and mRNA were extracted from parallel cultivated and transfected MDA-mb231 and HT-29 cells and MCF7 cells. Both protein and mRNA were extracted after 4, 24 and 96 hours from each of the transfected cell lines. Using immune blotting the levels of FBP1 protein expression at each time-point were probed in contrast to cells transfected with the empty vector. No expression was observed in either of the cell lines at 4 hours following transfection. In MDA-mb231

cells, successful expression was detected 24, and 96 hours upon transfection. In HT-29, FBP1 expression was detected only at 24 hours after transfection. Taken together with the observations of the proteasomal degradation of FBP1 in stably transfected MDA-mb231 cells, these findings implicate that MDA-mb231 and HT-29 cells are both capable of acquiring the capacity to eliminate the over-expressed FBP1. However, a proteasomal mechanism of FBP1 degredation was repeatedly shown in MDA-mb231 using proteasomal inhibition to successfully rescue FBP1 expression. Whereas similar proteasome inhibition failed to rescue FBP1 expression in HT-29 cells. The underlying reason can be the discrepancy in the concentrations of proteasome inhibitors required for rescuing the ectopically introduced FBP1.

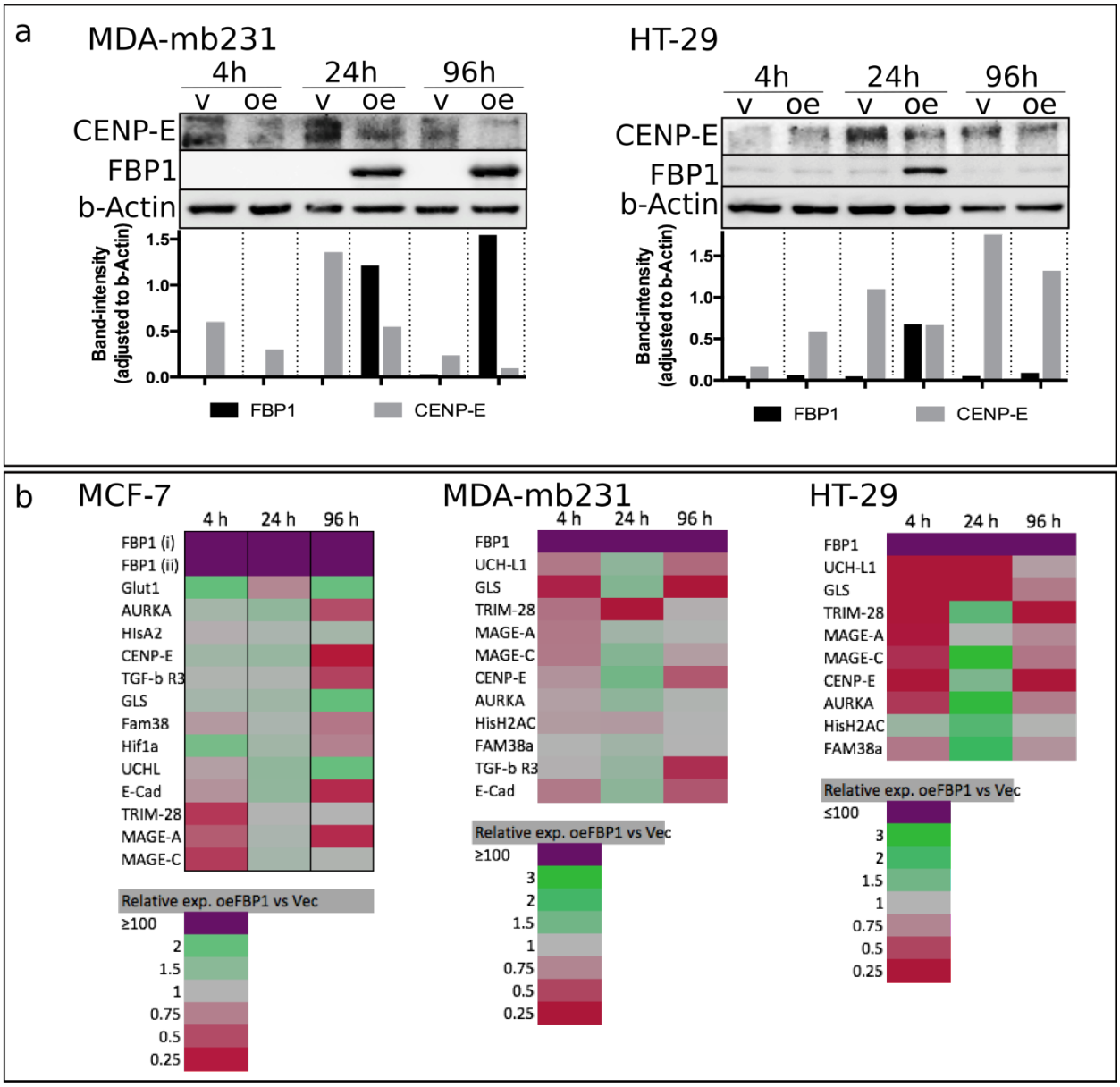

Figure 18: a) Western-blots showing the levels of transient over-expression of FBP1 4, 24 and 96 hours post-transfection and the concomitant levels of CENP-E. Left: MDA-mb231, Right: HT-29.
b) Quantitative rt-PCR analysis of several top down and up-regulated genes upon FBP1 over-expression.

Since the gene expression analysis demonstrated tangible and wide-range down-regulation of a plethora of genes coding for cell-cycle factors, especially M-Phase associated genes, upon the ectopic expression of FBP1. I probed the impact of FBP1 over-expression on the levels of the centromere protein E (CENP-E). CENP-E turned out as the most down-regulated gene in response to FBP1 over-expression in the full-scope gene expression analysis in MDA-mb231 cells, it stabilizes the interaction between the kinetochore and the microtubule and is therefore pivotal for chromosomal stability during M-phase and for correct chromosomal alignment on the metaphase prior to the anaphase. The immune blotting of protein extracts from transiently transfected cells showed a noticeable decrease in the CENP-E protein levels in FBP1 over-expressed cells compared to the controls harbouring an empty vector. Moreover, the plummeting CENP-E levels perfectly coincided with successful FBP1 protein expression as seen in both MDA-mb231 and HT-29 cells (Fig. 18 a).
Parallel to the immune detection of transiently expressed FBP1, mRNA was extracted from similarly treated samples and the top regulated genes from the expression profiles of MDA-mb231 cells with stable FBP1 over-expression were probed.

III-III-7 The ectopic expression of FBP1 inhibits glucose and acidification, hinders colony formation and leads to increased mitochondrial mass in MDA-mb231

After establishing the stable over-expression of FBP1 in MDA-mb231 and the observation of the proteasomal degradation of ectopically introduced fbp1, I sought to assess some of the metabolic effects of stable FBP1 over-expression in MDA-mb231. Unlike in MCF-7 cells, the ectopically expressed FBP1 showed no effect on glucose uptake levels measured using FACS analysis of 2-NBDG labelled cells (Fig. 19 a).

I assumed that this discrepancy is due to the very low basal levels of FBP1 expression in MDA-mb231 cells compared to MCF-7. This speculation is supported by the widening gap in glucose uptake between oeFBP1 and vector cells upon bortezomib treatment. As previously shown, bortezomib stabilizes and rescues ectopically expressed FBP1. Bortezomib treatment increased the overall glucose uptake in both vector and oeFBP1 cells (Fig. 19 a). However, the increase was markedly smaller in cells expressing oeFBP1 compared to their counterparts harbouring the empty vector, leading to an Fbp1-associated significant difference of glucose uptake in bortezomib treated cells. Further discrepancy in the effects of FBP1 over-expression in redox homeostasis and mitochondrial function was observed in MDA-mb231 cells compared to MCF-7 cells. MDA-mb231 with FBP1 over-expression exhibited markedly depleted ROS levels, as measured by FACS analysis of DHE labelled cells (Fig.19 b). Probing the cells with JC-1 hinted at diminished mitochondrial inner-membrane potential MIMP upon FBP1 over-expression (Fig. 19 c). However, cells with FBP1 over-expression bestowed larger overall mitochondrial mass, measured using the specific mitochondrial probe MitoTracker® green (Fig. 19 d). Most notably, the MDA-mb231 cells show diminished colony formation and expansion compared to the control cells with empty vector (Fig. 19 e). This observation perfectly consists with the aforementioned results of gene expression analysis that indicated an overall cell-cycle inhibition especially at the M-Phase levels.

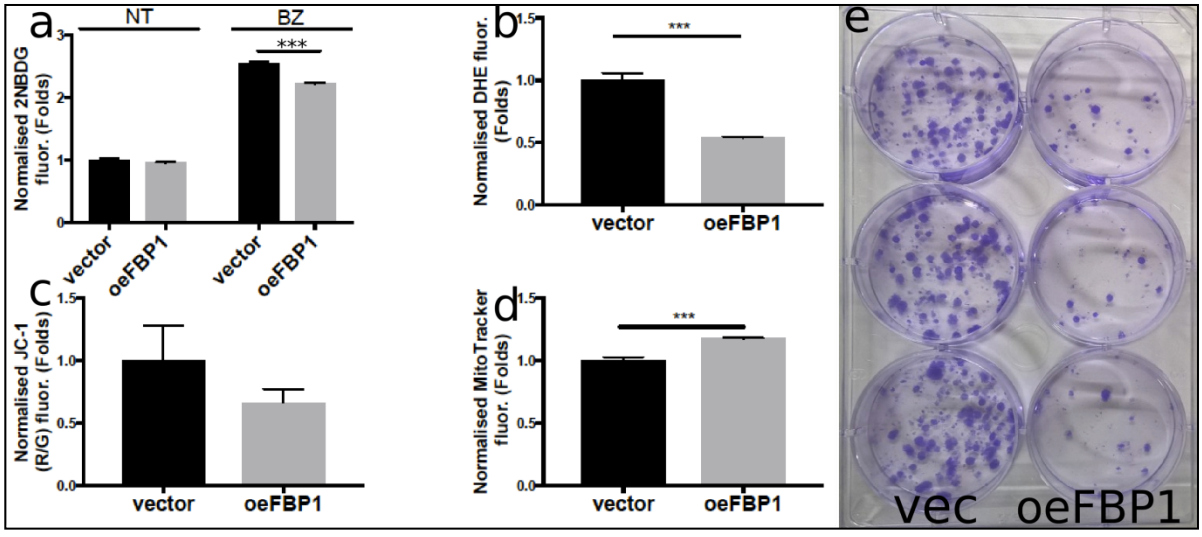

Figure 19: the effects of stable FBP1 expression in MDA-mb231 cells.

a) Glucose uptake in stably transfected MDA-mb231 cells (oeFBP1 vs vector). Glucose uptake was compared for non-treated and 24-h 25 nM bortezomib (BZ) treated cells. Glucose uptake was measured using FACS analysis of cells pre-incubated with full DMEM with 2-NBDG. 5000 cells of 3 biologically independent replicates were analysed (N=3, error-bar: SD). **b)** Basal ROS accumulation in MDA-mb231 cells (oeFBP1 vs vector) as measured using FACS analysis of DHE stained cells. 5000 cells of 3 biologically independent replicates were analysed (N=3, error-bar: SD).
c) Mitochondrial inner-membrane potential (MIMP) measured in stably transfected MDA-mb231 cells (oeFBP1 vs vector). D) Mitochondrial mass measured in stably transfected (oeFBP1 vs vector) MDA-MB231 cells. For **a,b,c&d)** 5000 cells of 3 biologically independent replicates were analysed (N=3, error-bar: SD). e) Colony forming assay CFA for stably transfected MDA-MB231 cells. 200 cells/well seeded initially and incubated for 3 weeks.

Consistent with the inhibited glucose uptake observed upon FBP-1 over-expression in both MDA-mb231 and MCF-7 cells, the ectopic introduction of FBP-1 into MDA-mb231 cells reduced the acidification rate in these cells compared to cells transfected with the empty vector. Both the pH and the impedance were measured using the Bionas flow-through system, allowing the online assessment of the acidification rate and adherence of the cells. Initially the acidification rate of the cells with FBP-1 over-expression was slightly higher than the control cells. However, this acidification rate dropped within the first 6 hours and stabilized at 70-80% of that of the control cells with the empty vector up to 24 hours after the measurement began (Fig. 20 a). This drop in acidification signifies a decrease in lactate production as a result of inhibited glucose uptake and glycolysis upon FBP-1 ectopic introduction into the originally FBP1-deficient MDA-mb231 cells. Monitoring the impedance showed almost no mentionable alterations upon FBP-1 expression indicating conserved viability and morphology and similar levels of adherence between the FBP1 over-expression and the control cells (Fig. 20 b).

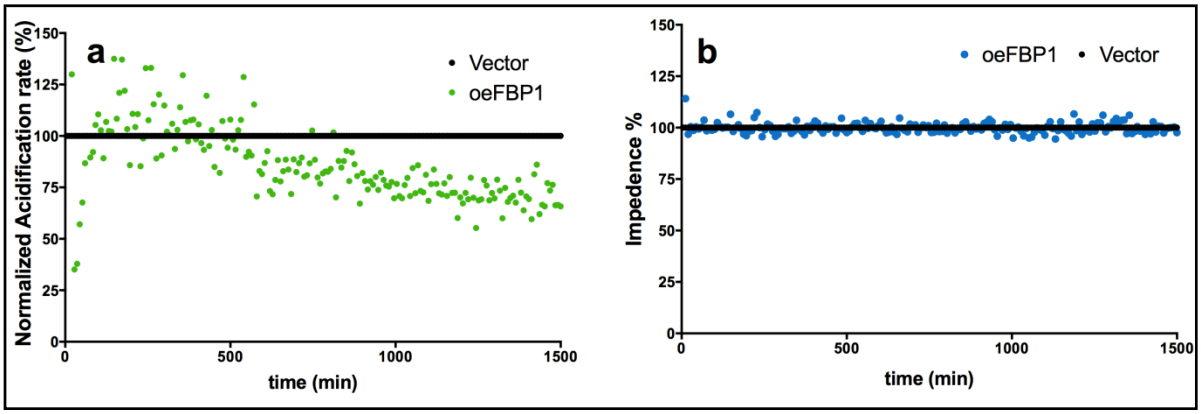

Figure 20: online monitoring of acidification and impedence in MDA-mb231 cells with FBP1 over-expression using the Bionas flow-through system:

a) Acidification rate (%) over time in MDA-mb231 oeFBP1 relative to that of the control cells with the empty vector. **b)** Impedance (%) over time in MDA-mb231 oeFBP1 relative to that of the control cells with the empty vector.

III-IV: The impact of FBP1 on the responsiveness and sensitivity to various metabolic, oxidative and genotoxic treatments

Various alterations have been associated with FBP1 loss, which raises the potential of a changed responsiveness and sensitivity to genotoxic, metabolic and RedOx modulating treatments. In consistence with existing literature, our findings indicate a correlation between FBP1 expression and the level thereof with the basal levels of ROS accumulation. Moreover, our findings indicate an increased antioxidant capacity in cells as reflected by the increased metabolic flux through the pentose phosphate pathway PPP. Compatibly, we had also observed and reported decreased ROS accumulation in yeast upon DNA-damaging treatments in FBP1 knockout strains compared to parental ones. Moreover, FBP1 K.O. strains exhibited decreased sensitivity to low doses of the DNA-methylating agent MMS.

Taken together, the aforementioned observations all point out at the potential of altered sensitivity to particular treatments in cancer cells upon FBP1 loss. Therefore, I chose to test this prospect using the CRISPR-Cas9 stable deletion already established in MCF7 cells (MCF-7 *fbp1*$^{\Delta/\Delta}$) compared to the parental wild-type cells.

III-IV-1: FBP1-loss increases MCF-7 resistance to DNA-chelating agents, in addition to slightly improving resistance to direct and indirect inhibitors of the topo-isomerase activity

Since I have shown, using mutational analysis in *S.cerevisiae,* that the sensitivity to treatment with methyl-methanesulfonate MMS correlates to FBP1 expression and enzymatic activity. I aimed to probe if FBP1 has similar sensitizing effects to DNA-methylation and other forms of genotoxicity in MCF-7 cells. Surprisingly, no difference in sensitivity to MMS was observed in the SRB cell-survival assay (Fig 21 a). Since our findings in yeast were primarily dependent on drop-tests, whose results are primarily dependent on cell growth rather than survival, I also tested long-term colony forming assays to assess any additional growth-dependent differences in

MMS sensitivity that might remain obscure in a short-term survival assay. However, no substantial differences in sensitivity to MMS between wild-type and *fbp1*$^{\Delta/\Delta}$. MCF-7 cells were observed with the colony-forming assay either. (Fig 21 f and g) On the contrary, the loss of FBP1 in MCF-7 cells bestowed an increased resistance to the DNA-chelating agent cis-platin (almost double the IC_{50} value) in addition to the direct (camptothecin) and indirect (daunorubicin) topoisomerase inhibitors (Fig 21 b,c and d respectively).

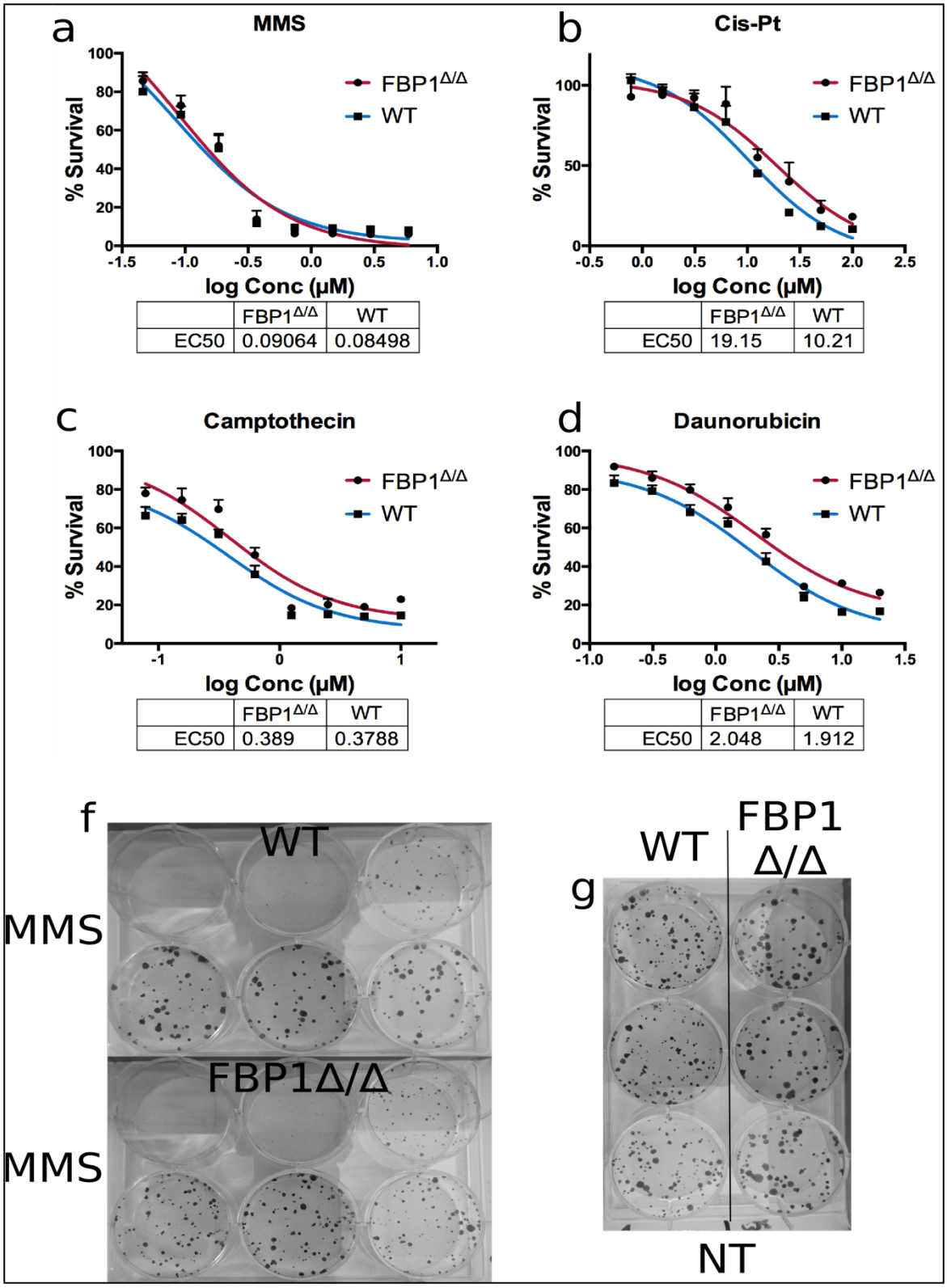

Figure 21: a) b) c) d) SRB survival assays of MCF-7 cells (fbp1Δ/Δ vs WT). Cells were fixed 48 hours after treatment. Points depict the percentage of cell survival corresponding to each given concentration and survival curves were plotted with GrapPad Prism using the sigmoidal non-linear regression tool, (N=4, error-bar: SD). **f)** Colony formation assay of MCF-7 cells (fbp1Δ/Δ vs WT) upon MMS treatment. Cells were treated with a 2:1 serial dilution of MMS starting with 0.001% (v/v) then incubated for two weeks. Resulting colonies were fixed and stained using PFA & crystal violet solution. g) Colony formation assay of non-treated MCF-7 (fbp1Δ/Δ vs WT). Cells were maintained in non-

treated full DMEM for 2 full weeks. Afterwards cells were fixed and stained with PFA & crystal violet solution.

III-IV-2: Absence of FBP1 correlates to increased survival upon oxidative treatments

Considering the correlation between FBP1 expression and increased ROS accumulation, I aimed to assess the effect of FBP1 on the sensitivity towards treatment eliciting oxidative stress. Cell survival assay showed that FBP1 loss slightly improves MCF-7 cells resistance to menadione as reflected by slightly improved survival upon treatment. Despite the unchanged sigmoidity of the survival curve, a look at the lower platue (corresponding to the higher menadione concentrations) suggests improved survival of a small fraction of fbp1 K.O cells compared to the wild-type population (Fig 22 a). However, the observed difference diminished at the last time-point of 72 hours following treatment, suggesting that the slightly improved resistance to menadione is temporary. Taken together with the fact that menadione is a stable one electron Redox-cycling agent that progressively generates reactive oxygen species, this indicates slowed-down ROS accumulation in the fbp1 K.O. cells compared to the wild-type cells. High concentrations of ascrobate have been reported to exhibit oxidative-dependent cytotoxicity against cancer cells. Similarly to menadione treatment, the loss of FBP1 slightly improved cell survival upon exposure to high concentrations of ascorbate. Additionally, the absence of FBP1 promoted growth induction upon treatment with lower concentrations of ascorbate (Fig 22 b). Consistently, fbp1 K.O cells accumulated less ROS upon menadione treatment compared to the wild-type cells. Moreover, the over-expression of FBP1 in MCF-7 cells further increased ROS accumulation following menadione exposure (Fig 22 c).

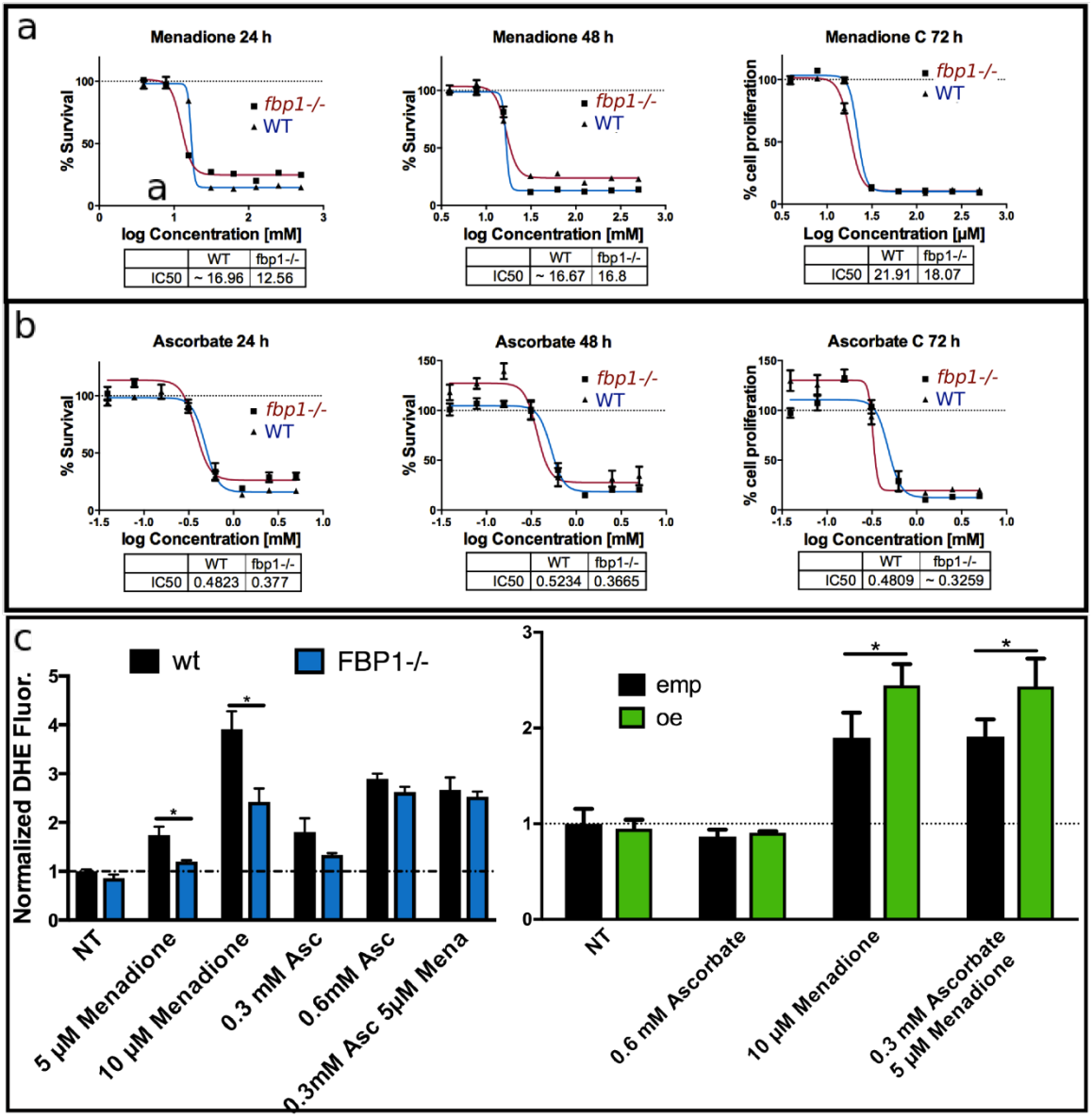

Figure 22: FBP1 promotes sensitivity to oxidative treatments.
a) SRB survival assay of MCF-7 (fbp1Δ/Δ vs WT) 24, 48 and 72 hours following menadione treatment. Points depict the percentage of cell survival corresponding to each given concentration and survival curves were plotted with GrapPad Prism using the sigmoidal non-linear regression tool, (N=4, error-bar: SD). **b)** SRB survival assay of MCF-7 (fbp1Δ/Δ vs WT) 24, 48 and 72 hours following ascorbate (vitamin C) treatment. Points depict the percentage of cell survival corresponding to each given concentration and survival curves were plotted with GrapPad Prism using the sigmoidal non-linear regression tool, (N=4, error-bar: SD). **c)** ROS accumulation in MCF-7 cells (fbp1Δ/Δ vs WT; oeFBP1 vs vector) upon 4 hours of menadione, ascorbate or co-treatment with both. ROS levels were determined using FACS analysis of DHE stained cells.

III-IV-3: In spite of unchanged sensitivity to metformin, Fbp1 strongly sensitizes MCF-7 cells to a combination of ascorbate and metformin

Metformin is a biguanide used as a first choice treatment for type II diabetes mellitus, its effects are mainly attributed to increasing insulin sensitivity and glucose uptake in addition to inhibiting gluconeogenesis in the liver [101]. Metformin is thought to work

as a mitochondrial decoupler by inhibiting mitochondrial complex I. Statistical correlation of metformin use to decreased incident of malignancy in diabetics shed light on a potential anti-cancer use of this widely prescribed drug[102]. Due to its effects on respiration and glucose uptake, I speculated that sensitivity to metformin should be affected with altered Fbp1 expression. However, no tangible effect was observed between wild-type and Fbp1 K.O MCF-7 cells in their sensitivity to metformin (Fig. 23 a and b).

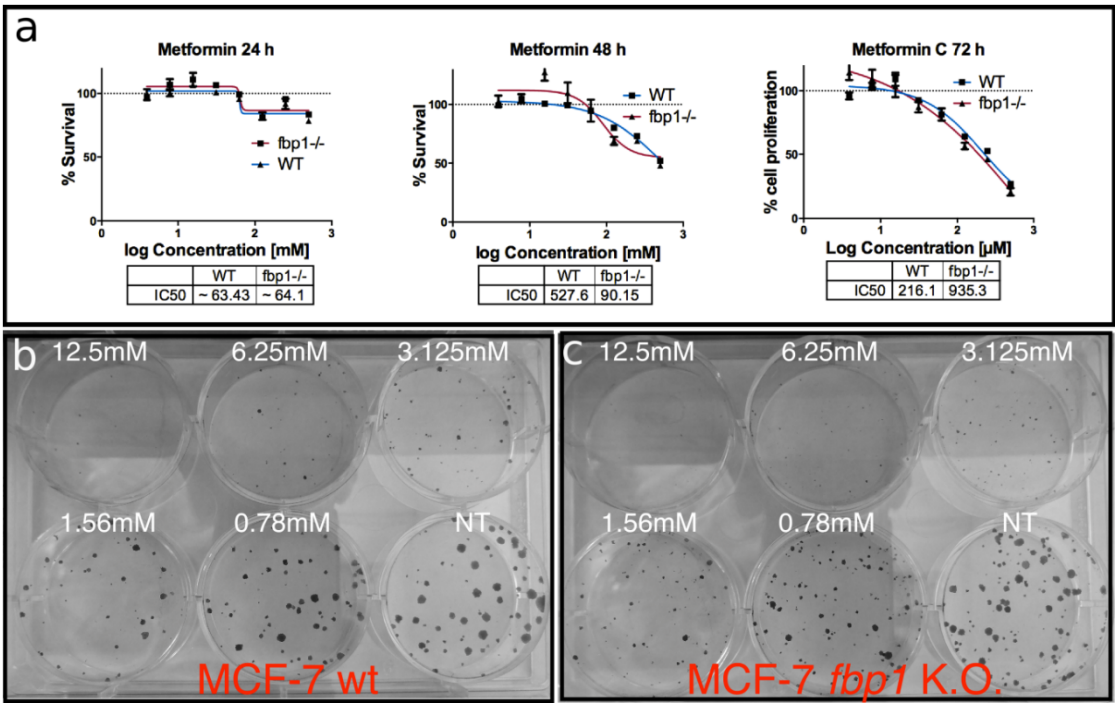

Figure 23: FBP1-loss slightly increases MCF-7 cells sensitivity to metformin.
a) SRB survival assay of MCF-7 (fbp1Δ/Δ vs WT) 24, 48 and 72 hours following metformin treatment. Points depict the percentage of cell survival corresponding to each given concentration and survival curves were plotted with GrapPad Prism using the sigmoidal non-linear regression tool, (N=4, error-bar: SD). **b)** and **c)** Colony formation assay of MCF-7 cells (fbp1Δ/Δ vs WT) upon treatment with metformin. Cells were treated with a 1:1 serial dilution of metformin starting with 12.5mM and incubated for two weeks. Resulting colonies were fixed and stained using PFA& crystal violet solution.

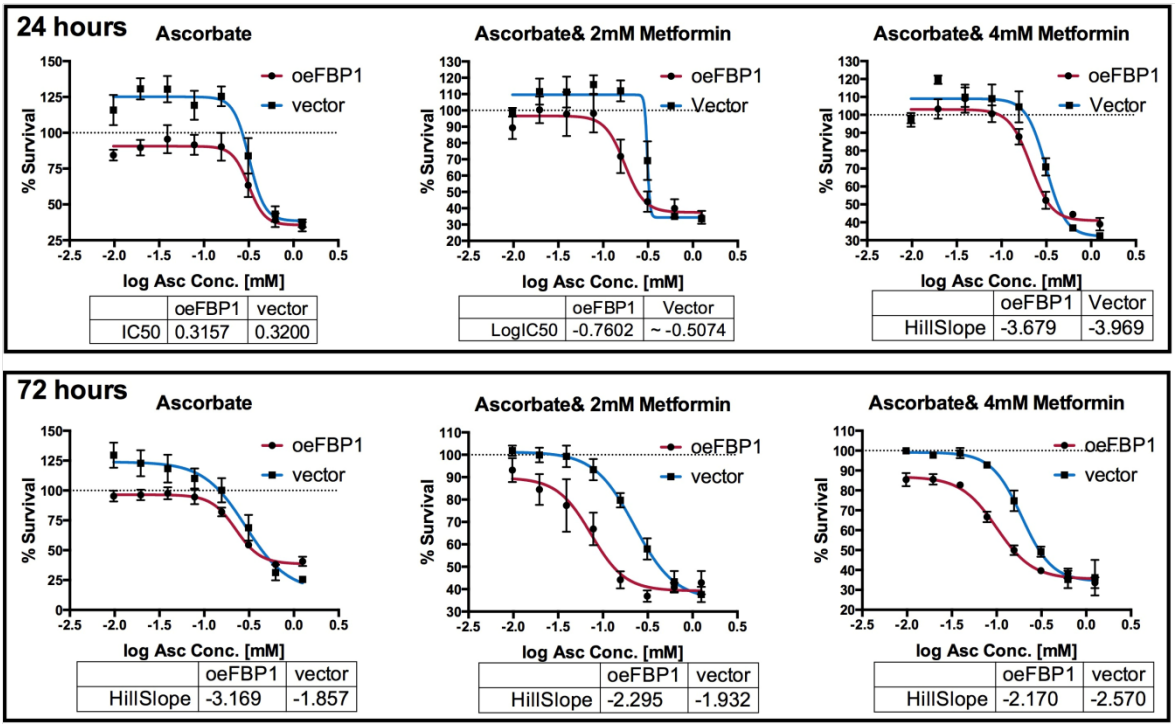

Figure 24: the over-expression of FBP1 intensifies the outcome of ascorbate & metformin co-treatment.

III-V: Fbp1 from yeast to cancer

III-V-1 The decoupling mutation of the yeast Fbp1 almost attenuates the FBPase catalysis of the human homolog but partially rescues proliferation of Fbp1-deficient MCF7 in glucose deprived DMEM

Aiming to extrapolate the findings from the mutational analysis of yeast Fbp1 towards the human homolog. I mirrored the decoupling mutation from yeast Asn75→Ala75 by mutagenizing the corresponding evolutionary conserved residue in the human enzyme Asn65→Ala65. To characterize the effects of this mutation, I introduced the Asn65 mutant into Fbp1-deficient MCF-7 cells and compared its ability to rescue the FBPase catalysis to that of the wild-type Fbp1. I had already established that the knockout of *fbp1* in MCF-7 cells completely annulled the FBPase activity and abolished growth and survival in glucose-free medium (see Fig 9). The

immunoblotting verified the successful expression of both the wild-type and mutated (Asn65→Ala65) Fbp1 as well as the complete absence of Fbp1 in the MCF-7 fbp1$^{\Delta/\Delta}$ cells harbouring the empty vector. Despite being slightly more expressed compared to the wt-Fbp1, the mutated Fbp1 exhibited almost diminished FBPase activity (≈10% of wtFbp1). The effect of this mutation on the on the FBPase catalysis in human cells diverges from that observed in yeast in which the enzymatic activity remains intact.

III-V-2: despite the presence of mRNA, the yeast FBP1-homologue protein was not expressed successfully in cell lines and also failed to replace the enzymatic activity of the endogenous homologue

Aiming to decouple the enzymatic activity of FBP1 from other effects arising from non-enzymatic interactions, I attempted to replace the endogenous human FBP1 in cell lines with the yeast homologue of the enzyme. Upon transfecting MCF-7 cells with the mammalian expression vector harbouring yeast-FBP1 pcDNA3.1-y*fbp1*, successful transcription of yeast-fbp1 mRNA was verified (Fig. 25 b). Nonetheless, no correspondent yeast-FBP1 protein was detected, and the yeast homologue also failed to restore FBPase activity in FBP1-deficient MCF-7 cells (Fig. 25 b). Hence indicating the failure of cell lines to express yeast-FBP1. The situation was similar in MDA-MB231 cells, in which no successful expression of yeast FBP1 could be confirmed. Neither the wild-type form of yeast-FBP1 nor an inactive mutated from S133A could be successfully expressed in MDA-MB231 cells (Fig. 25 e).

III-V-3 mutating proline 5 in human FBP1 does not rescue the protein from degradation in MDA-MB231 cells

The N-terminal proline in yeast FBP1 has been shown essential for its catabolite-induced ubiquitination and degradation based on the N-end rule. Therefore, and due to the hugh levels of evolutionary conservation between yeast and mammalian FBP1 homologues, I regarded it possible that the proline 5 residue of human FBP1 (the closest proline to the N-terminal) can be essential for the newly observed proteasomal degradation of FBP1 in MDA-MB231 cells. Nonetheless, mutagenizing human FBP1 to replace proline 5 with alanine P5A did not avert the degradation in mda-MB231 cells and akin to wild-type FBP1, the protein was only detected upon proteasome inhibition with Bortezomib (Fig. 25 f).

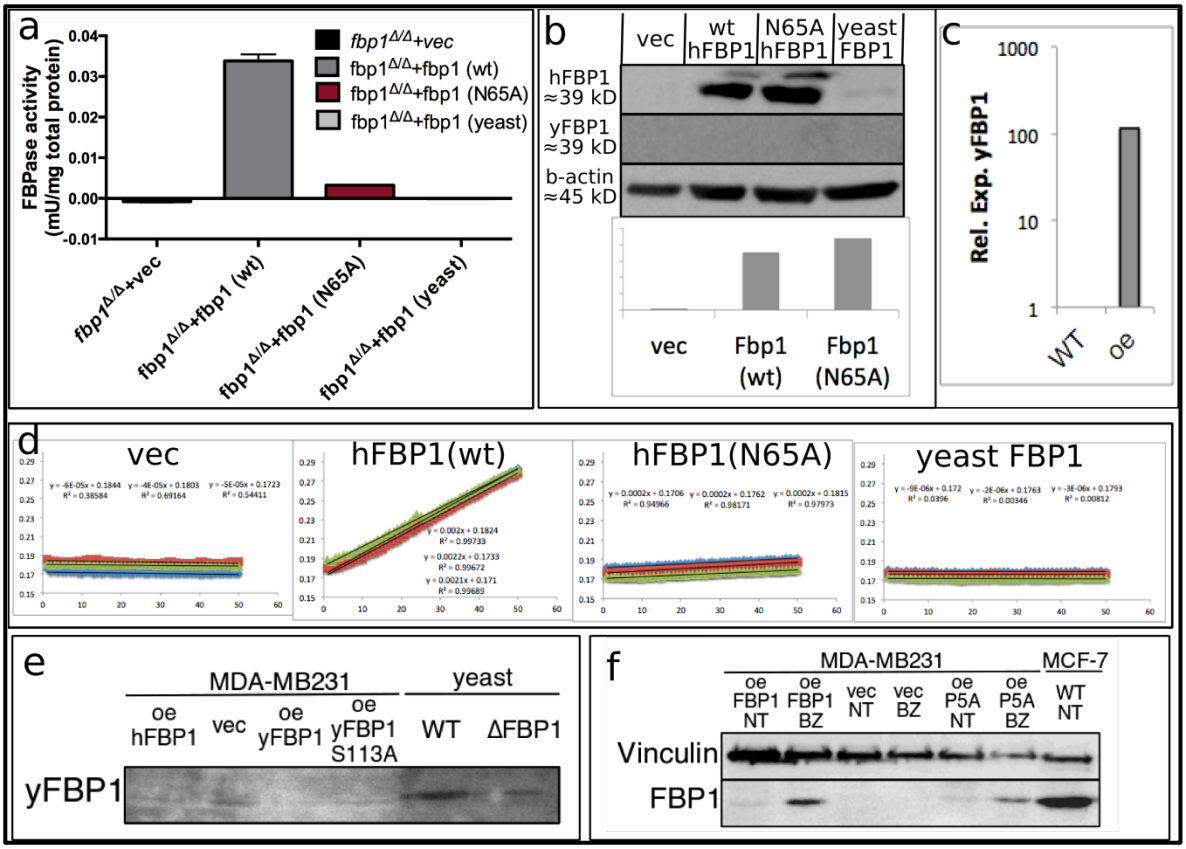

Figure 25: The mutated human Fbp1 Asn65→Ala65 and the yeast homolog of Fbp1 fail to rescue the FBPase catalysis in Fbp1-deficient MCF-7 cells. a) The quantified FBPase activity measured in total native protein extracts.
b) Immunoblotting of full denatured lysates of MCF-7 Fbp1Δ/Δ cells with different forms of ectopically introduced Fbp1. c) Relative transcription of yeast-Fbp1 mRNA. d) The row graphs of the enzymatic activity assay (a), depicting the increase in the NADPH absorption (Abs_{340}) over time. e) Western-blot showing the lack of yeast-Fbp1 expression in MDA-MB231 cells harbouring the expression vector. f) Western-blot showing the impact of bortezomib BZ (50nM) in rescuing the expression of wild type and P5A mutant Fbp1.

III-VI The loss of Fbp1 bestows improved growth and survival upon MCF-7 cells in hypoxic conditions

Since Fbp1 loss has been demonstrated beneficial for survival of cancer cell in hypoxic conditions in both a direct metabolic and indirect effect on gene transcriptional manner. I aimed to probe the effects of Fbp1 on the survival and growth under hypoxia in the context of the Fbp1 deletion and over-expression system established in MCF-7. Akin to previous reports, the absence of Fbp1 conferred higher growth and survival upon Fbp1 K.O MCF-7 cells compared to the parental cell line as seen in the SRB viability assay. Consistently, dead-cell staining using propedium iodide also demonstrated 1 fold decrease in the dead cell fraction compared to the wild-type MCF-7 cells (Fig 26 c). The over-expression of Fbp1 added no additional

disadvantage to that conveyed by the presence of endogenous Fbp1. These observations make it plausible that the full loss of Fbp1, at least in part, promoted by the presence of hypoxic niches in the tumour where selective pressure favours the absence of Fbp1. Despite the suggested advantage of Fbp1-loss in maintaining glycolysis in absence of oxygen and promoting complete reliance on fermentation, Fbp1-deficient MCF-7 cells exhibited no increased advantage over the parental MCF-7 wt cell line when it came to glucose uptake. Fbp1-loss correlated to slightly higher glucose uptake under normoxic and hypoxic conditions alike (Fig 26 d).

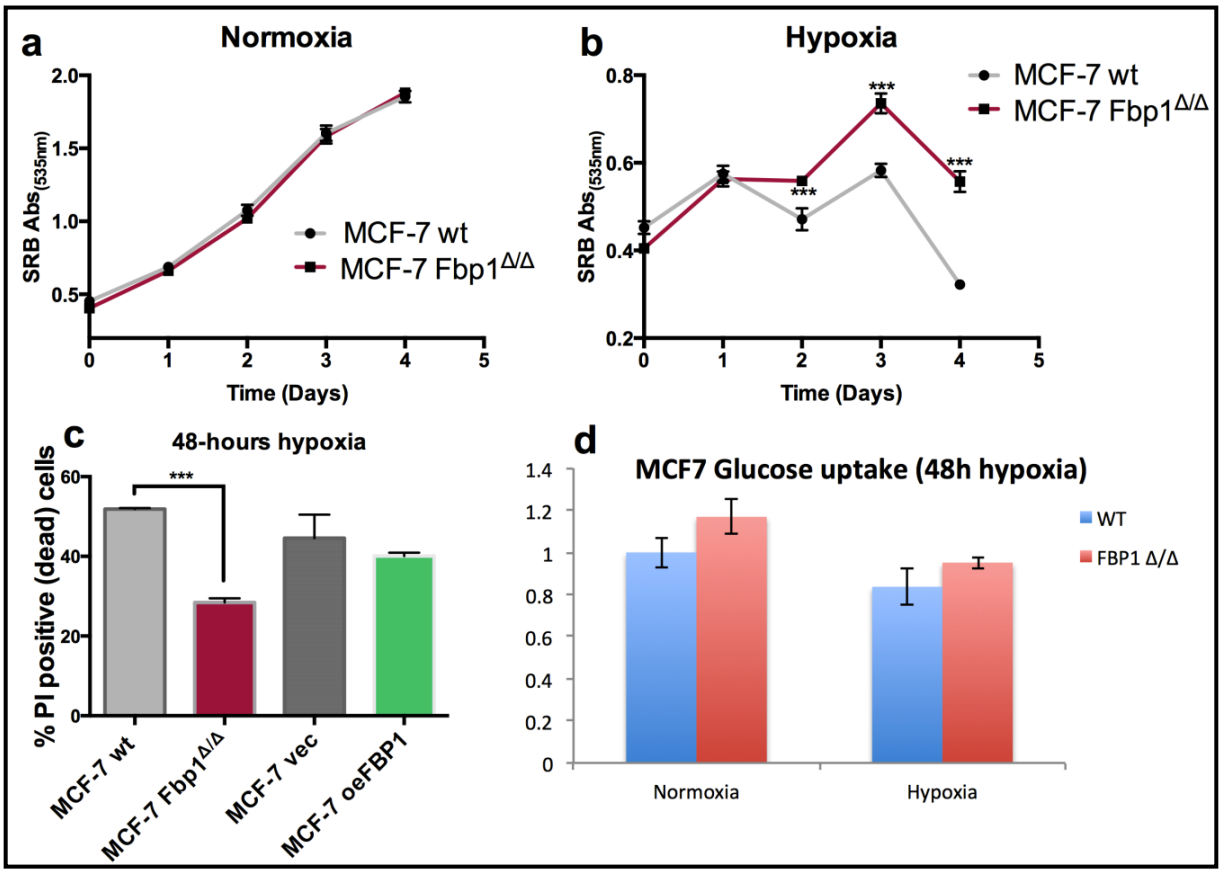

Figure 26: Fbp1-loss bestows survival and growth advantages onto MCF-7 cells under hypoxic conditions. a) Growth curves of WT and FBP1$^{\Delta/\Delta}$ under atmospheric oxygen levels. b) Growth curves of WT and FBP1$^{\Delta/\Delta}$ under hypoxic conditions (1% oxygen saturation). c) Fractions of dead cells upon hypoxia quantified using FACS analysis of PI stained cells (N=3, SD). d) Glucose uptake in MCF-7 cells upon incubation in normoxic vs hypoxic conditions (N=3, SD).

IV-Discussion

"The best way to have a good idea is to have a lot of ideas". Linus Pauling

In the course of my PhD work I explored the impact of Fbp1 in two different systems; the budding yeast and breast cancer cell lines (luminal and basal-like). The main commonality between the two systems is the additional effects attributed to Fbp1. The impact of Fbp1 is best realized by comparing the Fbp1 -deficient cells to their wild-type Fbp1 -expressing counterparts. In yeast the knock-out of Fbp1 produces strains with higher resistance to the MMS-induced growth and the inhibition of colony formation [94]. Whereas, the absence of Fbp1 in cancerous cells predicts worse prognosis, and is linked to faster growth, more extreme glycolytic phenotype and invasiveness and metastasis [60, 61, 64, 103, 104]. I aimed to further explore the impact of Fbp1 in both systems to reach a common understanding of the roles linked to this enzyme.

The results presented shed light on several aspects of Fbp1 roles in both studied models, emphasize previous reports from a new perspective, showcase novel observations of the post-translational control of Fbp1 levels and suggest new explanations for the observed effects of this enzyme. Although no particular single common mechanism has been found, the findings suggest several shared trends between the two systems (yeast and cancer cells) that should be subject of further investigation. In this section I will present the most important conclusions from my work, discuss the implications in light of the existing literature and suggest further experimental work to build on the presented findings.

In an order akin to that of the results section, I will begin with discussing the implications of my work on the yeast system, followed by those derived from my work on the cancerous cells. Commonalities between the two systems will be pointed out whenever appropriate, and then recapped and further elaborated on at the end of this section.

IV-I The over expression of mutagenised Fbp1 in yeast revealed the possibility of decoupling of the enzymatic activity from MMS sensitization

Via site directed mutagenesis, I individually targeted evolutionary conserved residues with structural and functional relevance in yeast [85]. The over-expression of the mutated Fbp1 in an array of different genetic backgrounds yielded strains with varying levels of FBPase activity, growth and survival upon MMS treatment and proliferation rates. Despite the apparent correlation between FBPase catalysis and MMS-induced growth inhibition, we identified one mutant that particularly defies this pattern and thus uncouples the enzymatic activity from MMS-sensitisation. Replacing Alanine for the Asparagine in position 65 yields a mutated Fbp1 that retains the catalytic activity but contributes no additional sensitivity towards MMS[85]. This is best depicted by plotting the measured enzymatic activity of each mutated Fbp1 against the quantified growth on MMS-containing agar media, a pattern of inversed correlation between growth on MMS-agar and FBPase catalytic activity is observed that applies to all tested mutants except Asn65. The exclusion of Asn65 also leads to a starkly improved linearity reflected by an increase in the R^2 "coefficient of determination" value from 0.37 to 0.84 (Fig 28).

This provides evidence of decoupled enzymatic catalysis from the additional MMS sensitization phenotype and suggests that a novel non-catalytic function/interaction underlies the additional Fbp1-associated increase in sensitivity towards MMS.

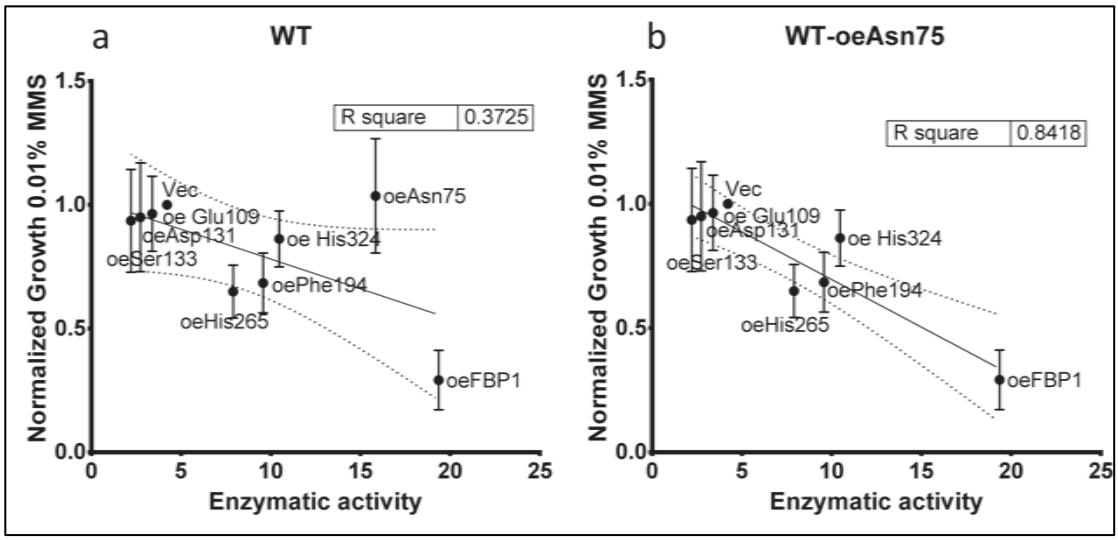

Figure 28 featured in my publication in Microbial Cell ″ 2017 Ghanem et al." [85]

Figure 28: Asn75 defies the pattern of inversed linear correlation between the enzymatic activity and growth on agar containing MMS. Depicted is the linear correlation between the measured enzymatic activity of the mutants (see Fig. 3) and the quantified growth on MMS-correlating to each mutant when over-expressed in wild-type BY4147 cells. **a)** Including Asn75 **b)** excluding Asn75.

Moreover, a clear distinction must be made between two different hallmarks of the Fbp1-associated MMS-sensitization; 1) Growth inhibition and 2) cellular damage and survival upon treatment. The first effect is seen in the spot assays of cells in liquid cultures on MMS-containing agar, while the second effect by PI staining and colony forming assays of cells treated in the liquid cultures.

The effect of Fbp1 on cellular growth was observed upon over-expression of Fbp1 in both wild type and *fbp1*Δ genetic backgrounds. Clear difference was also observed between wild type and *fbp1*Δ cells without the introduction of ectopic Fbp1 expression. In contrast, no differences in cell survival and death were observed between wild type and Fbp1-deficient cells upon MMS-exposure. While the ectopic over-expression of Fbp1 in cells only leads to increased MMS-associated disruption of cell-integrity and survival when the ectopic expression of fbp1 is added to its endogenous expression.

IV-II Potential underpinnings of the MMS-sensitising effect of Fbp1: altered RedOx homeostasis, gluconeogenesis/glycolysis futile cycling and RAS regulation by phosphorylated sugars is considered

On one hand, the decoupling of the enzymatic activity from MMS-sensitization suggests a novel activity related to the mutated Asn75, or modified reaction kinetics responsible for the observed decoupling of both effects. On the other hand, the observed synergy between the ectopically (wild-type or mutated Fbp1) and the endogenously expressed Fbp1 in increasing the MMS-inflicted cell damage, in addition to the positive correlation between the enzymatic activity of the mutants and the MMS-sensitization (except in Asn75 case) both suggest a quantitative mechanism in which the FBPase activity itself, or a by-product thereof is responsible for the cellular damage. The former possibility can be an outcome of futile cycles due to Fbp1 over-production [105], which would jeopardise the glycolytic flow and tips the energy homeostasis, hence limits cells' ability to repair their DNA and cope with the MMS-inflicted damage. As potentially harmful by-products, ROS accumulate in the cases of DNA damage including post MMS exposure [94, 106]. It has been previously shown that Fbp1 absence in yeast abrogates ROS accumulation upon

MMS exposure. My results also speak for a similar pattern, with the over-expression of Fbp1 or its active mutants leading to an immediate increase in ROS accumulation upon MMS exposure and to a long term ROS accumulation when cells are kept in stationary phase. Therefore, FBPase activity seems to correlate to an increased oxidative stress [60]. This notion was also postulated in cancer cells, where Fbp1 presence slows down glycolysis by competing for metabolic intermediates with PFK1, hence enforcing an increased reliance on respiration and ROS accumulation as a by-product thereof [107]. Future endeavours to elucidate the links between Fbp1 enzymatic activity and its additional MMS-sensitising role should focus on the aforementioned possibilities. The screened mutants can be of used for this purpose since they offer varying degrees of enzymatic activity. To further highlight ROS contribution to increased MMS sensitisation, the correlation between the FBPase activity and the amount of accumulated ROS should be quantitatively assessed; preferably using various ROS probes with relative specificity for different reactive oxygen species. These include: DHE for superoxide, H2DCFDA and boronate for hydrogen peroxide and MitoSox for quantification of mitochondrial superoxide and thus probing the possible link between FBPase catalysis, respiration and ROS accumulation [108, 109]. ROS scavenging also offers a way of investigating the causality between the severity of oxidative stress and the observed growth inhibition in MMS spot assays. Additionally, the genetically encoded redox sensitive GFPs (roGFPs), would provide additional means for elucidating the effects of Fbp1 on the intracellular RedOx homeostasis reflected in the GSH/GSSG balance or in H_2O_2 levels [110, 111]. My preliminary results using the Grx1-coupled roGFP2 sensor indicate higher levels of glutathione oxidation upon MMS-treatment in wild-type y486 cells compared to Fbp1-deficient ones as indicated by the higher levels of oxidized roGFP2 fluorescence (λ_{Ex}=390 nm). Consistently, the absence of Fbp1 also correlates to deminished oxidised roGFP fluorescence in the non-treated samples reflecting lower cytosolic GSSG levels in Fbp1-deficient cells. A separate preliminary experiment showed that Fbp1-deficient yeast exhibited a stronger fluorescence signal for reduced roGFP (λ_{Ex}=480nm) and a weaker signal for oxidised roGFP (λ_{Ex}=390nm) thus suggesting an enrichment of cytosolic GSH on the expense of free cytosolic GSSG hence reflecting larger anti-oxidant capacity in Fbp1-deficient cells.

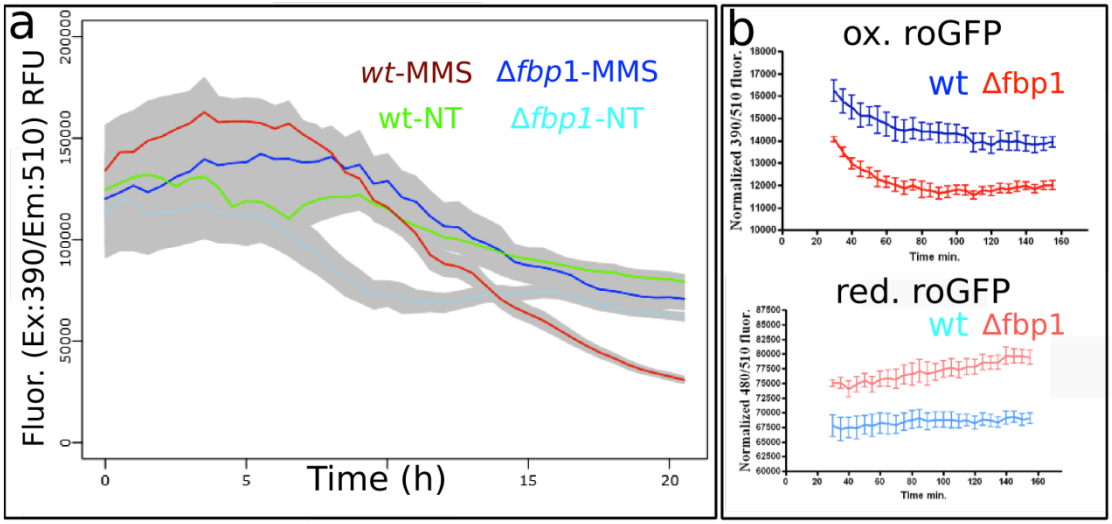

Figure 29: a) Dynamic measurement of the fluorescence levels of oxidised roGFP2 (λ_{Ex}=390 nm, λ_{Em}=510 nm) adjusted to the corresponding $O.D_{600}$ values. Featured are real time fluorescence measurements of non-treated and MMS treated wild-type and *Δfbp1* strains.
b) Dynamic measurements of the fluorescence levels of oxidised and reduced roGFP2 in MMS-treated wild-type and *fbp1Δ* strains adjusted to the corresponding O.D600 values.

It must be clearly stated that the abovementioned results using roGFP are preliminary and in no way to be accepted as a stand-alone evidence for the increase in GSH/GSSG ratio in light of different Fbp1 expression. Nevertheless, these observations add up well to the existing evidence that Fbp1 expression quantitatively correlates to higher ROS production as previously reported [94] and also seen in the results presented in this thesis (Fig. 7). Moreover, the diminished oxidative stress in Fbp1-deficient cells consists with reports of similar observations in cancerous cells [60, 107] and also with my findings in ductal breast cancer cells MCF-7, in which both endogenous and ectopic expression of Fbp1 increased ROS accumulation (Fig. 7) and further sensitised cells to oxidative agents (Fig. 22). Based on the above results, GFP-based RedOx sensors can be harnessed for the reliable and dynamic probing of the cytosolic RedOx homeostasis and anti-oxidant capacity provided that the results get quantified relative to control measurements performed in fully oxidising and reducing conditions for calibration.

To test the contribution of FBP1-associated futile cycling to the growth inhibition and increased sensitivity to MMS, lower glycolytic intermediates such as pyruvate in addition to amino acids that can feed into the TCA can be provided in the culture medium in an attempt to annul the Fbp1 associated MMS-sensitisation by circumventing the proposed futile cycling in the upper glycolytic pathway [105]. This

approach is especially interesting in combination with ectopic over-expression of Fbp1 that is more likely to produce futile cycling than the endogenously expressed levels. The over-expression mutants with gradually increasing activity can also be used as a system of controlling the severity of the potential futile cycling.

Very recent work on RAS regulation by glycolytic intermediates suggested an agonistic effect of fructose 1,6 bisphosphate on RAS via the guanosine nucleotide exchange factors GEFs Cdc25 and Sdc25 (homologs of the mammalian RAS GEF SOS1) [112]. This suggests a novel connection between Fbp1 and RAS regulation via F1,6bP, the substrate of Fbp1 and brings new light to Fbp1 as an anti-proliferative regulator. The absence of Fbp1 should conceivably lead to an accumulation of its substrate F1,6bP and hence RAS over-activation. Therefore a mechanism in which the absence of Fbp1 sustains enough RAS activation upon MMS is very plausible in theory. In presence of glucose, Fbp1 should have no noticeable effects on the abundance of F1,6bP due to its glucose-mediated transcriptional repression and proteasomal degradation [21, 89, 113, 114]. However, MMS treatment seems to readily engage Fbp1 by overcoming its glucose repression [94]. The growth inhibition on MMS in presence of endogenously expressed Fbp1 can be assumed a protective mechanism especially that it comes at no cost on cells' integrity and survival. MMS sensitivity in yeast has been shown to depend upon glucose abundance, and the enzymatic activity of both GAPDH and PYK, (lower glycolytic enzymes) was inhibited 4 hours upon treatment [106]. Altogether this suggests a potential role of the accumulating upper glycolytic metabolites, including F1,6bP, as modulators of the outcome of MMS treatment in *S. cerevisiae*. Whether differential RAS activation by F1,6bP could offer an explanation to the link between Fbp1 and the response to MMS treatment intriguingly remains an open question to be answered. The elucidation of this potential link should make use of CDK25 and SOS1 mutants with impaired interaction to F1,6bP, such mutants have been already established and reported to abolish the F1,6bP activation of RAS [112, 115, 116]. The mutation library of Fbp1 presented in this thesis is also a suitable tool for the above-suggested endeavour since it offers a way of titrating Fbp1 activity and thus the availability of intracellular F1,6bp. Additionally, probing the effects of the decoupling mutant Asn75 in light of various RAS backgrounds would be of additional interest, since the effect of

F1,6bp on RAS is not obviously concentration-dependent suggesting that the impact of different enzyme dynamics of Fbp1 on RAS activation could vary unpredictably.
Altogether, all the aforementioned potential mechanisms of Fbp1-dependent MMS sensitisation rely upon metabolic, oxidative or signalling components common between yeast and mammalian cells. Indeed, many of the observed effects of Fbp1 that can underlie the MMS sensitisation have also been observed in cancerous cell lines including the results presented in this thesis.
Increased oxidative and metabolic stress has been observed upon Fbp1 introduction to cell lines. Impeded growth, proliferation and colony formation are also common hallmarks between yeast and cancer cells harbouring ectopic expression of fully functional Fbp1. Consistently cells with Fbp1 over-expression demonstrated multiple signs of glycolytic inhibition. Hence substantiating the notion that Fbp1 is central for counteracting the Warburg effect and the resulting rapid proliferation.

IV-III Fbp1 abrogates glucose uptake and glycolysis in cancer cells and promotes a respiratory metabolic program

Recently Fbp1 loss has been indicated as a detrimental event in the metabolic reprogramming essential for cancer initiation or later gain of invasive and metastatic properties [60, 61, 64, 107]. The findings of this thesis fall in line with the reported effects of Fbp1 on cancer cell metabolism. These could be summed up as reduced glucose sensitivity and uptake, slowed down glycolysis and reliance on respiration also resulting in higher ROS levels and oxidative stress. An examining view of the existing body of knowledge on Fbp1, and its repression in various types of cancers suggests two distinct means by which Fbp1 excerpts its metabolic “tumour suppressor” effects. The first is a direct consequence of Fbp1 catalytic activity. By splitting F1,6bP into F6P and inorganic phosphate, the enzyme directly contributes to the intracellular abundance of 6-phospho hexoses [117]. Additionally, F1,6bP has an activating role on PKM2 by stabilising its tetrameric enzymatically active form. By depleting its own substrate F1,6bP, Fbp1 indirectly deactivates PKM2 by hindering its tetramer formation [118, 119]. PKM2 inactivation leads to a slowed down dephosphprylation of PEP and thus an increased accumulation of lower glycolytic

intermediates in addition to the above mentioned phospho-hexoses accumulation. The accumulation of glycolytic intermediates has an inhibitory effect of glucose uptake in part by promoting the expression of the theoredoxin interacting protein TXNIP. Both G6P and GA3P trigger the nuclear translocation of MondoA and ChRheb, which subsequently trigger TXNIP transcription [120, 121]. TXNIP then closes the negative feedback loop by triggering the internalization and subsequent degradation of GLUT1 and thus inhibiting overall glucose uptake [122]. Consistent with the suggested mechanisms, my findings robustly show an inverse correlation between Fbp1 levels and TXNIP in various contexts, especially upon glucose replenishment. Seen in light of the inhibited glucose uptake in presence of Fbp1 and the increasing difference of TXNIP expression upon glucose replenishment, the Fbp1-associated down-regulation of TXNIP is best explained as an outcome of inhibited glucose uptake and not as a cause thereof.

The metabolic quantification presented in this thesis also suggests an Fbp1-elicited overall down-regulation of glycolysis and and a higher intracellular lactate levels in Fbp1-deficient cells. The predicted increase of hexose-phosphates as a result of Fbp1 activity can grant basis for the assumption that Fbp1 supplies the pentose phosphate shunt with an abundance of G6P. However, the findings in this thesis defy this notion by clearly depicting an increase of flux through the pentose phosphate shunt upon Fbp1 deletion. Moreover the Fbp1-deficient MCF-7 cells exhibit higher levels of upper glycolytic intermediates compared to the parental MCF-7 cells. The apparent contradiction in these observations is simply resolved by the clear observation that both endogenous and ectopically introduced Fbp1 significantly reduce glucose uptake and sensitivity. Hence, the inhibited glucose uptake due to Fbp1 over-expression translates to a decreased flow through both glycolysis and pentose phosphate pathway, and the contrary applies to Fbp1-loss.

IV-IV The existing evidence suggests an anti-tumour outcome of the indirect inhibition of PKM2 by FBP1 in addition to competition between the two proteins as transcriptional co-activators

As part of their metabolic reprogramming, cancer cells favour the embryonic pyruvate kinase isozyme M2 PKM2 over the M1 isozyme predominantly expressed in

differentiated tissues[123]. The flexible post-translational regulation of PKM2 and its non-enzymatic roles, including as a transcriptional co-activator, bestow cancer cells with metabolic advantages that support their special demands of precursors to fuel their rapid proliferation [124, 125]. PKM2 is subject to allosteric regulation by fructose 1,6 bis phosphate F1,6bP, the substrate of Fbp1. Binding of F1,6bP promotes an active tetrameric configuration of PKM2[118]. Hence Fbp1 is speculated to have an indirect inhibitory effect on PKM2 by depleting F1,6bP.

The interplay between Fbp1 and PKM2 has been highlighted as part of Fbp1 tumour-suppressor and anti glycolytic effects [60, 107]. This is despite the fact that idle PKM2 has been assumed advantageous for fuelling cancer metabolism and proliferation in various cellular and animal studies [126, 127]. The inactive PKM2 is thought to allow the funnelling of glycolytic intermediates for anabolic processes including amino-acid synthesis, especially serine [128], and the pentose phosphate shun t[129]. In addition, the enzymatically inactive dimer form of PKM2 has been demonstrated to translocate into the nucleus, where it operates as a transcriptional co-factor of several regulators including β-catenin and Hif-1α [130, 131], through which PKM2 exert a self-propagating feedback loop which ends up in further activation of Hif-1a and further up-regulation of glycolytic enzymes including PKM2 itself [132, 133]. Nevertheless, the two above listed mechanisms fall short of describing the particular outcome of Fbp1 related inhibition of PKM2. The results presented here, consistently with earlier research on Fbp1 loss in breast cancer [60], demonstrate an increased flux through both glycolysis and the pentose phosphate pathway. Thus suggesting an over-all increase in the flux over glucose catabolic pathways in Fbp1 knockout cells as a result of an overall increase of glucose uptake. To ensure that the effect of Fbp1 on PKM2 holds true in the stable cellular system I established, I verified the increased activity of PKM2 in Fbp1-deficient MCF-7 cells compared to their wild-type counterparts (Fig 30).

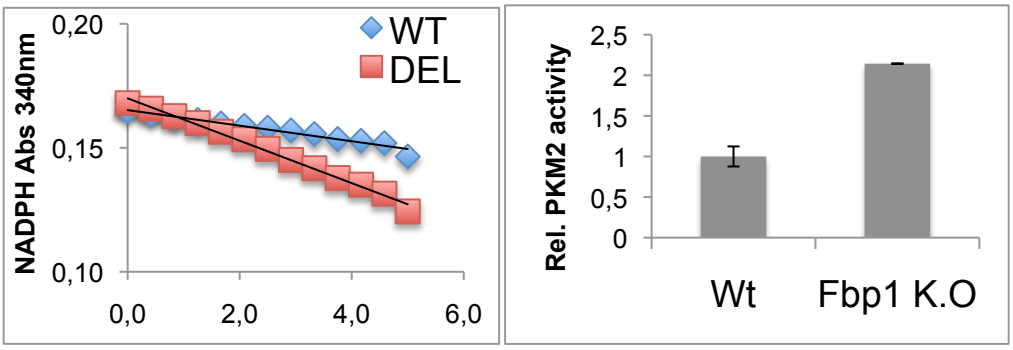

Figure 30: Fbp1 deletion causes PKM2 induction.
Left) PKM2 induced decrease in NADH absorbance over time. Right) The relative activity of PKM2 in the native lysate of Fbp1-deficient MCF-7 cells compared to MCF7-wt.

Moreover, PKM2 was reported to exhibit a predominantly monomeric conformation in Fbp1 positive breast cancer cells, as opposed to the active tertrameric form seen in Fbp1-deficient cells[60]. It is the dimeric form of PKM2 that is deemed to elicit co-transcriptional regulation promoting cancer metabolism and proliferation [125, 132, 134]. Hence the predominance of the monomeric inactive form in presence of Fbp1 grants another ground for assuming the Fbp1-induced PKM2 inactivation of no particular advantage for tumour metabolism.

Fbp1 and PKM2 seem yet to also collide as co-transcriptional regulators with opposite effects. This prediction arises from the recently described inhibitory interaction between Fbp1 and and Hif1a[61]. The described interaction involves the translocation of Fbp1 into the nucleus, where it subsequently binds to Hif1a and inhibits its transcriptional effect and, thus impedes the metabolic rewiring required for the metabolic reprogramming required to support rapid proliferation [61]. The inhibitory interaction of Fbp1 to Hif1a is non-enzymatic since it was exhibited to work using inactive truncations of Fbp1[61]. Consistently the findings of this thesis demonstrated that Fbp1-loss bestows cells with an increased tolerance to ???whatand improved survival upon hypoxia.

Taken together, evidence has been presented for non-enzymatic interactions of Fbp1 and PKM2 to Hif1a with either an inhibitory or a co-activation outcome, respectively [61, 132]. This suggests a potential competition between Fbp1 and PKM2 in binding Hif1a. It is plausible that Fbp1 can inhibit PKM2 co-transcriptional cancerous activity by preventing its interaction with Hif1a or/and other transcriptional regulators. Intriguingly, the over-expression of Fbp1 under a constitutively induced promoter was

sufficient to abrogate EMT in luminal breast cancer cells [60]. Normally, Snail expression is sufficient to induce EMT in luminal cell lines with E-Cadherin, Fbp1 and several other targets being repressed in the process. The continued expression of irrepressible Fbp1 (constitutively expressed) prevented EMT and maintained E-Cadherin expression [60]. Recently it has been demonstrated that PKM2 participates in the epigenetic silencing of E-Cadherin in EMT contexts by interacting with the co-transcriptional repressor TGIF2, which subsequently recruits histone deacetylases to E-Cadherin promoter [135]. All this makes it more imperative to thoroughly investigate the multiplex interaction between Fbp1 and PKM2 on metabolic and transcriptional regulation levels. To achieve this, the impact of Fbp1 on PKM2 conformation and activation state and the resulting effects on cellular metabolism should be examined in cells exhibiting various levels of PKM2 activity and Fbp1 content. In addition, assessing the adversary effects of FBP1 on the transcription of characterized targets of PKM2 co-activation role should help determine if Fbp1 competes with PKM2 for binding Hif1α and/or other transcriptional regulators.

Finally, it is also apt to hint here that G6PD, the entry enzyme to the pentose phosphate pathway, also demonstrated higher enzymatic activity in Fbp1-deficient yeast, especially in the context of MMS treatment that increases the demand on ribose phosphates for *de-novo* nucleotide synthesis. Therefore, the overall antagonistic effect of Fbp1 on glucose catabolism seems rather general and evolutionary conserved.

Further unravelling of the interaction between Fbp1 and PKM2 is imperative for a better understanding of the metabolic reprogramming essential for cancer initiation, progress and acquisition of invasive properties.

IV-V Fbp1 as an indirect ROS inducing factor

It has become widely accepted that reactive oxygen species transcend their previously assumed purely harmful role to actively participate in cell signalling [136, 137].

Diverse roles have been attributed to ROS including the participation of H_2O_2 as a secondary transducer of various extracellular growth signals including insulin EGF and VGEF[138]. Additionally, ROS accumulation and DNA damage show reciprocal

feedback with unchecked accumulation of ROS leading to DNA damage and ROS production being an essential part of the cellular response to DNA damage [139]. Further studies illuminated the mechanism by which DNA damage triggers ROS production. The histone H2AX conveys the DNA damage signal to NOX1, which produces reactive oxygen species that are determinant of the outcome and the cell-death and senescence decisions[140]. MMS treatment is no exception to other types of DNA damage in inducing high levels of ROS that are detected in yeast within 1 hour of exposure [85, 94, 106]. Intriguingly, the absence of endogenously expressed Fbp1 abrogated ROS accumulation in yeast in contexts of MMS treatment and chronological aging[94]. Consistently, Fbp1-deficient MCF-7 cells exhibited diminished basal ROS levels compared to the parental cell line while the ectopic over-expression of Fbp1 in the same cell line correlated to increased ROS abundance. Moreover, Fbp1 over-production correlates to diminished tolerance to oxidizing treatments. Altogether, this indicates Fbp1 as an important mediator for the regulation of ROS production. The effect of Fbp1 on ROS stems from its respiratory inducing effects as a result of the direct and indirect metabolic reprogramming roles discussed above.

Therefore, it is very plausible that the loss of Fbp1 relieves the intracellular oxidative stress, thus allowing a wider tolerance margin towards oxidative agents. This state of relieved oxidative stress permits cells with damaged and unstable DNA to continue proliferating due to the lack of ROS signalling required to engage apoptosis or senescence[140]. This last point also sheds light at a potential mechanism by which the loss of Fbp1 can also promote cancer initiation and recurrence.

In accordance with the literature, the results of this thesis suggest an evolutionary conserved pro-oxidant role of Fbp1 as a result of increased respiration. Hence future work should focus on the premise of Fbp1 and gluconeogenesis as pro ROS signalling components. The impact of Fbp1 activity on ROS can be relevant to its observed roles including the MMS-sensitisation effect in yeast as suggested by the observation that direct ROS scavenging using TEMPO rescued the growth on MMS-containing agar[94]. While the enzymatic activity of Fbp1 could explain the increase in ROS as a result of increased respiration, other indirect ways as result of non-catalytic interactions cannot be ruled out, especially since similar interactions have

been reported in human cancer cells. The screened mutants library and especially the decoupling mutant would make a good tool for probing the relation between the catalytic activity of Fbp1 and ROS production and the general intracellular RedOx homeostasis.

IV-VI Evidence of ectopic Fbp1 slowing down the cell cycle hints at metabolic regulation of cell cycle progression

In their quest for division, cells must ensure sufficient supply of energy and metabolic intermediates required for the biosynthesis of macromolecules for the daughter cells[141]. Hence the cell cycle and cellular metabolism are tightly synchronised so to supply the energy and biomaterial necessary for DNA replication and cell division in general[142, 143]. Introducing Fbp1 into the Fbp1-dificient MDA-MB-231 cells correlated to a wide-scale transcriptional inhibition of a variety of cell cycle related factors. This sort of gobal inhibition of Fbp1 has not been previously reported and therefore sheds new light on the anti proliferative impact of Fbp1. The moderate transcriptional inhibition of a majority of mitotic factors in addition to considerable number of G1/S factors could be seen as an outcome of impeded cell growth and proliferation upon Fbp1 introduction. In a slowly proliferating population, less cells are likely to be engaging in mitotic events and therefore the expression of the factor required for this phase is diminished. Nevertheless, particular aspects of the reciprocal regulation between metabolism and the cell cycle suggest potential mechanisms by which Fbp1 could affect certain cell cycle components. These include the up-regulation of the thymidylate synthase by the E2F transcriptional factor being subject to ROS regulation of the latter[144, 145]. Our analysis indicated thymidylate synthase as one of the most down regulated targets upon Fbp1 expression in MDA-MB231. This suggests an indirect inhibitory effect of E2F by Fbp1 due to the Fbp1 induced alterations in ROS production and accumulation. Intriguingly, the MDA-MB-231 cells represent the only context in which the ectopically expressed Fbp1 diminished ROS accumulation, a very unexpected result that possibly relates to ectopic Fbp1 being subject of proteasomal degradation in MDA-MB-231 cells. Moreover metabolism impinges on the cell cycle more directly via signalling queues that sense nutrient and energy scarcity and relay an off signal to

the cell cycle regulators. A prone applicable example is AMPK sensing critically elevated AMP (or ADP) and phosphorylating the tumour suppressor p53 (Ser15) that conveys the signal to p21, which subsequently imposes G1/S cell cycle arrest[146, 147]. Therefore, it is plausible that the metabolically disadvantageous enforced expression of Fbp1 could elicit G1/S cell cycle arrest akin to glucose scarcity or deprivation. Pondering this novel observation of Fbp1-associated cell cycle inhibition, PMK2 also pops into the picture since its nuclear non-catalytic activity modulates the workings of M-phase proteins responsible for efficient and error-proof chromosomal segregation[148]. Since Fbp1 indirectly affects the tertiary structure of PKM2 by consuming F1,6bP[60], it also inevitably affects its nuclear sub-localisation and thus its cell cycle related function as well.

IV-VII Fbp1 and gluconeogenesis regulation from yeast to cancer, evaluation of the inter-species and heterologous approach

The notion of the high evolutionary conservation of Fbp1 leading to similarities in the regulation in yeast and cancer cell lines is central to this thesis. Indeed, the high degree of similarity in the glycolytic pathway, and the aerobic fermentation associated to both cancer cells and yeast are all valid reasons to place high values at the predictive capacity of the findings in yeast for the situation in cancer cells.

Nevertheless, the effects of the particular decoupling observed in the yeast mutation N75A did not simply extend to the corresponding mutation of the human enzyme N65A. This is evident in the almost completely diminished enzymatic activity of this mutant in the human enzyme compared to the almost intact enzymatic activity observed in the corresponding mutation in yeast. Despite the disparity of the effects of this peculiar mutation on the enzymatic activity, the general FBP1-associated effects in both yeast and cancer cells exhibited comparable tendencies. Both yeast and cancer cells exhibited slower growth upon ectopic FBP1 expression, in addition to hallmarks of oxidation stress and imbalanced redox. Moreover, this work also demonstrated initial evidence of reduced sensitivity towards some genotoxic agents in FBP1-deficient, most prominently cis-platin. Nevertheless, Fbp1 absence made no difference for MMS sensitivity in the tested MCF-7 cell line. MMS induced DNA damage is mostly reversed by base excision repair BER mechanisms[94]. Therefore,

the reported deviation between yeast and mammals in the BER mechanisms including the absence of two factors can offer an explanation for the absence of the Fbp1-related differences in MMS-sensitivity in human cancer cells. Interestingly, the findings in this thesis in addition to earlier works provide evidence that Fbp1 deletion mitigates the burst in ROS shortly after MMS exposure. Meanwhile, mammalian BER has been reported especially superior to yeast BER in handling oxidative DNA damage[60, 149]. Therefore, I speculate that the superior BER system in human cells prevents the translation of Fbp1-associated oxidative stress into an increased sensitivity to MMS-induced DNA damage.

Perhaps the biggest advantage of the dual yeast/human-cells system is that it inspired to consider the possibility of previously unreported post-translational degradation of Fbp1 in human cancer cells. In this thesis, I described a first-hand observation of Fbp1 degradation when ectopically expressed in the Fbp1-negative basal-like breast cancer cell line MDA-MB231. Although no reports on any proteasomal degradation of Fbp1 in cancer existed at that point, my familiarity with catabolite degradation of the yeast homologue enabled me to consider this possibility in cancer cells. Later reports of proteasomal degratation of Fbp1 in hepatocellular carcinoma added further confidence to my observation[95]. Nevertheless, my efforts have yielded no evidence for the same ubiquitination machinery implicated in Fbp1 degradation in hepatocellular carcinoma also underlying my observation in breast cancer cells. None of the three genes TRIM28, MAGE-A3 or MAGE-C2 showed any peculiar variations in their levels of expression between MDA-MB231 cells and MCF-7 cells or in MDA-MB231 cells upon Fbp1 over-expression. While this does not completely rule out the complicity of these factors in the observed degradation in MDA-MB231 cells, it at least signifies the potential of other mechanisms. Recently, the GID ubiquitin ligase, a complex with 8 evolutionary conserved components, has been showcased to mediate the catabolite degradation of Fbp1 and other gluconeogenic enzymes in yeast[21]. Hence further work to understand the mechanism underlying the ubiquitination proteasomal degradation in breast cancer cells and cancers in general, should also consider the possibility of evolutionary conserved pathways.

In retrospect, I view my experience in addressing my topic in a yeast/cancer dual system favourably. While the effects of mutagenising particular evolutionary conserved residues might vary between the two systems, it is no surprise that overall mechanisms exhibit high similarity. While the evolutionary conservation of large segments of metabolic pathways, DNA damage and repair mechanisms should be kept in mind when pursuing such approaches, extra attention should be dedicated to disparity between the two systems so that deviations in outcomes could be predicted and explained. The most unique aspect of this approach is viewing the cancer-associated metabolic reprogramming and the Warburg effect as a regressive phenomenon that awakens ancient 'selfish' and 'originally unicellular' metabolic programmes in a multi-cellular organism with well known destructive outcomes [45, 46]

This view has been recently echoing in the milieu of cancer research[150, 151] and while it does not yet provides no direct contribution to treatment, it offers a fresh and dynamic framework of a wider comprehension and discussion of the evolutionary and metabolic aspects of malignancy that can hopefully contribute to a more robust and total approach against cancer.

V-Conclusions

The results presented in this thesis emphasise the reported impact of Fbp1 on response to genotoxicity in yeast, and support its antiproliferative role in both yeast and cancer cells. In light of various recent reports on Fbp1 repression in various tumours, this thesis further reiterates Fbp1 as a probable tumour suppressor with metabolic and non-metabolic functions. This overall conclusion is supported by the following experimental observations:

- Despite the general correlation between the enzymatic activity of Fbp1 and the previously described MMS-sensitisation, the mutational analysis of Fbp1 in yeast revealed the possibility of decoupling the enzymatic activity from this additional effect.
- The ectopic expression of Fbp1 slows down the growth of both luminal MCF-7 and basal like MDA-MB231 breast cancer cells.
- In cancer cells, FBP1 expression changes glucose sensitivity and inhibits glucose uptake, glycolysis and pentose phosphate pathway.
- Fbp1 is essential for survival in glucose free DMEM.
- The ectopic introduction of Fbp1 in the originally Fbp1-dificient MDA-MB231 cells correlated to a generalised transcriptional inhibition of cell cycle factors, especially M-phase factors.
- Basal-like breast cancer MDA-MB231 cells developed the capacity to proteolitically degrade ectopically expressed Fbp1 upon long-term selection of successfully transfected cells.
- Fbp1 expression exhibited pro-oxidant roles in both yeast and cancer cells, manifested in higher base-line and post-MMS ROS levels, reduced reductive capacity, and tolerance to oxidative treatments.

These summarised findings suggest variable sources for the observed effects with Fbp1 and hence warrant further investigation into the mechanisms underlying these observations. Further work on this should consider two major potential sources of Fbp1 antiproliferative impact. The metabolic effects, mainly stemming from alterations in the altered availability of phospho -hexoses and the non catalytic protein-protein interactions, some of which have already been implicated in recent

reports. Moreover, the potential for proteasomal degradation of Fbp1 should be further investigated, especially in precancerous contexts in which the gradual ablation of Fbp1 could prompt tumour initiation or an increase in tumour aggressiveness. Exploring these possibilities will be essential for devising potential prevention strategies relying on the prevention of Fbp1 loss or ambitious treatment approaches based on the later de-repression/prevention of post-translational deactivation of Fbp1.

VI-References:

1. Shyh-Chang, N. and G.Q. Daley, *Metabolic switches linked to pluripotency and embryonic stem cell differentiation.* Cell Metab, 2015. **21**(3): p. 349-50.
2. Vander Heiden, M.G., L.C. Cantley, and C.B. Thompson, *Understanding the Warburg effect: the metabolic requirements of cell proliferation.* Science, 2009. **324**(5930): p. 1029-33.
3. Vander Heiden, M.G., *Targeting cancer metabolism: a therapeutic window opens.* Nat Rev Drug Discov, 2011. **10**(9): p. 671-84.
4. Israelsen, W.J. and M.G. Vander Heiden, *ATP consumption promotes cancer metabolism.* Cell, 2010. **143**(5): p. 669-71.
5. Scholnick, P., D. Lang, and E. Racker, *Regulatory mechanisms in carbohydrate metabolism. IX. Stimulation of aerobic glycolysis by energy-linked ion transport and inhibition by dextran sulfate.* J Biol Chem, 1973. **248**(14): p. 5175.
6. Goodman, G., M.E. Gershwin, and D. Bercovich, *Fullerene and the origin of life.* Isr Med Assoc J, 2012. **14**(10): p. 602-6.
7. Schimel, D.S., *Terrestrial Ecosystems and the Carbon-Cycle.* Global Change Biology, 1995. **1**(1): p. 77-91.
8. Frayn, K.N., *The glucose-fatty acid cycle: a physiological perspective.* Biochem Soc Trans, 2003. **31**(Pt 6): p. 1115-9.
9. Berg JM, T.J., Stryer L, *Glycolysis Is an Energy-Conversion Pathway in Many Organisms.*, in *Biochemistry*. 2002, W H Freeman: New York.
10. Bouche, C., S. Serdy, C.R. Kahn, and A.B. Goldfine, *The cellular fate of glucose and its relevance in type 2 diabetes.* Endocr Rev, 2004. **25**(5): p. 807-30.
11. Li, Z. and H. Zhang, *Reprogramming of glucose, fatty acid and amino acid metabolism for cancer progression.* Cell Mol Life Sci, 2016. **73**(2): p. 377-92.
12. Tsun, Z.Y. and R. Possemato, *Amino acid management in cancer.* Semin Cell Dev Biol, 2015. **43**: p. 22-32.
13. Gray, L.R., S.C. Tompkins, and E.B. Taylor, *Regulation of pyruvate metabolism and human disease.* Cell Mol Life Sci, 2014. **71**(14): p. 2577-604.
14. Jiang, P., W. Du, and M. Wu, *Regulation of the pentose phosphate pathway in cancer.* Protein Cell, 2014. **5**(8): p. 592-602.
15. Stanton, R.C., *Glucose-6-phosphate dehydrogenase, NADPH, and cell survival.* IUBMB Life, 2012. **64**(5): p. 362-9.
16. Ying, H., A.C. Kimmelman, C.A. Lyssiotis, S. Hua, G.C. Chu, E. Fletcher-Sananikone, J.W. Locasale, J. Son, H. Zhang, J.L. Coloff, H. Yan, W. Wang, S. Chen, A. Viale, H. Zheng, J.H. Paik, C. Lim, A.R. Guimaraes, E.S. Martin, J. Chang, A.F. Hezel, S.R. Perry, J. Hu, B. Gan, Y. Xiao, J.M. Asara, R. Weissleder, Y.A. Wang, L. Chin, L.C. Cantley, and R.A. DePinho, *Oncogenic Kras maintains pancreatic tumors through regulation of anabolic glucose metabolism.* Cell, 2012. **149**(3): p. 656-70.
17. Duvel, K., J.L. Yecies, S. Menon, P. Raman, A.I. Lipovsky, A.L. Souza, E. Triantafellow, Q. Ma, R. Gorski, S. Cleaver, M.G. Vander Heiden, J.P. MacKeigan, P.M. Finan, C.B. Clish, L.O. Murphy, and B.D. Manning, *Activation of a metabolic*

gene regulatory network downstream of mTOR complex 1. Mol Cell, 2010. **39**(2): p. 171-83.
18. Jiang, P., W. Du, X. Wang, A. Mancuso, X. Gao, M. Wu, and X. Yang, *p53 regulates biosynthesis through direct inactivation of glucose-6-phosphate dehydrogenase.* Nat Cell Biol, 2011. **13**(3): p. 310-6.
19. Kohan, A.B., I. Talukdar, C.M. Walsh, and L.M. Salati, *A role for AMPK in the inhibition of glucose-6-phosphate dehydrogenase by polyunsaturated fatty acids.* Biochem Biophys Res Commun, 2009. **388**(1): p. 117-21.
20. Kelleher, J.K., *Gluconeogenesis from labeled carbon: estimating isotope dilution.* Am J Physiol, 1986. **250**(3 Pt 1): p. E296-305.
21. Chen, S.J., X. Wu, B. Wadas, J.H. Oh, and A. Varshavsky, *An N-end rule pathway that recognizes proline and destroys gluconeogenic enzymes.* Science, 2017. **355**(6323).
22. Xiong, Y., Q.Y. Lei, S. Zhao, and K.L. Guan, *Regulation of glycolysis and gluconeogenesis by acetylation of PKM and PEPCK.* Cold Spring Harb Symp Quant Biol, 2011. **76**: p. 285-9.
23. Sedivy, J.M. and D.G. Fraenkel, *Fructose bisphosphatase of Saccharomyces cerevisiae. Cloning, disruption and regulation of the FBP1 structural gene.* J Mol Biol, 1985. **186**(2): p. 307-19.
24. Jones, M.E., M.N. Berry, and J.W. Phillips, *Futile cycles revisited: a markov chain model of simultaneous glycolysis and gluconeogenesis.* J Theor Biol, 2002. **217**(4): p. 509-23.
25. Mor, I., E.C. Cheung, and K.H. Vousden, *Control of glycolysis through regulation of PFK1: old friends and recent additions.* Cold Spring Harb Symp Quant Biol, 2011. **76**: p. 211-6.
26. Weber, G., *Enzymology of cancer cells (second of two parts).* N Engl J Med, 1977. **296**(10): p. 541-51.
27. Hers, H.G. and E. Van Schaftingen, *Fructose 2,6-bisphosphate 2 years after its discovery.* Biochem J, 1982. **206**(1): p. 1-12.
28. Jenkins, C.M., J. Yang, H.F. Sims, and R.W. Gross, *Reversible high affinity inhibition of phosphofructokinase-1 by acyl-CoA: a mechanism integrating glycolytic flux with lipid metabolism.* J Biol Chem, 2011. **286**(14): p. 11937-50.
29. Emery, J.L., A.J. Howat, S. Variend, and G.F. Vawter, *Investigation of inborn errors of metabolism in unexpected infant deaths.* Lancet, 1988. **2**(8601): p. 29-31.
30. Adams, A., C. Redden, and S. Menahem, *Characterization of human fructose-1,6-bisphosphatase in control and deficient tissues.* J Inherit Metab Dis, 1990. **13**(6): p. 829-48.
31. Dunaway, G.A., *A review of animal phosphofructokinase isozymes with an emphasis on their physiological role.* Mol Cell Biochem, 1983. **52**(1): p. 75-91.
32. Benkovic, S.J. and M.M. deMaine, *Mechanism of action of fructose 1,6-bisphosphatase.* Adv Enzymol Relat Areas Mol Biol, 1982. **53**: p. 45-82.
33. Crochet, R.B., J.D. Kim, H. Lee, Y.S. Yim, S.G. Kim, D. Neau, and Y.H. Lee, *Crystal structure of heart 6-phosphofructo-2-kinase/fructose-2,6-bisphosphatase (PFKFB2) and the inhibitory influence of citrate on substrate binding.* Proteins, 2017. **85**(1): p. 117-124.

34. Pilkis, S.J., M.R. El-Maghrabi, M. McGrane, J. Pilkis, and T.H. Claus, *Regulation by glucagon of hepatic pyruvate kinase, 6-phosphofructo 1-kinase, and fructose-1,6-bisphosphatase.* Fed Proc, 1982. **41**(10): p. 2623-8.
35. Pilkis, S.J., M.R. el-Maghrabi, and T.H. Claus, *Fructose-2,6-bisphosphate in control of hepatic gluconeogenesis. From metabolites to molecular genetics.* Diabetes Care, 1990. **13**(6): p. 582-99.
36. Pilkis, S.J., M.R. El-Maghrabi, M. McGrane, J. Pilkis, E. Fox, and T.H. Claus, *Fructose 2,6-bisphosphate: a mediator of hormone action at the fructose 6-phosphate/fructose 1,6-bisphosphate substrate cycle.* Mol Cell Endocrinol, 1982. **25**(3): p. 245-66.
37. Ispolatov, I., M. Ackermann, and M. Doebeli, *Division of labour and the evolution of multicellularity.* Proc Biol Sci, 2012. **279**(1734): p. 1768-76.
38. Michod, R.E., *Evolution of individuality during the transition from unicellular to multicellular life.* Proc Natl Acad Sci U S A, 2007. **104 Suppl 1**: p. 8613-8.
39. Michod, R.E., *Evolution of the individual.* Am Nat, 1997. **150 Suppl 1**: p. S5-S21.
40. Aktipis, C.A., A.M. Boddy, G. Jansen, U. Hibner, M.E. Hochberg, C.C. Maley, and G.S. Wilkinson, *Cancer across the tree of life: cooperation and cheating in multicellularity.* Philos Trans R Soc Lond B Biol Sci, 2015. **370**(1673).
41. Li, Z.J., S.C. Mack, T.H. Mak, S. Angers, M.D. Taylor, and C.C. Hui, *Evasion of p53 and G2/M checkpoints are characteristic of Hh-driven basal cell carcinoma.* Oncogene, 2014. **33**(20): p. 2674-80.
42. Rodeck, U., *Growth factor independence and growth regulatory pathways in human melanoma development.* Cancer Metastasis Rev, 1993. **12**(3-4): p. 219-26.
43. Muenst, S., H. Laubli, S.D. Soysal, A. Zippelius, A. Tzankov, and S. Hoeller, *The immune system and cancer evasion strategies: therapeutic concepts.* J Intern Med, 2016. **279**(6): p. 541-62.
44. Hanahan, D. and R.A. Weinberg, *Hallmarks of cancer: the next generation.* Cell, 2011. **144**(5): p. 646-74.
45. Gabbert, H., R. Wagner, R. Moll, and C.D. Gerharz, *Tumor dedifferentiation: an important step in tumor invasion.* Clin Exp Metastasis, 1985. **3**(4): p. 257-79.
46. Vincent, M., *Cancer: a de-repression of a default survival program common to all cells?: a life-history perspective on the nature of cancer.* Bioessays, 2012. **34**(1): p. 72-82.
47. Huang, S., *The war on cancer: lessons from the war on terror.* Front Oncol, 2014. **4**: p. 293.
48. Setala, K., *Carcinogenesis--devolution towards an ancient nucleated pre-eukaryotic level.* Med Hypotheses, 1984. **15**(3): p. 209-30.
49. Warburg, O., *Note on the metabolism of tumours.* Biochemische Zeitschrift, 1930. **228**: p. 257-258.
50. Shaw, R.J., *Glucose metabolism and cancer.* Curr Opin Cell Biol, 2006. **18**(6): p. 598-608.
51. Diaz-Ruiz, R., M. Rigoulet, and A. Devin, *The Warburg and Crabtree effects: On the origin of cancer cell energy metabolism and of yeast glucose repression*, in *Biochim Biophys Acta*. 2011. p. 568-76.
52. Hardie, D.G. and D. Carling, *The AMP-activated protein kinase--fuel gauge of the mammalian cell?* Eur J Biochem, 1997. **246**(2): p. 259-73.

53. Huang, D., C. Li, and H. Zhang, *Hypoxia and cancer cell metabolism.* Acta Biochim Biophys Sin (Shanghai), 2014. **46**(3): p. 214-9.
54. Vincent, M.D., *The animal within: carcinogenesis and the clonal evolution of cancer cells are speciation events sensu stricto.* Evolution, 2010. **64**(4): p. 1173-83.
55. Roder, P.V., B. Wu, Y. Liu, and W. Han, *Pancreatic regulation of glucose homeostasis.* Exp Mol Med, 2016. **48**: p. e219.
56. DeBerardinis, R.J. and N.S. Chandel, *Fundamentals of cancer metabolism.* Sci Adv, 2016. **2**(5): p. e1600200.
57. Petersen, M.C., D.F. Vatner, and G.I. Shulman, *Regulation of hepatic glucose metabolism in health and disease.* Nat Rev Endocrinol, 2017. **13**(10): p. 572-587.
58. Macheda, M.L., S. Rogers, and J.D. Best, *Molecular and cellular regulation of glucose transporter (GLUT) proteins in cancer.* J Cell Physiol, 2005. **202**(3): p. 654-62.
59. Chen, M., J. Zhang, N. Li, Z. Qian, M. Zhu, Q. Li, J. Zheng, X. Wang, and G. Shi, *Promoter hypermethylation mediated downregulation of FBP1 in human hepatocellular carcinoma and colon cancer.* PLoS One, 2011. **6**(10): p. e25564.
60. Dong, C., T. Yuan, Y. Wu, Y. Wang, T.W. Fan, S. Miriyala, Y. Lin, J. Yao, J. Shi, T. Kang, P. Lorkiewicz, D. St Clair, M.C. Hung, B.M. Evers, and B.P. Zhou, *Loss of FBP1 by Snail-mediated repression provides metabolic advantages in basal-like breast cancer.* Cancer Cell, 2013. **23**(3): p. 316-31.
61. Li, B., B. Qiu, D.S. Lee, Z.E. Walton, J.D. Ochocki, L.K. Mathew, A. Mancuso, T.P. Gade, B. Keith, I. Nissim, and M.C. Simon, *Fructose-1,6-bisphosphatase opposes renal carcinoma progression.* Nature, 2014. **513**(7517): p. 251-5.
62. Li, J., Y. Wang, Q.G. Li, J.J. Xue, Z. Wang, X. Yuan, J.D. Tong, and L.C. Xu, *Downregulation of FBP1 Promotes Tumor Metastasis and Indicates Poor Prognosis in Gastric Cancer via Regulating Epithelial-Mesenchymal Transition.* PLoS One, 2016. **11**(12): p. e0167857.
63. Sheng, H., L. Ying, L. Zheng, D. Zhang, C. Zhu, J. Wu, J. Feng, and D. Su, *Down Expression of FBP1 Is a Negative Prognostic Factor for Non-Small-Cell Lung Cancer.* Cancer Invest, 2015. **33**(5): p. 197-204.
64. Zhu, Y., M. Shi, H. Chen, J. Gu, J. Zhang, B. Shen, X. Deng, J. Xie, X. Zhan, and C. Peng, *NPM1 activates metabolic changes by inhibiting FBP1 while promoting the tumorigenicity of pancreatic cancer cells.* Oncotarget, 2015. **6**(25): p. 21443-51.
65. Watson, J.D. and F.H. Crick, *Molecular structure of nucleic acids; a structure for deoxyribose nucleic acid.* Nature, 1953. **171**(4356): p. 737-8.
66. Chargaff, E., *Preface to a grammar of biology. A hundred years of nucleic acid research.* Science, 1971. **172**(3984): p. 637-42.
67. Curtis, H.J., *Formal discussion of: somatic mutations and carcinogenesis.* Cancer Res, 1965. **25**(8): p. 1305-8.
68. Marjanovic, N.D., R.A. Weinberg, and C.L. Chaffer, *Cell plasticity and heterogeneity in cancer.* Clin Chem, 2013. **59**(1): p. 168-79.
69. Hanahan, D. and R.A. Weinberg, *The hallmarks of cancer.* Cell, 2000. **100**(1): p. 57-70.
70. Farber, S. and L.K. Diamond, *Temporary remissions in acute leukemia in children produced by folic acid antagonist, 4-aminopteroyl-glutamic acid.* N Engl J Med, 1948. **238**(23): p. 787-93.

71. Lippman, A.J., C. Helson, L. Helson, and I.H. Krakoff, *Clinical trials of cis-diamminedichloroplatinum (NSC-119875).* Cancer Chemother Rep, 1973. **57**(2): p. 191-200.
72. Holohan, C., S. Van Schaeybroeck, D.B. Longley, and P.G. Johnston, *Cancer drug resistance: an evolving paradigm.* Nat Rev Cancer, 2013. **13**(10): p. 714-26.
73. Gottesman, M.M., *Mechanisms of cancer drug resistance.* Annu Rev Med, 2002. **53**: p. 615-27.
74. Bouwman, P. and J. Jonkers, *The effects of deregulated DNA damage signalling on cancer chemotherapy response and resistance.* Nat Rev Cancer, 2012. **12**(9): p. 587-98.
75. Sui, X., R. Chen, Z. Wang, Z. Huang, N. Kong, M. Zhang, W. Han, F. Lou, J. Yang, Q. Zhang, X. Wang, C. He, and H. Pan, *Autophagy and chemotherapy resistance: a promising therapeutic target for cancer treatment.* Cell Death Dis, 2013. **4**: p. e838.
76. Hu, X., K. Bardhan, A.V. Paschall, D. Yang, J.L. Waller, M.A. Park, A. Nayak-Kapoor, T.A. Samuel, S.I. Abrams, and K. Liu, *Deregulation of apoptotic factors Bcl-xL and Bax confers apoptotic resistance to myeloid-derived suppressor cells and contributes to their persistence in cancer.* J Biol Chem, 2013. **288**(26): p. 19103-15.
77. Gietz, R.D., R.H. Schiestl, A.R. Willems, and R.A. Woods, *Studies on the transformation of intact yeast cells by the LiAc/SS-DNA/PEG procedure.* Yeast, 1995. **11**(4): p. 355-60.
78. Laemmli, U.K., *Cleavage of structural proteins during the assembly of the head of bacteriophage T4.* Nature, 1970. **227**(5259): p. 680-5.
79. Skalecki, K., W. Mularczyk, and A. Dzugaj, *Kinetic properties of D-fructose-1,6-bisphosphate 1-phosphohydrolase isolated from human muscle.* Biochem J, 1995. **310 (Pt 3)**: p. 1029-35.
80. Zou, C., Y. Wang, and Z. Shen, *2-NBDG as a fluorescent indicator for direct glucose uptake measurement.* J Biochem Biophys Methods, 2005. **64**(3): p. 207-15.
81. Zhao, H., S. Kalivendi, H. Zhang, J. Joseph, K. Nithipatikom, J. Vasquez-Vivar, and B. Kalyanaraman, *Superoxide reacts with hydroethidine but forms a fluorescent product that is distinctly different from ethidium: potential implications in intracellular fluorescence detection of superoxide.* Free Radic Biol Med, 2003. **34**(11): p. 1359-68.
82. Perelman, A., C. Wachtel, M. Cohen, S. Haupt, H. Shapiro, and A. Tzur, *JC-1: alternative excitation wavelengths facilitate mitochondrial membrane potential cytometry.* Cell Death Dis, 2012. **3**: p. e430.
83. Vichai, V. and K. Kirtikara, *Sulforhodamine B colorimetric assay for cytotoxicity screening.* Nat Protoc, 2006. **1**(3): p. 1112-6.
84. Bauer, A.S., P.V. Nazarov, N.A. Giese, S. Beghelli, A. Heller, W. Greenhalf, E. Costello, A. Muller, M. Bier, O. Strobel, T. Hackert, L. Vallar, A. Scarpa, M.W. Buchler, J.P. Neoptolemos, S. Kreis, and J.D. Hoheisel, *Transcriptional variations in the wider peritumoral tissue environment of pancreatic cancer.* Int J Cancer, 2018. **142**(5): p. 1010-1021.
85. Ghanem, A., A. Kitanovic, J. Holzwarth, and S. Wolfl, *Mutational analysis of fructose-1,6-bis-phosphatase FBP1 indicates partially independent functions in gluconeogenesis and sensitivity to genotoxic stress.* Microb Cell, 2017. **4**(2): p. 52-63.

86. Entian, K.D., R.F. Vogel, M. Rose, L. Hofmann, and D. Mecke, *Isolation and primary structure of the gene encoding fructose-1,6-bisphosphatase from Saccharomyces cerevisiae.* FEBS Lett, 1988. **236**(1): p. 195-200.
87. Rogers, D.T., E. Hiller, L. Mitsock, and E. Orr, *Characterization of the gene for fructose-1,6-bisphosphatase from Saccharomyces cerevisiae and Schizosaccharomyces pombe. Sequence, protein homology, and expression during growth on glucose.* J Biol Chem, 1988. **263**(13): p. 6051-7.
88. Hammerle, M., J. Bauer, M. Rose, A. Szallies, M. Thumm, S. Dusterhus, D. Mecke, K.D. Entian, and D.H. Wolf, *Proteins of newly isolated mutants and the amino-terminal proline are essential for ubiquitin-proteasome-catalyzed catabolite degradation of fructose-1,6-bisphosphatase of Saccharomyces cerevisiae.* J Biol Chem, 1998. **273**(39): p. 25000-5.
89. Schork, S.M., M. Thumm, and D.H. Wolf, *Catabolite inactivation of fructose-1,6-bisphosphatase of Saccharomyces cerevisiae. Degradation occurs via the ubiquitin pathway.* J Biol Chem, 1995. **270**(44): p. 26446-50.
90. Rittenhouse, J., P.B. Harrsch, J.N. Kim, and F. Marcus, *Amino acid sequence of the phosphorylation site of yeast (Saccharomyces cerevisiae) fructose-1,6-bisphosphatase.* J Biol Chem, 1986. **261**(9): p. 3939-43.
91. Choe, J.Y., H.J. Fromm, and R.B. Honzatko, *Crystal structures of fructose 1,6-bisphosphatase: mechanism of catalysis and allosteric inhibition revealed in product complexes.* Biochemistry, 2000. **39**(29): p. 8565-74.
92. York, J.D., J.W. Ponder, and P.W. Majerus, *Definition of a metal-dependent/Li(+)-inhibited phosphomonoesterase protein family based upon a conserved three-dimensional core structure.* Proc Natl Acad Sci U S A, 1995. **92**(11): p. 5149-53.
93. Xu, G.J., A.G. Datta, V.N. Singh, H. Suda, S. Pontremoli, and B.L. Horecker, *Rabbit liver fructose 1,6-bisphosphatase: labeling of the active and allosteric sites with pyridoxal 5-phosphate and sequence of a nonapeptide from the active site.* Arch Biochem Biophys, 1981. **210**(1): p. 98-103.
94. Kitanovic, A. and S. Wolfl, *Fructose-1,6-bisphosphatase mediates cellular responses to DNA damage and aging in Saccharomyces cerevisiae.* Mutat Res, 2006. **594**(1-2): p. 135-47.
95. Jin, X., Y. Pan, L. Wang, L. Zhang, R. Ravichandran, P.R. Potts, J. Jiang, H. Wu, and H. Huang, *MAGE-TRIM28 complex promotes the Warburg effect and hepatocellular carcinoma progression by targeting FBP1 for degradation.* Oncogenesis, 2017. **6**(4): p. e312.
96. van 't Veer, L.J., H. Dai, M.J. van de Vijver, Y.D. He, A.A. Hart, M. Mao, H.L. Peterse, K. van der Kooy, M.J. Marton, A.T. Witteveen, G.J. Schreiber, R.M. Kerkhoven, C. Roberts, P.S. Linsley, R. Bernards, and S.H. Friend, *Gene expression profiling predicts clinical outcome of breast cancer.* Nature, 2002. **415**(6871): p. 530-6.
97. Polyak, K., *Heterogeneity in breast cancer.* J Clin Invest, 2011. **121**(10): p. 3786-8.
98. McHugh, B.J., A. Murdoch, C. Haslett, and T. Sethi, *Loss of the integrin-activating transmembrane protein Fam38A (Piezo1) promotes a switch to a reduced integrin-dependent mode of cell migration.* PLoS One, 2012. **7**(7): p. e40346.

99. Gardner, M.K., *CENP-E hangs on at dynamic microtubule ends.* Nat Cell Biol, 2013. **15**(9): p. 1030-2.
100. Bai, M., J. Ni, S. Shen, Q. Huang, J. Wu, Y. Le, and L. Yu, *Aurora-A kinase-inactive mutants disrupt the interaction with Ajuba and cause defects in mitotic spindle formation and G2/M phase arrest in HeLa cells.* BMB Rep, 2014. **47**(11): p. 631-6.
101. Zheng, J., S.L. Woo, X. Hu, R. Botchlett, L. Chen, Y. Huo, and C. Wu, *Metformin and metabolic diseases: a focus on hepatic aspects.* Front Med, 2015. **9**(2): p. 173-86.
102. Pryor, R. and F. Cabreiro, *Repurposing metformin: an old drug with new tricks in its binding pockets.* Biochem J, 2015. **471**(3): p. 307-22.
103. Shi, L., C. He, Z. Li, Z. Wang, and Q. Zhang, *FBP1 modulates cell metabolism of breast cancer cells by inhibiting the expression of HIF-1alpha.* Neoplasma, 2017. **64**(4): p. 535-542.
104. Yu, J., J. Li, Y. Chen, W. Cao, Y. Lu, J. Yang, and E. Xing, *Snail Enhances Glycolysis in the Epithelial-Mesenchymal Transition Process by Targeting FBP1 in Gastric Cancer.* Cell Physiol Biochem, 2017. **43**(1): p. 31-38.
105. Navas, M.A., S. Cerdan, and J.M. Gancedo, *Futile cycles in Saccharomyces cerevisiae strains expressing the gluconeogenic enzymes during growth on glucose.* Proc Natl Acad Sci U S A, 1993. **90**(4): p. 1290-4.
106. Kitanovic, A., T. Walther, M.O. Loret, J. Holzwarth, I. Kitanovic, F. Bonowski, N. Van Bui, J.M. Francois, and S. Wolfl, *Metabolic response to MMS-mediated DNA damage in Saccharomyces cerevisiae is dependent on the glucose concentration in the medium.* FEMS Yeast Res, 2009. **9**(4): p. 535-51.
107. Schieber, M.S. and N.S. Chandel, *ROS links glucose metabolism to breast cancer stem cell and EMT phenotype.* Cancer Cell, 2013. **23**(3): p. 265-7.
108. Winterbourn, C.C., *The challenges of using fluorescent probes to detect and quantify specific reactive oxygen species in living cells.* Biochim Biophys Acta, 2014. **1840**(2): p. 730-8.
109. Puleston, D., *Detection of Mitochondrial Mass, Damage, and Reactive Oxygen Species by Flow Cytometry.* Cold Spring Harb Protoc, 2015. **2015**(9): p. pdb prot086298.
110. Morgan, B., M.C. Sobotta, and T.P. Dick, *Measuring E(GSH) and H2O2 with roGFP2-based redox probes.* Free Radic Biol Med, 2011. **51**(11): p. 1943-51.
111. Meyer, A.J. and T.P. Dick, *Fluorescent protein-based redox probes.* Antioxid Redox Signal, 2010. **13**(5): p. 621-50.
112. Peeters, K., F. Van Leemputte, B. Fischer, B.M. Bonini, H. Quezada, M. Tsytlonok, D. Haesen, W. Vanthienen, N. Bernardes, C.B. Gonzalez-Blas, V. Janssens, P. Tompa, W. Versees, and J.M. Thevelein, *Fructose-1,6-bisphosphate couples glycolytic flux to activation of Ras.* Nat Commun, 2017. **8**(1): p. 922.
113. Holzer, H., *Proteolytic catabolite inactivation in Saccharomyces cerevisiae.* Revis Biol Celular, 1989. **21**: p. 305-19.
114. Hedges, D., M. Proft, and K.D. Entian, *CAT8, a new zinc cluster-encoding gene necessary for derepression of gluconeogenic enzymes in the yeast Saccharomyces cerevisiae.* Mol Cell Biol, 1995. **15**(4): p. 1915-22.
115. Boriack-Sjodin, P.A., S.M. Margarit, D. Bar-Sagi, and J. Kuriyan, *The structural basis of the activation of Ras by Sos.* Nature, 1998. **394**(6691): p. 337-43.

116. Schomerus, C., T. Munder, and H. Kuntzel, *Site-directed mutagenesis of the Saccharomyces cerevisiae CDC25 gene: effects on mitotic growth and cAMP signalling.* Mol Gen Genet, 1990. **223**(3): p. 426-32.
117. Horecker, B.L., E. Melloni, and S. Pontremoli, *Fructose 1,6-bisphosphatase: properties of the neutral enzyme and its modification by proteolytic enzymes.* Adv Enzymol Relat Areas Mol Biol, 1975. **42**: p. 193-226.
118. Ashizawa, K., M.C. Willingham, C.M. Liang, and S.Y. Cheng, *In vivo regulation of monomer-tetramer conversion of pyruvate kinase subtype M2 by glucose is mediated via fructose 1,6-bisphosphate.* J Biol Chem, 1991. **266**(25): p. 16842-6.
119. Ashizawa, K., P. McPhie, K.H. Lin, and S.Y. Cheng, *An in vitro novel mechanism of regulating the activity of pyruvate kinase M2 by thyroid hormone and fructose 1, 6-bisphosphate.* Biochemistry, 1991. **30**(29): p. 7105-11.
120. Li, M.V., B. Chang, M. Imamura, N. Poungvarin, and L. Chan, *Glucose-dependent transcriptional regulation by an evolutionarily conserved glucose-sensing module.* Diabetes, 2006. **55**(5): p. 1179-89.
121. Peterson, C.W., C.A. Stoltzman, M.P. Sighinolfi, K.S. Han, and D.E. Ayer, *Glucose controls nuclear accumulation, promoter binding, and transcriptional activity of the MondoA-Mlx heterodimer.* Mol Cell Biol, 2010. **30**(12): p. 2887-95.
122. Wu, N., B. Zheng, A. Shaywitz, Y. Dagon, C. Tower, G. Bellinger, C.H. Shen, J. Wen, J. Asara, T.E. McGraw, B.B. Kahn, and L.C. Cantley, *AMPK-dependent degradation of TXNIP upon energy stress leads to enhanced glucose uptake via GLUT1.* Mol Cell, 2013. **49**(6): p. 1167-75.
123. Mazurek, S., C.B. Boschek, F. Hugo, and E. Eigenbrodt, *Pyruvate kinase type M2 and its role in tumor growth and spreading.* Semin Cancer Biol, 2005. **15**(4): p. 300-8.
124. Mazurek, S., *Pyruvate kinase type M2: a key regulator of the metabolic budget system in tumor cells.* Int J Biochem Cell Biol, 2011. **43**(7): p. 969-80.
125. Luo, W. and G.L. Semenza, *Emerging roles of PKM2 in cell metabolism and cancer progression.* Trends Endocrinol Metab, 2012. **23**(11): p. 560-6.
126. Israelsen, W.J., T.L. Dayton, S.M. Davidson, B.P. Fiske, A.M. Hosios, G. Bellinger, J. Li, Y. Yu, M. Sasaki, J.W. Horner, L.N. Burga, J. Xie, M.J. Jurczak, R.A. DePinho, C.B. Clish, T. Jacks, R.G. Kibbey, G.M. Wulf, D. Di Vizio, G.B. Mills, L.C. Cantley, and M.G. Vander Heiden, *PKM2 isoform-specific deletion reveals a differential requirement for pyruvate kinase in tumor cells.* Cell, 2013. **155**(2): p. 397-409.
127. Walsh, M.J., K.R. Brimacombe, D. Anastasiou, Y. Yu, W.J. Israelsen, B.S. Hong, W. Tempel, S. Dimov, H. Veith, H. Yang, C. Kung, K.E. Yen, L. Dang, F. Salituro, D.S. Auld, H.W. Park, M.G. Vander Heiden, C.J. Thomas, M. Shen, and M.B. Boxer, *ML265: A potent PKM2 activator induces tetramerization and reduces tumor formation and size in a mouse xenograft model*, in *Probe Reports from the NIH Molecular Libraries Program*. 2010: Bethesda (MD).
128. Ye, J., A. Mancuso, X. Tong, P.S. Ward, J. Fan, J.D. Rabinowitz, and C.B. Thompson, *Pyruvate kinase M2 promotes de novo serine synthesis to sustain mTORC1 activity and cell proliferation.* Proc Natl Acad Sci U S A, 2012. **109**(18): p. 6904-9.
129. Fukuda, S., H. Miyata, Y. Miyazaki, T. Makino, T. Takahashi, Y. Kurokawa, M. Yamasaki, K. Nakajima, S. Takiguchi, M. Mori, and Y. Doki, *Pyruvate Kinase M2*

Modulates Esophageal Squamous Cell Carcinoma Chemotherapy Response by Regulating the Pentose Phosphate Pathway. Ann Surg Oncol, 2015. **22 Suppl 3**: p. S1461-8.
130. Yang, W., Y. Xia, H. Ji, Y. Zheng, J. Liang, W. Huang, X. Gao, K. Aldape, and Z. Lu, *Nuclear PKM2 regulates beta-catenin transactivation upon EGFR activation.* Nature, 2011. **480**(7375): p. 118-22.
131. Luo, W., H. Hu, R. Chang, J. Zhong, M. Knabel, R. O'Meally, R.N. Cole, A. Pandey, and G.L. Semenza, *Pyruvate kinase M2 is a PHD3-stimulated coactivator for hypoxia-inducible factor 1.* Cell, 2011. **145**(5): p. 732-44.
132. Demaria, M. and V. Poli, *PKM2, STAT3 and HIF-1alpha: The Warburg's vicious circle.* JAKSTAT, 2012. **1**(3): p. 194-6.
133. Bayley, J.P. and P. Devilee, *The Warburg effect in 2012.* Curr Opin Oncol, 2012. **24**(1): p. 62-7.
134. Hsu, M.C., W.C. Hung, H. Yamaguchi, S.O. Lim, H.W. Liao, C.H. Tsai, and M.C. Hung, *Extracellular PKM2 induces cancer proliferation by activating the EGFR signaling pathway.* Am J Cancer Res, 2016. **6**(3): p. 628-38.
135. Hamabe, A., M. Konno, N. Tanuma, H. Shima, K. Tsunekuni, K. Kawamoto, N. Nishida, J. Koseki, K. Mimori, N. Gotoh, H. Yamamoto, Y. Doki, M. Mori, and H. Ishii, *Role of pyruvate kinase M2 in transcriptional regulation leading to epithelial-mesenchymal transition.* Proc Natl Acad Sci U S A, 2014. **111**(43): p. 15526-31.
136. Woolley, J.F., A. Corcoran, G. Groeger, W.D. Landry, and T.G. Cotter, *Redox-regulated growth factor survival signaling.* Antioxid Redox Signal, 2013. **19**(15): p. 1815-27.
137. Schieber, M. and N.S. Chandel, *ROS function in redox signaling and oxidative stress.* Curr Biol, 2014. **24**(10): p. R453-62.
138. Sies, H., *Hydrogen peroxide as a central redox signaling molecule in physiological oxidative stress: Oxidative eustress.* Redox Biol, 2017. **11**: p. 613-619.
139. Storr, S.J., C.M. Woolston, Y. Zhang, and S.G. Martin, *Redox environment, free radical, and oxidative DNA damage.* Antioxid Redox Signal, 2013. **18**(18): p. 2399-408.
140. Kang, M.A., E.Y. So, A.L. Simons, D.R. Spitz, and T. Ouchi, *DNA damage induces reactive oxygen species generation through the H2AX-Nox1/Rac1 pathway.* Cell Death Dis, 2012. **3**: p. e249.
141. Keibler, M.A., T.M. Wasylenko, J.K. Kelleher, O. Iliopoulos, M.G. Vander Heiden, and G. Stephanopoulos, *Metabolic requirements for cancer cell proliferation.* Cancer Metab, 2016. **4**: p. 16.
142. Kalucka, J., R. Missiaen, M. Georgiadou, S. Schoors, C. Lange, K. De Bock, M. Dewerchin, and P. Carmeliet, *Metabolic control of the cell cycle.* Cell Cycle, 2015. **14**(21): p. 3379-88.
143. Lee, I.H. and T. Finkel, *Metabolic regulation of the cell cycle.* Curr Opin Cell Biol, 2013. **25**(6): p. 724-9.
144. Peters, G.J., H.H. Backus, S. Freemantle, B. van Triest, G. Codacci-Pisanelli, C.L. van der Wilt, K. Smid, J. Lunec, A.H. Calvert, S. Marsh, H.L. McLeod, E. Bloemena, S. Meijer, G. Jansen, C.J. van Groeningen, and H.M. Pinedo, *Induction of thymidylate synthase as a 5-fluorouracil resistance mechanism.* Biochim Biophys Acta, 2002. **1587**(2-3): p. 194-205.

145. Espada, L., N. Meo-Evoli, P. Sancho, S. Real, I. Fabregat, S. Ambrosio, and A. Tauler, *ROS production is essential for the apoptotic function of E2F1 in pheochromocytoma and neuroblastoma cell lines.* PLoS One, 2012. **7**(12): p. e51544.
146. Jones, R.G., D.R. Plas, S. Kubek, M. Buzzai, J. Mu, Y. Xu, M.J. Birnbaum, and C.B. Thompson, *AMP-activated protein kinase induces a p53-dependent metabolic checkpoint.* Mol Cell, 2005. **18**(3): p. 283-93.
147. Cai, X., X. Hu, X. Tan, W. Cheng, Q. Wang, X. Chen, Y. Guan, C. Chen, and X. Jing, *Metformin Induced AMPK Activation, G0/G1 Phase Cell Cycle Arrest and the Inhibition of Growth of Esophageal Squamous Cell Carcinomas In Vitro and In Vivo.* PLoS One, 2015. **10**(7): p. e0133349.
148. Jiang, Y., X. Li, W. Yang, D.H. Hawke, Y. Zheng, Y. Xia, K. Aldape, C. Wei, F. Guo, Y. Chen, and Z. Lu, *PKM2 regulates chromosome segregation and mitosis progression of tumor cells.* Mol Cell, 2014. **53**(1): p. 75-87.
149. Kelley, M.R., Y.W. Kow, and D.M. Wilson, 3rd, *Disparity between DNA base excision repair in yeast and mammals: translational implications.* Cancer Res, 2003. **63**(3): p. 549-54.
150. Trigos, A.S., R.B. Pearson, A.T. Papenfuss, and D.L. Goode, *How the evolution of multicellularity set the stage for cancer.* Br J Cancer, 2018. **118**(2): p. 145-152.
151. Chen, H., F. Lin, K. Xing, and X. He, *The reverse evolution from multicellularity to unicellularity during carcinogenesis.* Nat Commun, 2015. **6**: p. 6367.